Facet Model Optic Flow
and
Rigid Body Motion

by

Jong Soo Lee

A Dissertation submitted to the Faculty of
the Virginia Polytechnique Institute and State University
in partial fulfillment of the requirements for the degree of

Doctor of Philosophy
in
Electrical Engineering

APPROVED:

Dr. Robert M. Haralick (Chairman)

Dr. Roger W. Ehrich

Dr. Linda G. Shapiro

Dr. Paul M. Lapsa

Dr. Kai Bor Yu

August 1985

Blacksburg Virginia

Facet Model Optic Flow and Rigid Body Motion

by

Jong Soo Lee

(ABSTRACT)

The dissertation uses the facet model technique to compute the optic flow field directly from a time sequence of image frames. Two techniques, an iterative and a non-iterative one, determine 3D motion parameters and surface structure (relative depth) from the computed optic flow field. Finally we discuss a technique for the image segmentation based on the multi-object motion using both optic flow and its time derivative.

The facet model technique computes optic flow locally by solving over-constrained linear equations obtained from a fit over 3D (row, column, and time) neighborhoods in an image sequence. The iterative technique computes motion parameters and surface structure using each to update the other. This technique essentially uses the least square error method on the relationship between optic flow field and rigid body motion. The non-iterative technique computes motion parameters by solving a linear system derived from the relationship between optic flow field and rigid body motion and then computes the relative depth of each pixel using the motion parameters computed. The technique also estimates errors of both the computed motion parameters and the relative depth when the optic flow is perturbed.

ACKNOWLEDGEMENTS

I wish to express my sincere gratitude to each and every member of my advisory committee. Special recognition is given to my committee chairman, R. M. Haralick, for his guidance and patient assistance.

I would also like to thank my family, , , and , for their patience during the periods of time that I spent doing the work.

Table of Contents

Chapter		Page
I.	Introduction	1
II.	Related Literature Review	6
	2.1 Computing Optic Flow	7
	2.2 From Optic Flow to 3D Motion and Depth	20
	2.3 Determining Corresponding Points	24
	2.4 From Corresponding Points 3D Motion and Depth	30
III.	Facet Model Optic Flow	33
	3.1 Optic Flow Computation	34
	3.2 Discrete Orthogonal Polynomials for Facet Model	46
	3.3 Computed Optic Flow Images	59
IV.	Iterative Motion and Depth Recovery	88
	4.1 Rigid Body Motion	88
	4.2 Fundamental Optic Flow Equations	93
	4.3 Position and Motion Determination	102
	4.4 Convergence and Uniqueness	109
	4.5 Error Analysis of Small Noise Perturbation	120
	4.6 Motion Parameters Estimation	130
V.	Linear Estimation of Motion and Depth	149
	5.1 The Second Fundamental Optic Flow Equation	150
	5.2 Optic Flow Image and One Spatial Point	164
	5.3 Motion Parameter Estimation	168
	5.4 Estimation of Translational Motion and Depth	185
	5.5 Recapitulation and Experimental Result	193
VI.	Using Optic Flow and Its Time Derivative	212
	6.1 General Motion Equation	213
	6.2 Pure Translation Motion	221
	6.3 Pure Rotational Motion	226
	6.4 Motion Based Image Segmentation	230
VII.	Conclusion	243
	Bibliography	241

LIST OF FIGURES

	Page
Fig 2.1 - Fig 2.2	18 - 19
Fig 3.1 - Fig 3.2	35 - 36
Fig 3.3	38
Fig 3.4	57
Fig 3.5 - Fig 3.18	65 - 78
Fig 3.19 - Fig 3.23	83 - 87
Fig 4.1	94
Fig 4.2	119
Fig 4.3 - Fig 4.8	135 - 140
Fig 4.9 - Fig 4.10	142 - 143
Fig 4.11 - Fig 4.13	145 - 147
Fig 5.1 - Fig 5.2	199 - 200
Fig 5.3	202
Fig 5.4 - Fig 5.7	204 - 207
Fig 5.8 - Fig 5.10	209 - 211
Fig 6.1 - Fig 6.6	235 - 242

LIST OF TABLES

	Page
Table 4.1	141
Table 4.2	144
Table 4.3	148
Table 5.1	201
Table 5.2	203
Table 5.3	208

CHAPTER I

INTRODUCTION

When a scene containing objects in motion is imaged on a camera, a time-varying image or image time sequence is produced. From the image time sequence optic flow can be extracted. The optic flow can be used for the motion and surface structure determination of each object. Having velocity information for camera movement or for each moving object in such a scene is useful in areas such as robotic vision, navigation systems, and target tracking systems because an object trajectory in the scene may be calculated and predicted from the image time sequence. It can also be integrated with a complex vision system which uses various kinds of information from textural analysis, shape from shading, stereopsis, and so on.

Motion vision analysis is difficult due, in part, to a technical problem of dealing with massive amounts of data and the traditional problem of motion interpretation from a correspondence process of static scenes. This interpretation is different from that indicated by biological studies [GIBSON(1950bc), CORNSWEET(1970), KOLERS(1972)] on the eyes of various kinds of animals. From the studies, it is clear

that in biological system there are many visual processing operations whose primitives are points in motion.

An object in motion causes change in the observed optic array. The change in the optic array is called the optic flow field [GIBSON(1950ab)]. The field is the basic visual input for a domain-independent, motion-understanding system [BALLARD and BROWN(1982)]. The extraction of optic flow from a changing image is a low-level operation whose computational mechanisms need to be developed. Determining an object's motion parameters and spatial structure from optic flow is called an inverse problem.

In this dissertation, we describe a two-step technique for extracting 3D motion and structure information about a single object from a uniform time sequence of image frames taken from a dynamic perspective projection. We assume that all the objects in the scene are rigid and consider relative velocities of the objects with respect to the camera even if the camera is in motion.

In the first step of the technique, we use the facet model of a time-varying image [HARALICK and LEE(1983)] to compute the optic flow velocity image, i.e., the positional-velocity field of picture elements, by solving the over-constrained linear system on the velocity of pixels. In the second step, we show two techniques to recover motion parameters and relative depth from the optic flow image. One

determines motion parameters iteratively by updating relative depth using the parameters determined. We apply the above facet model technique to an image time sequence of a real street scene containing a turning taxicab to obtain optic flows and apply this iterative technique to the optic flows obtained to estimate quantitatively the 3D velocity of the taxicab. In comparision, DRESCHLER and NAGEL(1982) approximate this taxicab by a polyhedra from a sequence of corresponding corner points in the same image sequence.

The other technique in the second step establishes a linear system from the relationship between optic flow and rigid body motion. Solving the linear system, we determine the motion parameters and relative depth. We estimate the error bounds of motion parameters and relative depth for optic flow images under small noise perturbations.

This dissertation also describes a technique for segmenting image frames based on the 3D motion when the image contains multiple moving objects. Although POTTER(1975) uses the cross-template for the segmentation of images containing objects in two-dimensional motion, the Hough transform technique [HOUGH(1962), DUDA and HART(1972)] can be used for the image frame segmentation when a motion constraining transformation can be derived [ADIV(1983), LEE(1984)]. Segmentation of an optic flow field using the relationship between the rigid body motion and the optic

flow requires high-dimensional parameter space [LEE(1984)]. Assuming the time derivative of the optic flow is observable, we can segment the optic flow field in a reduced dimensional parameter space.

Furthermore, we can derive a second order polynomial equation involving three rotational components only from each optic flow and its time derivative and thus we can determine general 3D motion parameters of an object from the object's two optic flow points and their time derivatives. The general 3D motion parameters can also be determined from a nonlinear system of eight equations constructed from the object's two optic flows and their time derivatives. In comparison, the method by PRAZDNY(1981) requires 5 optic flow image points, the method by TSAI and HUANG [TSAI(1981,82,84)] requires 4 point correspondence for planar patch motion and 8 point correspondence for curved surface motion, and the method by NAGEL(1981bc) and NAGEL and NEUMAN(1981) requires 5 point correspondence. When the object only rotates or translates, we can determine the object's motion parameters in a closed form from a single point of optic flow and its time derivative. However, the method by YEN and HUANG(1983) requires 2 point correspondences over 2 frames and 1 point correspondence over 3 frames for pure rotational motion.

In the following chapter, we review the related

literature, and in chapter 3, we describe the computation of optic flow image from the facet model of image sequence. In chapter 4, we describe an iterative technique for recovering motion parameters and relative depth from the optic flow image. In chapter 5, we establish the linear system from the relationship between optic flow and rigid body motion and we also estimate motion parameters and relative depth with their error bounds when the optic flow image undergoes a small perturbation. In chapter 6, we introduce a technique determining motion and segmenting image frame from optic flow and its time derivative. We draw conclusions in chapter 7.

Chapter II

RELATED LITERATURE REVIEW

When objects in the environment are illuminated, light is reflected from surfaces of the objects. The reflected light forms a densely structured optic array at a point of observation. The optic array may be thought of as a bundle of narrow cones of light with their apices at the point of observation and their bases at distinct surface elements. Each surface element may produce a distinct light cone from a different intensity and spectral composition of the light at each surface element [LEE(1980)].

For moving objects or the observation point in motion, a light cone from a surface element moves with some velocity causing change of the optic array continuously over time, giving rise to an optic flow field. Formally, the optic field is a field of 2D velocities projected on the image plane of the projected 3D velocities of surface elements. For convenience and realism, the optic flow field is described in terms of and extracted from the changing pattern of light incident on an image plane that intercepts the time-varying optic array.

Motion has been conceptualized classically as an inference from analyzing each static 2D brightness intensity pattern of image time sequence [HELMHOLTZ(1925)]. However, motion and structure can be perceived directly from the optic flow field as one psychological theory indicates [GIBSON(1950abc)]. In that theory, motion and change are basic for a vision system while a static intensity pattern is a rare thing.

In the following, we discuss techniques computing optic flow in section 2.1 and techniques recovering 3D motions and depth from optic flow in section 2.2. In section 2.3 we consider techniques determining corresponding points and in section 2.4 we show techniques determining 3D motion and depth from corresponding points.

2.1 Computing Optic Flow

To compute the optic flow field directly from a time sequence of image frames, numerous techniques have been proposed. A technique can be assigned to one of two categories depending upon the requirement of a matching scheme. The so called 'non-matching' approaches, which do not require the correspondence process, determine two components of a flow vector based on the temporal and spatial brightness variation of the image and motion model.

When a surface models an image brightness, the brightness variation at an image point can be represented by the surface gradient at the point. Thus, the 'non-matching' approaches are sometimes called gradient based techniques [ULLMAN(1981)].

In their experimental studies of moving television images, LIMB and MURPHY(1975) use frame brightness difference for the temporal brightness variation and consecutive row pixel brightness difference for the spatial brightness variation in estimating the horizontal component of a flow vector. These brightness differences deserve consideration in a mathematical model of image and motion for the optic flow computation [CAFFORIO and ROCCA(1976,79), FENNEMA and THOMPSON(1979), THOMPSON and BARNARD(1981), HORN and SCHUNK(1981)].

A time-varying image can be represented mathematically by $I(x,z,t)$ where x and z are the image plane coordinates and t is the time coordniate. Suppose that the image is displaced a distance δx in the x-direction and a distance δz in the z-direction in a time δt. Then the intensity at image point $(x+\delta x, z+\delta z)$ at time $t+\delta t$ can be represented using the Taylor series expansion as

$$I(x+\delta x, z+\delta z, t+\delta t) = I(x,z,t) + \delta x \frac{\partial I}{\partial x} + \delta z \frac{\partial I}{\partial z} + \delta t \frac{\partial I}{\partial t}$$

$$+\frac{\delta x^2}{2}\frac{\partial^2 I}{\partial x^2}+\frac{\delta x\delta z}{2}\frac{\partial^2 I}{\partial x\partial z}+\frac{\delta z^2}{2}\frac{\partial^2 I}{\partial z^2}+\frac{\delta z\delta t}{2}\frac{\partial^2 I}{\partial z\partial t}$$

$$+\frac{\delta t^2}{2}\frac{\partial^2 I}{\partial t^2}+\frac{\delta t\delta x}{2}\frac{\partial^2 I}{\partial t\partial x}\cdots \qquad (2.1)$$

where the partial derivatives are computed at the image point (x,z) at the time t either from a differentiable image model or using a finite difference method.

For the optic flow computation, some techniques consider only the linear and constant terms in (2.1) while others consider the second or higher terms as well. In the following two subsections, we will first discuss techniques using the linear and constant terms in (2.1) and then techniques requiring higher terms.

2.1.1 Linear Model of Image and Motion

Neglecting the second and higher order terms as the error measurement in (2.1), we have

$$I(x+\delta x, z+\delta z, t+\delta t) = I(x,z,t) + \delta x\frac{\partial I}{\partial x} + \delta z\frac{\partial I}{\partial z} + \delta t\frac{\partial I}{\partial t} \qquad (2.2)$$

Assuming that the brightness remains the same after the motion, we can set $I(x+\delta x, z+\delta z, t+\delta t)=I(x,z,t)$. Thus, we have

$$\frac{\delta x}{\delta t}\frac{\partial I}{\partial x} + \frac{\delta z}{\delta t}\frac{\partial I}{\partial z} + \frac{\partial I}{\partial t} = 0 \qquad (2.3)$$

Setting $\delta t \to 0$, we have a linear relationship between the two optic flow components u and v as

$$u\frac{\partial I}{\partial x} + v\frac{\partial I}{\partial z} + \frac{\partial I}{\partial t} = 0 \qquad (2.4)$$

where $u = \lim_{\delta t \to 0} \frac{\delta x}{\delta t}$ and $v = \lim_{\delta t \to 0} \frac{\delta z}{\delta t}$.

This relationship is called the motion constraint or the optic flow equation [FENNEMA and THOMPSON(1979), THOMPSON and BARNARD(1981), HORN and SCHUNK(1981)].

Using the optic flow equation and assuming optic flow constancy over a moving image area, a flow vector can be computed [FENNEMA and THOMPSON(1979), THOMPSON and BARNARD(1981), HORN and SCHUNK(1981)]. CAFFORIO and ROCCA(1976) take the statistical analysis on the optic flow equation and estimate motion of multiple objects using a clustering scheme. CAFFORIO and ROCCA(1979) investigate the noise effect on the optic flow equation and consider a hardware implementation of motion estimation. FENNEMA and THOMPSON(1979) represent the optic flow equation in a polar coordinate system and determine the representative flow vector in a clustering scheme. THOMPSON and BARNARD(1981) derive a number of optic flow equations from the moving

image area and determine the flow vector by solving the equations using the pseudo inverse method. They compare the pseudo inverse method to the clustering method. Further discussion about these two methods is in [DUBOIS et al.(1981), NAGEL(1981a)]. DAVIS et al.(1983) use local optic flow component constancy which follows from the local 2D object motion assumption. From this constraint as well as the optic flow equation, they propagate, using geometry, the optic flow along a line segment with two given flow vectors at both end points.

Since it cannot be said generally which pixels move with the same velocity, HORN and SCHUNK(1981) use the global constraint that the estimated optic flow field should vary smoothly with the image plane coordinates. They combine the smoothness constraint and the motion constraint by a weighted sum of their error measurements and apply a minimization technique to the summed error to derive an iterative formula. The global smoothness constraint, however, causes unrealistic optic flows on stationary image areas or on the background across the occluding boundaries of moving areas.

To cope with this difficulty, YACHIDA(1983) assumes optic flows at prominent feature points like corners such as at the points A, B, ..., G in Fig 2.1 and propagates the flow vectors smoothly along the connecting edge points between

the corners. He computes the smooth flow vectors by the same equations derived by HORN and SCHUNK(1981) and their error measurements for termination of the propagation process. He mentions a difficulty in propagating the optic flow at the intersection (e.g. the point H in Fig 2.1) of an occluding and an occluded boundary. He solves the problem by terminating the propagation process when the error of newly estimated flow vector is equal to or larger than the previously estimated one. In Fig 2.1, the propagation of flow vectors to b direction is terminated by the propagation from d direction at a point between the points H and G.

Some researchers use additional constraints for the optic flow computation, but these are not absolutely necessary. Some researchers [NETRAVALI and ROBBINS(1979,80), PAQUIN and DUBIOS(1983)]. use the motion constraint only, with frame-to-frame prediction, to derive an iterative estimator by minimizing an error arising from the prediction. They simplify the estimator to use the optic flow (displacement vector) for encoding TV signals in real time. Using the optic flow equation as the linear measurement, the displacement vector is estimated as a random process by applying Kalman filter theory [STULLER and KRISHNAMURPHY(1983)].

Instead of imposing constraints on optic flows, we can derive additional constraints by differentiating the linear

model of image and motion. Specifically, we can differentiate the linear model of (2.2) with respect to x, producing

$$0 = \delta x \frac{\partial^2 I}{\partial x^2} + \delta z \frac{\partial^2 I}{\partial x \partial z} + \delta t \frac{\partial^2 I}{\partial x \partial t} \qquad (2.5)$$

Dividing both sides of (2.5) by δt and setting $G=\partial I/\partial x$, we have, for $\delta t \to 0$,

$$u \frac{\partial G}{\partial x} + v \frac{\partial G}{\partial z} + \frac{\partial G}{\partial t} = 0 \qquad (2.6)$$

Thus we derive another constraint (2.6) in the same form as the optic flow equation for the two optic flow components u and v. Although we use the x-directional derivative for G, any directional derivative can be used.

WOHN et al.(1983) use the gradient directional derivative and some other differential image features (e.g. curvature and moment) for G. However, feature estimation requiring high-order spatial derivatives is not reliable since the finite difference operation for the derivatives tends to amplify the noise. Thus, their estimated optic flows are often inaccurate. Such flow vectors are enhanced by a smoothing scheme which they devised with local $2\frac{1}{2}$D rigid motion to smooth those flow vectors which do not cross occluding boundaries.

Let P and Q be two optic flow image points where the optic flow vector is given by v and v', respectively. In the $2\frac{1}{2}$D rigid motion, they can compute the rotational velocity ω_q of a point Q with respect to a point P by

$$\omega_q = \frac{\Delta r \times \Delta v}{||\Delta r||^2} \tag{2.7}$$

and they define the dilation D_q by

$$D_q = \frac{\Delta r \cdot \Delta v}{||\Delta r||^2} \tag{2.8}$$

where

$$\Delta v = v' - v$$

$$\Delta r = \underline{Q} - \underline{P}$$

Thus for each pixel in a neighborhood, they can compute rotational velocity and dilation with respect to its center pixel position. For the center pixel, they average the computed values. To smooth a flow vector at a point P, they choose its neighbor P' which has the minimum variation of computed rotational velocities and dilations in its neighborhood and update the flow vector v_p at P by

$$v = v' - \Delta r \times \omega' \tag{2.9}$$

where ω' is the computed rotational velocity at the point P'. In Fig 2.2, the flow vector at P is recomputed with

respect to P' because the 3x3 neighborhood of P' has minimum variation of rotational velocities and dilations.

Similar multiple constraints are derived by TRETIAK and PASTOR(1984). They derive two independent equations directly from the motion constraint by differentiating the optic flow equation with respect to the image plane coordinates. The same two equations, however, can be derived from the linear model of image and motion.

Recently SCHUNK(1984) proved that the motion constraint is valid at the image points of intensity discontinuities at an occluding boundary and pointed out that rotational motion or perspective projection may cause a change in the brightness pattern of an image sequence due to the forshortening effects.

2.1.2 Nonlinear Model of Image and Motion

The linear model of intensity variation is too simple to represent edges and corners [SNYDER et al.(1980), NAGEL(1983)]. Thus, SNYDER et al. 80 represent (2.1) up to the second order at the time t+δt as

$$I(x+\delta x, z+\delta z, t+\delta t) = I(x,z,t+\delta t) + \delta x \frac{\partial I}{\partial x} + \delta z \frac{\partial I}{\partial z} + \frac{\delta x^2}{2}\frac{\partial^2 I}{\partial x^2} + \frac{\delta x \delta z}{2}\frac{\partial^2 I}{\partial x \partial z} + \frac{\delta z^2}{2}\frac{\partial^2 I}{\partial z^2} \qquad (2.10)$$

where the partial derivatives are computed at the image plane coordinate (x,z) at the time t+δt. Setting I(x+δx,z+δz,t+δt)=I(x,z,t) (brightness constancy after displacement), they derive

$$I(x,z,t) - I(x,z,t+\delta t) = \delta x \frac{\partial I}{\partial x} + \delta z \frac{\partial I}{\partial z} + \frac{\delta x^2}{2} \frac{\partial^2 I}{\partial x^2} + \frac{\delta x \delta z}{2} \frac{\partial^2 I}{\partial x \partial z} + \frac{\delta z^2}{2} \frac{\partial^2 I}{\partial z^2} \qquad (2.11)$$

For each pixel, they derive one quadratic equation (2.11) in the two unknown displacement vector components δx and δz. Thus, with the assumption of displacement vector constancy over a moving image area (i.e. I(x,z,t)=I(x,z,t+δt)), they can determine the displacement vector using clustering.

NAGEL(1983) fits the image model of (2.10) over a local neighborhood such that the partial derivatives are substituted for the fitting coefficients minimizing the sum of weighted squared differences between the measurement and the image model. Using the determined fitting coefficients and the proper transformation of the local coordinate system, he derives two coupled nonlinear equations for the two displacement vector components from (2.11) by minimizing the sum of the squared differences between the measurement and the approximating equation.

For the corner points defined by DRESCHLER and NAGEL(1982) or KITCHEN and ROSENFELD(1980), which are shown to be equivalent in [NAGEL(1983)], the two nonlinear equations can be further simplified into closed forms. This method is implemented and applied to a TV frame sequence and the results, which show sparse displacement vectors computed, are reported in [NAGEL and ENKELMANN(1982)]. To overcome the sparseness, NAGEL(1983) combines the above minimization problem with a global constraint called the 'oriented smoothness' constraint to estimate displacements for image area with minor intensity variation. This constraint imposes smooth variation of displacements only in the direction perpendicular to the gradient direction, allowing significant displacement change in other directions. Since the intensity gradient direction usually occurs across an occluding boundary, the above constraint allows significant displacement change across such a boundary. NAGEL and ENKELMANN(1984) implement the scheme and report preliminary results.

A higher order Taylor expansion than those in (2.1) has been used for the optic flow computation by HARALICK and LEE(1983). They fit a polynomial function to intensities in a local 3D neighborhood consisting of two image coordinates and one coordinate for time. They determine optic flow from the fit by locating the point which matches up with the relative origin. The details are described in chapter III.

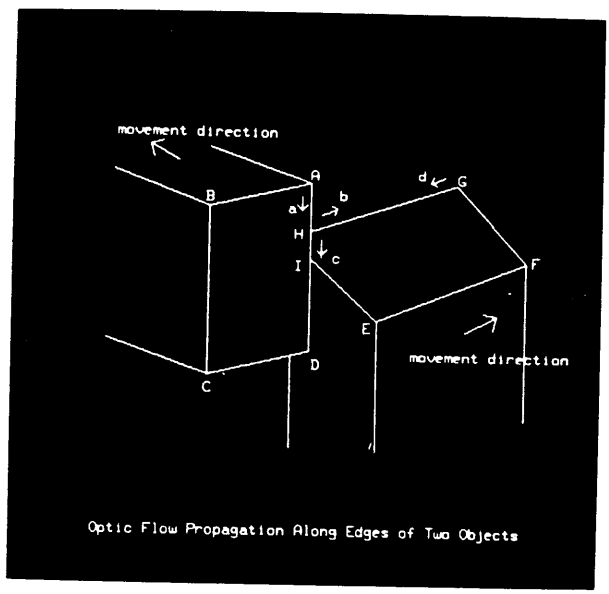

Fig 2.1 Propagation of Optic Flow Vectors

along the edges

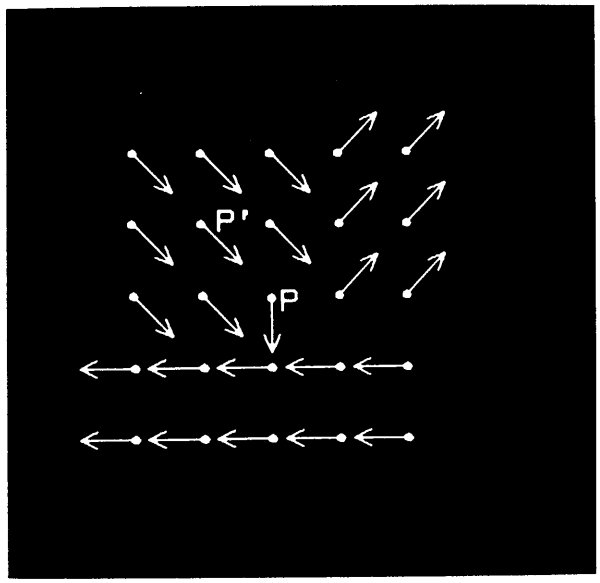

Fig 2.2 Updating Optic Flow Vector at P
with respect to Optic Flow vector at P'

2.2. From Optic Flow to 3D Motion and Depth

Early systems of moving image analysis concentrated on the extraction of 2D motion information from an image sequence. LEESE et al.(1970) and ENDLICH et al.(1971) use a matching scheme to automatically determine the cloud movement on the image plane from satellite images of clouds. AGGARWAL and DUDA(1975) analyze moving polygonal images to determine motion of polygons and to segment the images. With the help of a moving object model, CHOW and AGGARWAL(1977) analyze planar curvilinear motion. POTTER(1975) uses the 2D motion information from the 'cross-shaped' template for image segmentation.

From the psychophysical and biological study of a vision system perceiving three dimensional objects, researchers began to concentrate on the 3D scene analysis containing moving objects. Some researchers identify moving elements(tokens) from changing brightness pattern to get motion and structural information of a moving object. From the brightness difference of two image frames, LILLESTRAND(1972), ULSTAD(1973), LIMB and MURPHY(1975) obtain motion information and JAIN et. al.(1977,79), JAIN and NAGEL(1979ab), JAIN(1981), YALAMANCHILI et al.(1982) extract structural information of moving objects as well as their motion information. This differencing technique is

further developed for image segmentation and motion information extraction [JAIN et al.(1979), JAIN and NAGEL(1979a,b), JAIN(1981), YALAMANCHILI et al.(1982)]. This differencing technique is referred to as a peripheral process in the survey by Martin and AGGARWAL(1978) where the motion understanding is described on three levels, peripheral, attentive, and cognitive.

Moving object boundaries can be extracted directly from an image time sequence. HAYNES and JAIN(1983) define the time-varying 'edginess' as the product of the temporal brightness change and the static 'edginess' of the Sobel edge detector. They detect the moving object boundaries by thresholding the time-varying 'edginess'. SHAH and JAIN (1984) detect the time-varying corners in a similar way.

THOMPSON(1980) segments images containing multiple moving objects based on both the motion and the brightness. He assumes brightness motion constancy at image points from the same object and uses the motion constraint described in the previous section for the Hough transform to determine dominant motions. He segments images by merging regions having the same motion and similar brightness. Motion constancy is not realistic in general, especially when the motion involves some rotation.

In a restricted scene domain consisting of only vertical and horizontal surfaces, WILLIAMS(1980) searches over distances from the camera to the vertical surfaces and heights of horizontal surfaces which result in the best image model of one frame from the other.

Another approach which GIBSON(1950abc) pioneered derives 3D motion and structure information from the optic flow field obtained. GORDON(1965) shows an optic flow field of the ground plane observed by a moving observer and discusses the motion and depth perception from the optic flow field.

Optic flow field from a pure translational motion contains information about moving object surface structure as well as 3D motion. NAKAYAMA and LOOMIS(1974) show that relative depth can be determined from optic flow of an observer in translational motion. CLOCKSIN(1980) derives a mathematical formula for the surface orientation and the edge discrimination from optic flows generated by a pure translational motion. RIEGER and LAWTON(1983) employ an optimization procedure on thresholded difference vectors at discontinuities of the optic flow field to determine the instantaneous axis of translational motion.

Many researchers study optic flow field from general motion. KOENDERINK and VAN DOORN(1976) discuss the surface structure from a differential geometric analysis of optic flow field. PRAZDNY(1980,81) studies the curvilinear motion

of an observer and computes the egomotion parameters from at least five optic flow points. The computation involves solving a system of nonlinear (third order polynomial) equations for the rotational components. He also computes the depth map from the motion parameters determined. LONGUET-HIGGINS and PRAZDNY(1980) assume the first and second order spatial derivatives of the optic flow field are observable and compute the surface orientation and relative motion at each retinal point. They also show that the dilation, shear, and vorticity components of the first derivative can be used for the above 3D information.

BRUSS and HORN(1983) measure the discrepancy between the observed optic flow and the one expected by the computed motion parameters and use a least square technique to determine the motion parameters minimizing the discrepancy. In the case of pure translational and rotational motion, they derive equations in closed form for the motion parameters from the use of a proper error norm. For the general motion, they come up with a nonlinear system for the motion parameters. In chapter IV, we also use a least square technique to determine both the motion parameters and relative depth.

Given depth and optic flow at a point, BALLARD and KIMBALL(1983) compute 3D optic flow at the point and use it for the determination of motion parameters in decomposed

parameter spaces. They assume a small external force on moving objects and compute the acceleration from 3D flows. In chapter IV, we derive the temporal change of the optic flow field with no external force and determine motion and depth information.

2.3 Determining Corresponding Points

Optic flow can be computed without difficulty from the corresponding points in successive image frames. However, establishing the correspondence is generally recognized as a quite difficult task from the consideration of various factors [AGGARWAL et al.(1981)]. Marr and co-workers [GRIMSON and MARR(1979), MARR and HILDRETH(1980), MARR and POGGIO(1979)] study the correspondence problem in human stereo vision and develop a computational theory of human vision. ESKENAZI and CUNNINGHAM(1978) and MORAVEC(1979ab) derive a set of corresponding points from two cameras in a stereo arrangement. However, stereo vision requires extremely high resolution of the cameras to get an acceptable 3D description. AGGARWAL et al.(1981) consider two general approaches to the correspondence problem in their review; one based on iconic or picture-like models of an image pattern and the other based on the structure (identifiable tokens) present in the image pattern. In the

next subsection, we will discuss matching techniques using a template or an iconic model followed by token matching techniques.

2.3.1 Template Matching

The first approach usually takes a subimage (a template) containing a moving object from one frame and then matches it against the subsequent frame based on the chosen iconic representation. The iconic representation can be a portion of the image itself, a segmented binary image, or the edge image. Similarity (Dissimiliarity) is measured at each possible match and the match having the maximum (minimum) cross-correlation (absolute difference sum) is considered to be the best match. An equivalent process can be carried out through the use of the Fourier Transform of the iconic representation [LEESE et al.(1970)].

This search process usually requires much computation. To speed up the search process, several schemes have been introduced. BARNEA and SILVERMAN(1972) introduce a class of fast algorithms for image registration which speed up the search by essentially doing no calculation for similarity measure on positions when errors exceed the best match so far. VANDERBURG and ROSENFELD(1977) employ a two-stage template matching scheme in which, at first, a subtemplate is selected and used to determine positions which result in

a (dis)similarity measure above (below) a specified threshold. Next, the remainder of the template is evaluated at those chosen positions for the best match. Two difficulties in the two-stage matching scheme are in selecting the subtemplate and determining a proper threshold value of (dis)similarity measure. HALL et al.(1980) discuss the selection of the best subset for matching purposes in the sense of the minimum correlation length. GOSHTASBY et al.(1984) analytically derive the threshold value from the template size and false dismissal probability. Another scheme for the fast search is the coarse-fine matching scheme [GOSHTASBY et al.(1984)] which uses a similar strategy.

To establish point correspondence in multiple views at the specified positions, TSAI(1983) presents two methods called the joint moment method and the window variance method which result in a sharper similarity measure than the usual two frame cross-correlation. These methods, however, usually require more computation.

The techniques described up to now work only for image translation. Motion which produce a scaling or rotation of images can introduce much more computation [ALTMANN and REITBOCK(1984)].

2.3.2 Token Matching

Instead of matching picture-like models, one can identify a set of structures in one image frame and then search the corresponding structures in the subsequent image frame. Several researchers consider the object boundary structure for the match. POTTER(1975) generates a 'cross-shaped template' at a point by calculating the distance from the point to the closest object boundary in the row and column directions, and searches the corresponding point, in the next frame, at which the same size of the template is computed. MARTIN and AGGARWAL(1978) segment boundaries detected from both image frames into primitives such as straight lines and circular arcs and match a primitive of one frame against those of the other frame based on the length and curvature of the primitives. Using the generalized Hough Transform of an object boundary in one image frame, one can find the instance of that boundary in the subsequent frame [BALLARD(1981)].

Locating distinctive features present in images and imposing constraints on them, one can establish the correspondence of the feature points. ENDLICH et al.(1971) locate the brightness center by an ISODATA technique in successive image frames and establish the correspondence between sets of the brightnesss centers by assuming constant brightness motion. RENEDE and ROSENFELD(1980) apply a relaxation algorithm to establish the correspondence between sets of points selected by hand from two image frames with

the assumption of the global brightness displacement constancy. BARNARD and THOMPSON(1980) locate the feature points in an image pair by applying the Moravec interest operator [MORAVEC(1977)] and assign an initial match probability to each pair of feature points which lie within some specified distance of each other allowing for the possibility that the feature may not exist in the second image. They refine the probability for each pairing at a feature point iteratively by applying a relaxation algorithm such that the probability for a pairing is updated by the supporting evidence of similar pairings in the local neighborhood. DRESCHLER and NAGEL(1982) make some modifications in updating the probability by considering both evidence of the support and contradiction in the local neighborhood. At each point, the pairing assigned the highest probability is selected for the correspondence.

ULLMAN(1979) introduces a simple cost function to compare possible matches between two dot patterns and establishes the correspondence by minimizing the cost function. He shows that minimizing the cost function is optimal if the dots in the pattern move independently. PRAGER and ARBIB(1983) assume several feature types on dot patterns and they use a feature metric between feature types to define a distance between any two position-feature pairs. Using this distance, they define an attraction function for a nearest neighbor. With the help of the attraction function and with

the assumption of local consistency of displacement, they can establish the correspondence.

Some other structures present in images can be used. AYALA et al.(1982) segment image frames and establish correspondence between sets of segments based on the similarity of the segment feature values. They use features such as segment position, size, intensity, and area ratio. Since incorrect image segmentation from noise and occlusion introduces incorrect feature values, ROACH and AGGARWAL(1979) suggest using multiple methods arranged in a hierarchy. JACOBUS et al.(1980) encode boundary, region, and surface information in a graph form using a primitive called the half chunk and use a graph matching scheme to establish the correspondence.

The problem with most of these techniques is that they must employ some combinatorial computation to establish the match. This kind of computation is very expensive. Furthermore, these techniques require preprocessors to extract proper structures from image frames.

2.4 From Corresponding Points to 3D Motion and Depth

To determine 3D motion and structure of moving objects, a set of corresponding points can be used. ROACH and AGGARWAL(1980) require two known perspective views of five non-coplanar points in space to set up the problem and come up with 18 nonlinear equations in 18 unknowns. They solve the system of nonlinear equations iteratively with an initial guess for each unknown by using a modified finite difference Lavenberg-Marquetdt algorithm [BROWN and DENNIS(1972), LAVENBERG(1944)]. From experiments with noisy views of 3D points, they find that they obtain more accurate results with considerable overdetermination (two views of 12 or 15 points, three views of 7 or 8 points).

When the surface structure of a moving object is known, the motion estimation problem can be formulated differently. For a known planar surface, TSAI and HUANG(1981) define eight pure parameters which characterize the planar surface and can be uniquely determined by a linear method given two perspective views of four or more points. They derive a sixth order polynomial of one variable whose coefficients are expressed by the pure parameters and determine the motion parameters by solving the polynomial. Instead of solving the sixth order polynomial, the motion parameters can be determined by computing the singular value decomposition of a 3x3 matrix containing the pure parameters

TSAI et al.(1982). For a known curved surface, TSAI and HUANG(1984) show that two perspective views of seven points on the curved surface are sufficient to determine the 3D motion parameters. YEN and HUANG(1983) project image points centrally on the unit sphere at the origin and use the projected points in correspondence to determine the 3D motion parameters and their 3D positions. They analyze three types of motions; pure translation, pure rotation, and general motion, and interpret the uniqueness of the motion solution by a simple geometry of the points on the sphere. Unfortunately, we can not find any experimental results, especially of noisy views, in their paper.

NAGEL(1981b) uses two coordinate systems; one attached to the camera and the other to a moving object. He derives a relationship between known image point coordinates and unknown object point coordinates and sets up a minimization problem from the relationship and sets of image points in correspondence. DRESCHLER and NAGEL(1982) and NAGEL(1983) apply this technique to a sequence of feature (corner point) images obtained from a street scene containing a moving taxicab and approximate the cab by a polyhedra. See the estimated 3D motion of the taxicab from the iterative motion estimation technique in chapter IV for further discussion of this approach.

MARTIN and AGGARWAL(1983) assume orthographic projection

of images and develop a scheme describing a 3D object from multiple views of its occluding object boundary. They obtain the object boundaries from the thresholded brightness image. Their 3D description is a bounding volume approximation (to the actual object) represented by a volume segment data structure. AGGARWAL(1983) reviews techniques of deriving 3D descriptions from image sequences.

Chapter III

FACET MODEL OPTIC FLOW

Determination of the optic flow field is usually done by matching corresponding points on successive image frames. This kind of technique suffers from a potentially expensive combinatorial problem. In this chapter we discuss a facet model technique to the problem of estimating a subset of the optic flow field. We show how the first order derivative optic flow equation represents the intersection line of the isocontour plane with a successive image frame. To select a unique match point on this line we require that the gray tone intensities match. We show that this procedure amounts to requiring that gray tone intensities match, and first order partials in row, column, and time match. The complexity of the technique is linear in the number of pixels on the image. In section 3.1, we discuss the facet model technique for the optic flow computation, in section 3.2 we review discrete orthogonal polynomials for the facet model, and in section 3.3 we show how the facet model optic flow images compare with the Horn and Schunk optic flow images.

3.1 Optic Flow Computation

In this section we discuss the calculation of optic flow from a time sequence of image frames and illustrate the facet approach to the optic flow computation.

Consider the case of a one dimensional sequence of frames as shown in Fig 3.1. These frames are obviously translates of one another with a uniform motion. Instead of considering a correlation search to match each point on one frame with its corresponding place on the next frame, consider the sequence of frames as an image each of whose rows correspond to one frame. Corresponding points on different frames have the same intensity. Thus where the one-dimensional frames are organized as an image, the corresponding points will be on equal intensity contour lines as shown on Fig 3.2. The equal intensity contour line any point is on is easily computed as the line orthogonal to the gradient direction at that point. Thus by fitting a function to the image intensities in a local neighborhood about a point, as the facet model prescribes, and determining the gradient direction from the fit, the equal intensity contour line through the point can be determined. The match point on the next frame can be obtained without any search just as the intersection of the equal intensity contour line passing through the point with the next frame or row.

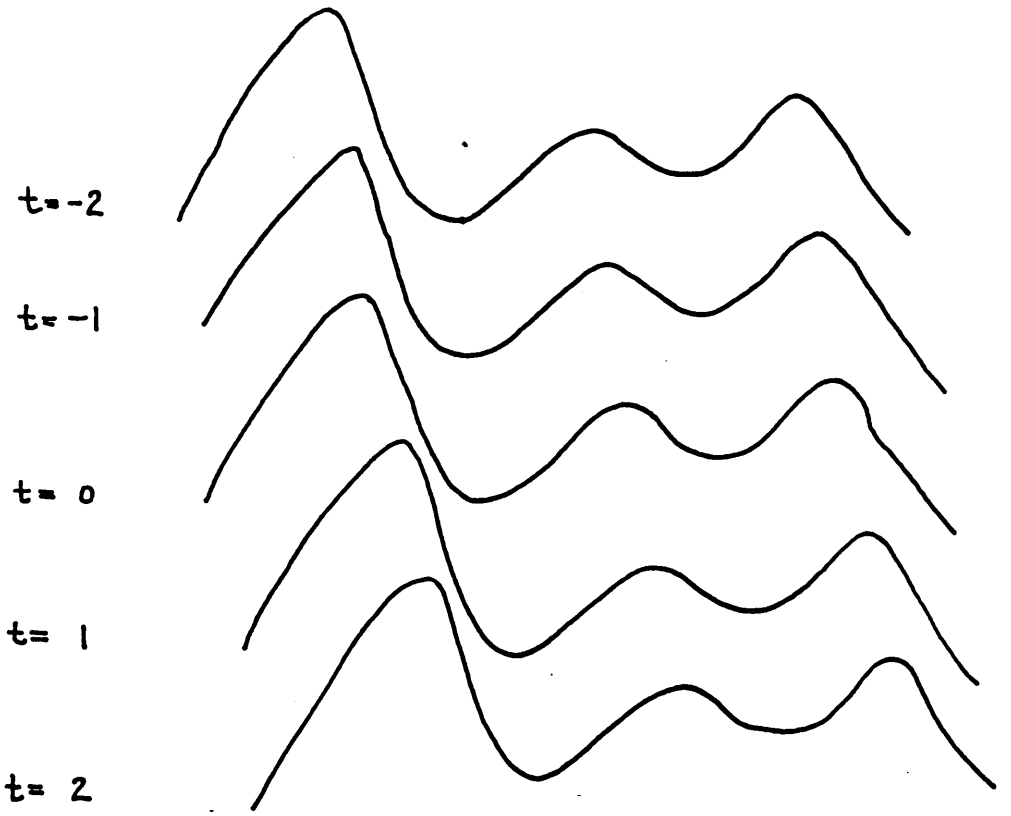

Fig 3.1. Illustrates a one-dimensional waveform which is translating in time.

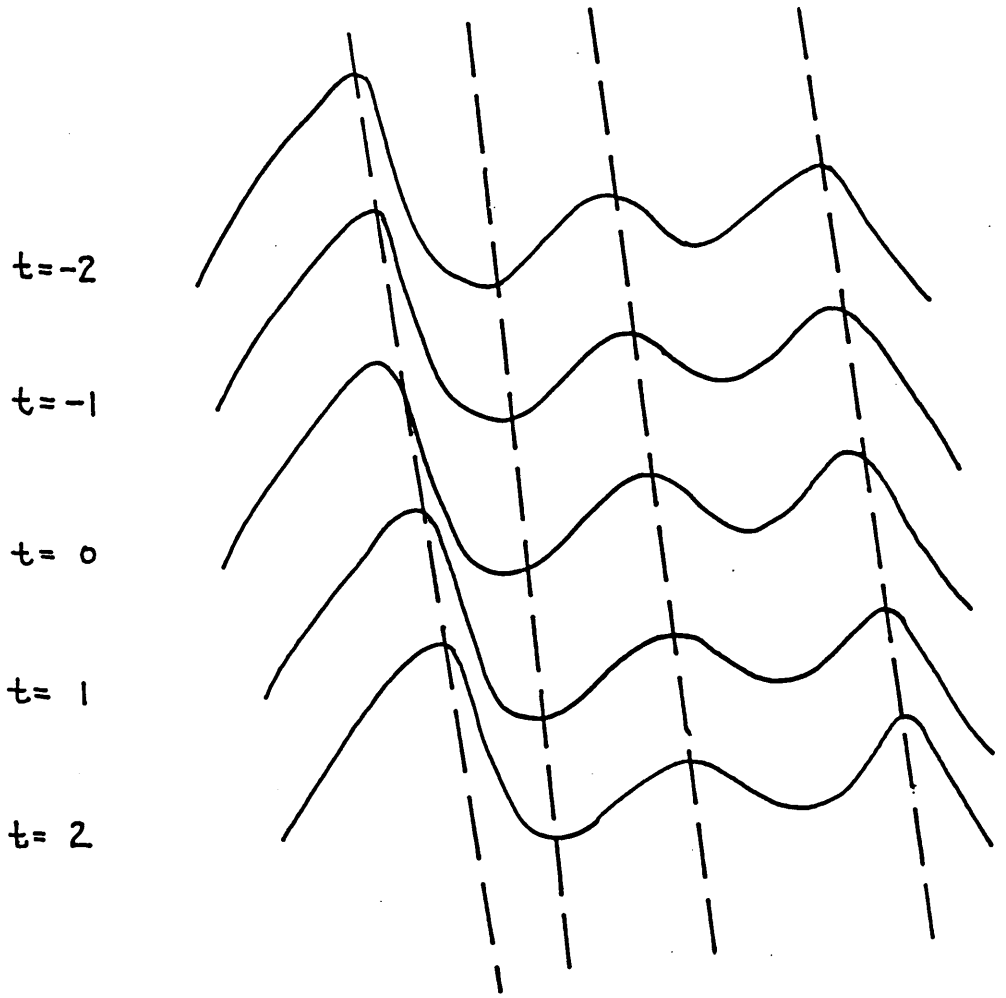

Fig 3.2. Shows the equal intensity contour lines which match corresponding points.

In a time-varying image sequence, the situation is similar, only the geometry is in a one dimensional higher space, a 4-dimensional space. To understand this geometry fix attention on one pixel on one frame. Use the 3D neighborhood (by row, by column, by image frame number) around the pixel and fit a function to the gray tone intensities in the 3D neighborhood. From the function fit determine the gradient vector at the given pixel position. The plane which is normal to the gradient vector is the equal intensity contour plane passing through the given pixel. To determine possible match points on the next frame intersect the equal intensity contour plane with the next image frame. As shown in Fig 3.3, the intersection is a line. The match point can be any place on this line. To determine it uniquely, find that position on the line whose gray tone intensity is equal to the grey tone intensity of the given pixel.

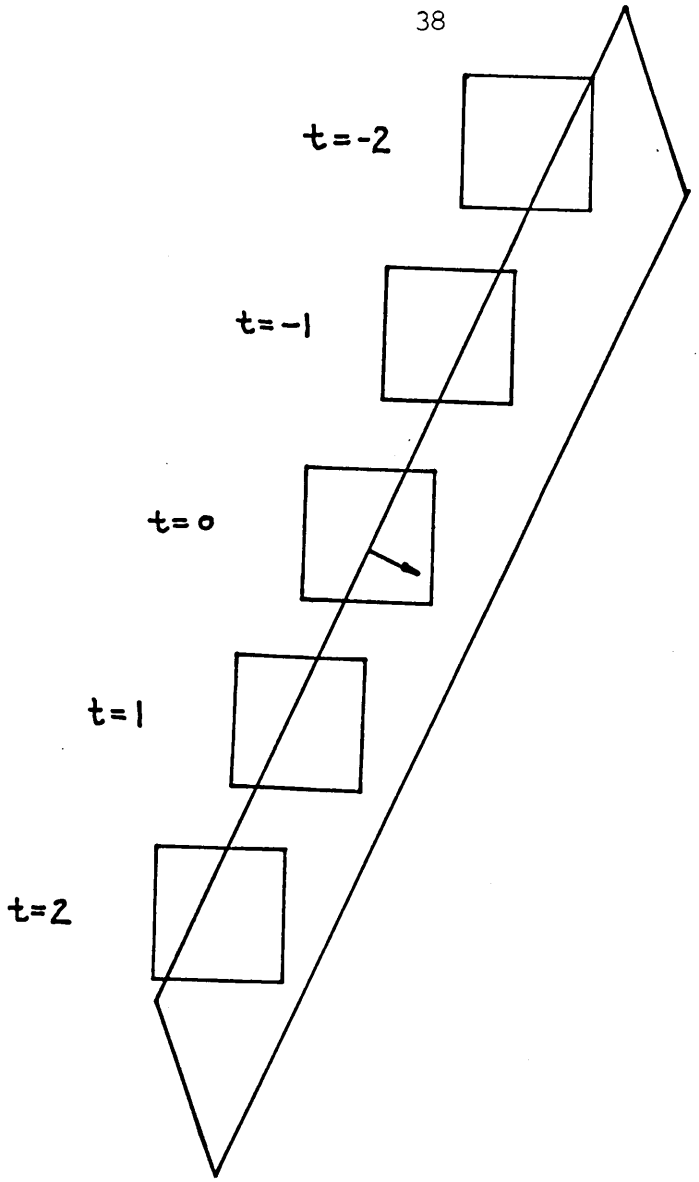

Fig 3.3. Shows a sequence of five frames, the gradient vector on frame t=0, and the plane orthogonal to the gradient vector and passing through the origin. The shaded area represents portions of frames to the left of the cutting plane. The lines on frames t=-1, t=0, and t=1 represent the intersection of the cutting plane with these frames.

3.1.1 Example

Consider a local 2D neighborhood whose gray tone intensity function appears like a paraboloid of the form $(r+1)^2 + (c+2)^2$. Suppose that image frames are taken each second and that due to the camera motion the paraboloid translates each successive frame by three rows and one column. Then upon fitting the gray tone intensities in a local 3D neighborhood whose center pixel has coordinates (0,0,0) in a relative coordinate frame we determine the function

$$f(r,c,t) = (r-3t+1)^2 + (c+t+2)^2$$

Thus the paraboloid is translating by (3 rows,-1 column) on successive frames.

The partial derivatives of f are

$$\frac{\partial f}{\partial r} = 2(r-3t+1)$$

$$\frac{\partial f}{\partial c} = 2(c+t+2)$$

$$\frac{\partial f}{\partial t} = 2(r-2t+1)(-3) + 2(c+t+2)$$

Evaluating these partials at (0,0,0) yields the gradient vector at the given pixel which is located at the origin of

the relative coordinate frame,

$$\text{grad } f = \begin{bmatrix} 2 \\ 4 \\ -2 \end{bmatrix}$$

The plane passing through (0,0,0) and orthogonal to this gradient vector is given by

$$2r + 4c - 2t = 0$$

Intersecting this plane with the next frame (t=1) produces the line

$$2r + 4c - 2 = 0$$

The gray tone intensity at (0,0,0) is given by $f(0,0,0) = 5$. To find the match point, find that (r,c) simultaneously satisfying the two equations

$$r + 2c - 1 = 0$$

$$f(r,c,1) = (r-2)^2 + (c+3)^2 = f(0,0,0) = 5$$

Substituting $r = 1 - 2c$ into $(r-2)^2 + (c+3)^2 = 5$ yields the quadratic equation $(c+1)^2 = 0$ from which $c = -1$ and $r = 3$, the correct translation parameters.

3.1.2 Translational Motion

As the example suggests, the difficulty of the

computation might be in determining a real root of a polynomial. It is natural to wonder, therefore, whether it is possible to have polynomials with no real roots. We demonstrate here that for the case of translational motion, there is no possibility of the polynomial roots being only complex. To see this express the local fitted functions $f(r,c,t)$ as

$$f(r,c,t) = g(r-\alpha t,\ c-\beta t) \tag{3.1}$$

explicitly indicating that the dependence between r, c, and and t is constrained to be translational.

The equation of the isodensity contour plane passing through (0,0) is given by

$$(r-\alpha t)\ g_r + (c-\beta t)\ g_c = 0 \tag{3.2}$$

where $g_r = \dfrac{\partial g}{\partial r}(0,0)$

$g_c = \dfrac{\partial g}{\partial c}(0,0)$

At $t = t_0$ this plane cuts the $t = t_0$ frame producing the line

$$(r-\alpha t_0)\ g_r + (c-\beta t_0)\ g_c = 0$$

At the desired point (r,c) on this line we must satisfy the match condition

$$g(r-\alpha t_0,\ c-\beta t_0) = g(0,0)$$

Assuming g is a function for which all partial derivatives exist we may represent $g(r-\alpha t,\ c-\beta t)$ by its Taylor series around (0,0)

$$g(r-\alpha t, c-\beta t) = g(0,0) + (r-\alpha t_0)\, g_r + (c-\beta t_0) g_c$$

$$+ \frac{(r-\alpha t_0)^2}{2} g_{rr} + (r-\alpha t_0)(c-\beta t_0) g_{rc} + \frac{(c-\beta t_0)^2}{2} g_{cc}$$

$$+ \ldots +$$

Substituting $g(r-\alpha t,\ c-\beta t)$ for g(0,0) and substituting $-(c-\beta t_0) g_c / g_r$ for $r-\alpha t_0$ yields

$$(c-\beta t_0)^2 \left[\frac{g_c^2}{g_r^2} \frac{g_{rr}}{2} - \frac{g_c g_{rc}}{g_r} + \frac{g_{cc}}{2} \right] + (c-\beta t_0)^3 [\ldots] + \ldots + = 0 \qquad (3.3)$$

Factoring out a $(c-\beta t_0)^2$ from the left hand side and noting that the right hand side is zero permits us to write $(c-\beta t_0)^2 = 0$ from which we can solve for the double real root $c = \beta t_0$

3.1.3 Comparison

There is a relationship between the facet point of view and the usual optic flow equation. Letting f_r, f_c, and f_t

designate the partial derivatives of f with respect to r, c, and t, evaluated at the origin, the equation of the isocontour plane is given by

$$rf_r + cf_c + tf_t = 0 \tag{3.4}$$

Intersecting this plane with the next image plane which is taken at t_0 seconds latter produces the line

$$-f_t = \frac{r}{t_0} f_r + \frac{c}{t_0} f_c \tag{3.5}$$

Equation (3.5) is the usual optic flow equation [Horn and Schunk 81]. The quantity r/t_0 represents a movement of r rows over t_0 seconds and is therefore the row velocity. Likewise c/t_0 represents the column velocity.

The difference in what we have done is that we have given equation (3.5) an enlarged meaning. It is the equation of a line containing the possible match points on the t_0 image frame. But since the match point must have the same brightness, we use the additional constraint that the match point (r,c) must satisfy the equal brightness constraint:

$$f(r,c,t_0) = f(0,0,0) \tag{3.6}$$

This brightness constraint is used in the usual derivation of the optic flow equation so it would seem to be superfluous to use again. From our perspective we see that the isodensity contour plane is really only isodensity at

the origin and as it moves away from the origin, it must be regarded as an approximation. Thus the intersection line on the successive frame is not guaranteed to have all its points be of the same brightness as the given pixel. In the ideal case, the match condition just tells us to select that point on the line having the same brightness as the given pixel. In a non-ideal case, we can select that point on the match line which is closest to the brightness of the given pixel.

3.1.4 Why It Works

In this section we give a detailed explanation of why the procedure works. We assume that all derivatives of third or higher order are negligible and that the match conditions consist of matching gray tone intensity and gray tone first partials in row, columns, and time.

Let f with a subscript designate the corresponding partial derivative of f evaluated at r = c = t = 0. A Taylor series of f about (0,0,0) neglecting third or higher order terms is given by

$$f(r,c,t) = f(0,0,0) + \Delta r f_r + \Delta c f_c + \Delta t f_t + \frac{\Delta r^2}{2} f_{rr} + r c f_{rc} + \frac{\Delta c^2}{2} f_{cc} + r t f_{rt} + c t f_{ct} + \frac{\Delta t^2}{2} f_{tt} \qquad (3.7)$$

At $(\Delta r, \Delta c)$ having relative neighborhood coordinates on relative time image Δt matches pixel (0,0) on time image 0 if

$$(1)\quad f(\Delta r, \Delta c, \Delta t) = f(0,0,0)$$

$$(2)\quad \frac{\partial f}{\partial r}(\Delta r, \Delta c, \Delta t) = \frac{\partial f}{\partial r}(0,0,0) = f_r$$

$$(3)\quad \frac{\partial f}{\partial c}(\Delta r, \Delta c, \Delta t) = \frac{\partial f}{\partial c}(0,0,0) = f_c$$

$$(4)\quad \frac{\partial f}{\partial t}(\Delta r, \Delta c, \Delta t) = \frac{\partial f}{\partial t}(0,0,0) = f_t$$

Condition (1) states that the gray tone intensities must match. Condition (2) and (3) states that the gray tone spatial pattern around the original and the match pixel must match. Condition (4) states that since the motion is uniform with no acceleration the gray tone time derivatives must match. Applying these constraints to the Taylor series we have, respectively,

$$\Delta r f_r + \Delta c f_c + \Delta t f_t + \frac{\Delta r^2}{2} f_{rr} + \Delta r \Delta c f_{rc} + \frac{\Delta c^2}{2} f_{cc} + \Delta r \Delta t f_{rt} + \Delta c \Delta t f_{ct} + \frac{\Delta t^2}{2} f_{tt} = 0 \qquad (3.8)$$

$$\Delta r f_{rr} + \Delta c f_{rc} + \Delta t f_{rt} = 0 \qquad (3.9)$$

$$\Delta r f_{rc} + \Delta c f_{cc} + \Delta t f_{ct} = 0 \qquad (3.10)$$

$$\Delta r f_{rt} + \Delta c f_{ct} + \Delta t f_{tt} = 0 \qquad (3.11)$$

Multiplying equation (3.9) by r, equation (3.10) by c, equation (3.11) by t and adding yields

$$\Delta r^2 f_{rr}+2\Delta r\Delta c f_{rc}+\Delta c^2 f_{cc}+2\Delta r\Delta t f_{rt}+2\Delta c\Delta t f_{ct}+\Delta t^2 f_{tt}=0 \qquad (3.12)$$

Substituting this back into equation (3.8) yields

$$\Delta r f_r + \Delta c f_c + \Delta t f_t = 0 \qquad (3.13)$$

the usual optic flow equation! Thus, the technique of using equation (3.13) and the grey tone intensity match condition (3.8) in essence works because it assumes that all first partials are matching. However, now we see that there need not be any problem of root finding. We just need to solve the overconstrained system of equations

$$\begin{bmatrix} f_r & f_c \\ f_{rr} & f_{rc} \\ f_{rc} & f_{cc} \\ f_{rt} & f_{ct} \end{bmatrix} \begin{bmatrix} \Delta r \\ \Delta c \end{bmatrix} = -\Delta t \begin{bmatrix} f_t \\ f_{rt} \\ f_{ct} \\ f_{tt} \end{bmatrix} \qquad (3.14)$$

for the row column position $(\Delta r, \Delta c)$ on the specified image Δt.

3.2 Discrete Orthogonal Polynomials for Facet Model

The facet technique described in the last section requires estimating underlying functions over grey tone intensities in each 3D neighborhood (by row, by column, and by image frame number) to compute optic flow. The underlying

functions from which the optic flow vectors are computed are easy to represent as linear combinations of the polynomials in any polynomial basis set. That polynomial basis set which permits the independent estimation of each coefficient would be the easiest to use. Such a polynomial basis set is the discrete orthogonal polynomial basis set.

In this section, we briefly describe a technique, which was introduced already in the literature [Forsythe(1957), Haralick(1984)], for constructing a discrete orthogonal polynomial basis set and we show how the basis set is used to determine underlying functions over grey tone intensities of image sequence.

3.2.1 Construction of Discrete Orthogonal Polynomial Basis

Fitting grey tone intensities in a 3D neighborhood requires three dimensional discrete orthogonal polynomials which can be constructed by taking the tensor products of one dimensional discrete orthogonal polynomials. Here, we show how the one dimensional discrete orthogonal polynomials are constructed and then we construct the three dimensional discrete orthogonal polynomials by the tensor products.

For a symmetric index set R where $i \varepsilon R$ implies $-i \varepsilon R$, we construct the discrete orthogonal polynomial $P_n(r)$, for n^{th} order iteratively where is defined $P_0(r) = 1$ for $r \varepsilon R$.

Let $P_0(r),\ldots,P_{n-1}(r)$ have been defined and $P_n(r)$ be defined where in general $P_n(r) = r^n + a_{n-1}r^{n-1} + \ldots + a_1 r + a_0$. To define $P_n(r)$ we use the orthogonality of $P_n(r)$ with respect to polynomials $P_0(r)$, $P_1(r),\ldots,$ $P_{n-1}(r)$, therefore

$$\sum_{r\varepsilon R} P_k(r)\,(r^n + a_{n-1}r^{n-1} + \ldots + a_1 r + a_0) = 0 \qquad (3.15)$$

$$\text{for } k = 0, \ldots, n-1.$$

There are n unknowns a_0, $a_1,\ldots,$ a_{n-1} in n equations which can be solved by standard techniques.

Introducing the first five polynomials, we have

$$P_0(r) = 1$$

$$P_1(r) = r$$

$$P_2(r) = r^2 - \mu_2/\mu_0 \qquad (3.16)$$

$$P_3(r) = r^3 - (\mu_4/\mu_2)r$$

$$P_4(r) = \frac{r^4 + (\mu_2\mu_4 - \mu_6)r^2 + (\mu_2\mu_6 - \mu_4^2)}{\mu_0\mu_4 - \mu_2}$$

where $\mu_k = \sum_{s\varepsilon R} s^k$.

The discrete orthogonal polynomials can be generated numerically by the three term recurrence [Forsythe(1957)] instead. Specifically, we can generate the polynomials from

$$
\begin{aligned}
P_0(r) &= 1 \\
P_1(r) &= rP_0(r) - a_1P_0(r) \\
P_2(r) &= rP_1(r) - a_2P_1(r) - b_1P_0(r) \\
&\quad . \qquad\qquad . \\
&\quad . \qquad\qquad . \\
&\quad . \qquad\qquad . \\
P_{i+1}(r) &= rP_i(r) - a_{i+1}P_i(r) - b_iP_{i-1}(r) \quad (i = 1,2,\ldots)
\end{aligned}
\tag{3.17}
$$

where

$$
a_{i+1} = \frac{\sum_{s\varepsilon R} sP_i(s)^2}{\sum_{s\varepsilon R} P_i(s)^2} \quad \text{and} \quad b_i = \frac{\sum_{s\varepsilon R} sP_i(s)P_{i-1}(s)}{\sum_{s\varepsilon R} P_{i-1}(s)^2}
$$

When a symmetric index set $\{-N,\ldots-1,0,1,\ldots N\}$ is chosen in (3.17), $a_1=0$, and thus $P_1(r)=P_1(-r)$ which makes $a_2=0$. Continuing this furhter, we have $a_{i+1}=0$, for i=0,1..., which makes (3.17) the two term recurrence.

Three dimensional discrete orthogonal polynomials can be constructed from three sets of one dimensional discrete orthogonal polynomials by taking tensor products. Let R, C, and T be index sets satisfying the symmetry condition. Let $\{P_0(r),\ldots,P_N(r)\}$, $\{Q_0(r),\ldots,Q_M(r)\}$, and $\{S_0(r),\ldots,S_L(r)\}$ be sets of one dimensional discrete orthogonal polynomials

on the index sets R, C, and T, respectively. Then any subset of the tensor products $\{P_0(r)Q_0(r)S_0(r), \ldots, P_n(r)Q_m(c)S_q(t), \ldots, P_N(r)Q_M(c)S_L(t)\}$ forms a three dimensional discrete orthogonal basis set on RxCxT. This fact can be easily proved. Let $P_i(r)Q_j(c)S_k(t)$ and $P_n(r)Q_m(c)S_q(t)$ be any two distinctive polynomials in a three dimensional basis set. Then the sum of their product over RxCxT is

$$\sum_{(r,c,t)\varepsilon RxCxT} P_i(r)Q_j(c)S_k(t)P_n(r)Q_m(c)S_q(t) \qquad (3.18)$$

$$= \sum_{r\varepsilon R} P_i(r)P_n(r) \sum_{c\varepsilon C} Q_j(c)Q_m(c) \sum_{t\varepsilon T} S_k(t)S_q(t)$$

Because $i\neq n$ or $j\neq m$, or $k\neq 1$ for the two distinct polynomials, at least one sum must be zero.

Let {-2, -1, 0, 1, 2} be the index set of R, C, and T. Then, we have three one dimensional orthogonal basis sets $\{1, r, r^2-2/3, r^3-3.4r\}$, $\{1, c, c^2-2/3, c^3-3.4c\}$, and $\{1, t, t^2-2/3, t^3-3.4t\}$ of degree up to cubic on the index set R, C, and T, respectively. Taking tensor products on the three basis sets, we have three dimensional discrete orthogonal basis set consisting of 64 polynomials of degree up to 9^{th} order. Of these 64 polynomials, $\{1, r, c, t, r^2-2/3, c^2-2/3, t^2-2/3, rc, ct, rt, r^3-3.4r, c^3-3.4c, t^3-3.4t,$

$r^2c-2/3c$, $rc^2-2/3r$, $c^2t-2/3t$, $ct^2-2/3c$, $r^2t-2/3t$, $rt^2-2/3r$, rct} are of degree 3 or less.

3.2.2 Fitting with Discrete Orthogonal Polynomial Basis

Let a three dimensional discrete orthogonal polynomial basis set over an index set RxCxT be $\{P_0(r)Q_0(c)S_0(t),\ldots,P_n(r)Q_m(c)S_1(t),\ldots,P_N(r)Q_M(c)S_L(t)\}$. Let d(r,c,t) represent a data value observed at (r,c,t)εRxCxT. Then the exact fitting problem is to determine the coefficients a_{000}, ..., a_{nm1}, ..., a_{NML} such that

$$d(r,c,t) = \sum_{n=0}^{N} \sum_{m=0}^{M} \sum_{1=0}^{L} a_{nm1}P_n(r)Q_m(c)S_1(t). \qquad (3.19)$$

Determination of coefficients is easy because of the orthogonality property. For a coefficient a_{ijk}, we multiply both sides of the above equation by $P_i(r)Q_j(c)S_k(t)$ and sum over all (r,c,t)εRxCxT. Specifically, we have

$$\sum_{(r,c,t)\varepsilon RxCxT} P_i(r)Q_j(c)S_k(t)d(r,c,t)$$

$$= \sum_{(r,c,t)\varepsilon RxCxT} P_i(r)Q_j(c)S_k(t) \sum_{n=0}^{N} \sum_{m=0}^{M} \sum_{l=0}^{L} a_{nml} P_n(r)Q_m(c)S_l(t)$$

$$= \sum_{n=0}^{N} \sum_{m=0}^{M} \sum_{l=0}^{L} a_{nml} \sum_{(r,c,t)\varepsilon RxCxT} P_n(r)Q_m(c)S_l(t)P_i(r)Q_j(c)S_k(t)$$

$$= a_{ijk} \sum_{(r,c,t)\varepsilon RxCxT} P_i^2(r)Q_j^2(c)S_k^2(t)$$

Let the polynomials be normalized such that the square sum over the index set is unity. Then we have

$$a_{ijk} = \sum_{(r,c,t)\varepsilon RxCxT} P_i(r)Q_j(c)S_k(t)d(r,c,t). \qquad (3.20)$$

The approximate fitting problem is to determine coefficients $a_{000},\ldots,a_{nml},\ldots,a_{NML}$ such that

$$e^2 = \sum_{(r,c,t)\varepsilon RxCxT} [d(r,c,t) - \sum_{n} \sum_{m} \sum_{l} a_{nml} P_n(r)Q_m(c)S_l(t)]^2 \qquad (3.21)$$

is minimized. Because the right side of the above equation is parabola open upward with respect to each coefficient, the value of a coefficient can be determined by taking the partial derivative of the equation with respect to each coefficient and setting the partial to zero. Specifically,

we determine the coefficient using the orthogonality property as follows.

$$\frac{\partial e^2}{\partial a_{ijk}} = 2 \sum_{(r,c,t)\varepsilon RxCxT} P_i(r)Q_j(c)\,S_k(t)\,[d(r,c,t) - \sum_n \sum_m \sum_l a_{nml}P_n(r)Q_m(c)S_l(t)]$$

$$= 2[\sum_{(r,c,t)\varepsilon RxCxT} P_i(r)Q_j(c)S_k(t)d(r,c,t) - a_{ijk} \sum_{(r,c,t)\varepsilon RxCxT} P_i^2(r)Q_j^2(c)S_k^2(t)\,] \qquad (3.22)$$

$$= 0.$$

Hence, for the normalized discrete orthogonal polynomials, we have

$$a_{ijk} = \sum_{(r,c,t)\varepsilon RxCxT} P_i(r)Q_j(c)S_k(t)d(r,c,t). \qquad (3.23)$$

Using the coefficients computed, we can compute the residual fitting error by

$$e^2 = \sum_{(r,c,t)\varepsilon RxCxT} [d(r,c,t) - \sum_n \sum_m \sum_l a_{nml}P_n(r)Q_m(c)S_l(t)]^2$$

$$= \sum_{(r,c,t)\varepsilon RxCxT} d^2(r,c,t) - 2\sum_n \sum_m \sum_l a_{nml} \sum_{(r,c,t)\varepsilon RxCxT} P_n(r)Q_m(c)S_l(t)d(r,c,t)$$

$$+ \sum_n \sum_m \sum_l a^2_{nml} \sum_{(r,c,t)\varepsilon RxCxT} P_n^2(r)Q_m^2(c)S_l^2(t)$$

$$= \sum_{(r,c,t)\varepsilon RxCxT} d^2(r,c,t) - \sum_n \sum_m \sum_l a^2_{nml} \qquad (3.24)$$

Let all the pixels in an image time sequence be referenced to a common 2D grid where a point is specified by the row and column coordinates and let each image in the sequence be specified by time coordinate. Then the observed brightness intensity at the row coordinate r and the column coordinate c on the image at the time coordinate t can be represented by g(r,c,t). Let an odd sized symmetric index set RxCxT be chosen for 3D neighborhood such that each pixel in the neighborhood in a time sequence of image frames is referenced uniquely by the coordinate difference between the center pixel and itself. Then for each pixel at the coordinates (r,c,t), its 3D neighborhood can be expressed by

$$\{ (r+r', c+c', t+t') \mid r'\varepsilon R, c'\varepsilon C, \text{ and } t'\varepsilon T \}$$

Determining a coefficient a_{ijk} for a 3D orthogonal polynomial $P_i(r)Q_j(c)S_k(t)$ for the above neighborhood, we have

$$a_{ijk} = \sum_{(r',c',t')\varepsilon RxCxT} g(r+r',c+c',t+t')P_i(r')Q_j(c')S_k(t') \qquad (3.25)$$

Determination of all coefficients of the polynomials in the basis set need not proceed independently. Some of the partial sums needed for one are useful in another. Some of the previously computed partial sums are useful as well [Lee(1981)]. For example, to determine coefficients a_{ijh} of the polynomial $P_i(r)Q_j(c)S_h(t)$ for i=0,...,N, j=0,...,M, and a fixed h, the partial sums,

$$B(r,c) = \sum_{t'\varepsilon T} g(r,c,t+t')S_h(t')$$

can be used.

In the same way, for the coefficients a_{igh} of the polynomials $P_i(r)Q_g(c)S_h(t)$ for i=0,...,N and fixed g and h, the partial sum

$$A(r) = \sum_{c'\varepsilon C} B(r,c+c')Q_g(c') \qquad (3.26)$$

can be used. Hence the coefficient a_{fgh} for fixed f,g, and h is determined by

$$a_{fgh} = \sum_{r'\varepsilon R} A(r+r')P_f(r'). \qquad (3.27)$$

For the constant polynomial, its convolution complexity can be reduced to 3 operations on the sums

determined already. For example, let $P_f(r) = k$, k is a constant and let the coefficient, a_{fgh}, be computed for the neighborhood whose center is at the coordinate (r-1,c,t) by

$$a'_{fgh} = \sum_{r' \varepsilon R} A(r-1+r')P_f(r') = k \sum_{r' \varepsilon R} A(r-1+r') \qquad (3.28)$$

Then the coefficient a_{fgh} for the neighborhood whose center is at (r,c,t) is determined by

$$a_{fgh} = \{ a'_{fgh} - A(r-1-W) + A(r+W) \} k \qquad (3.29)$$

where $W=|R|/2$.

Specifically, let

$$B_0(r,c) = \sum_{t \varepsilon R} g(r,c,t)$$

$$B_1(r,c) = \sum_{t \varepsilon R} S_1(t)g(r,c,t)$$

$$B_2(r,c) = \sum_{t \varepsilon R} S_2(t)g(r,c,t)$$

$$B_3(r,c) = \sum S_3(t)g(r,c,t)$$

Then the fitting coefficients a_{ijh} can be determined from the convolution path shown in Fig 3.4.

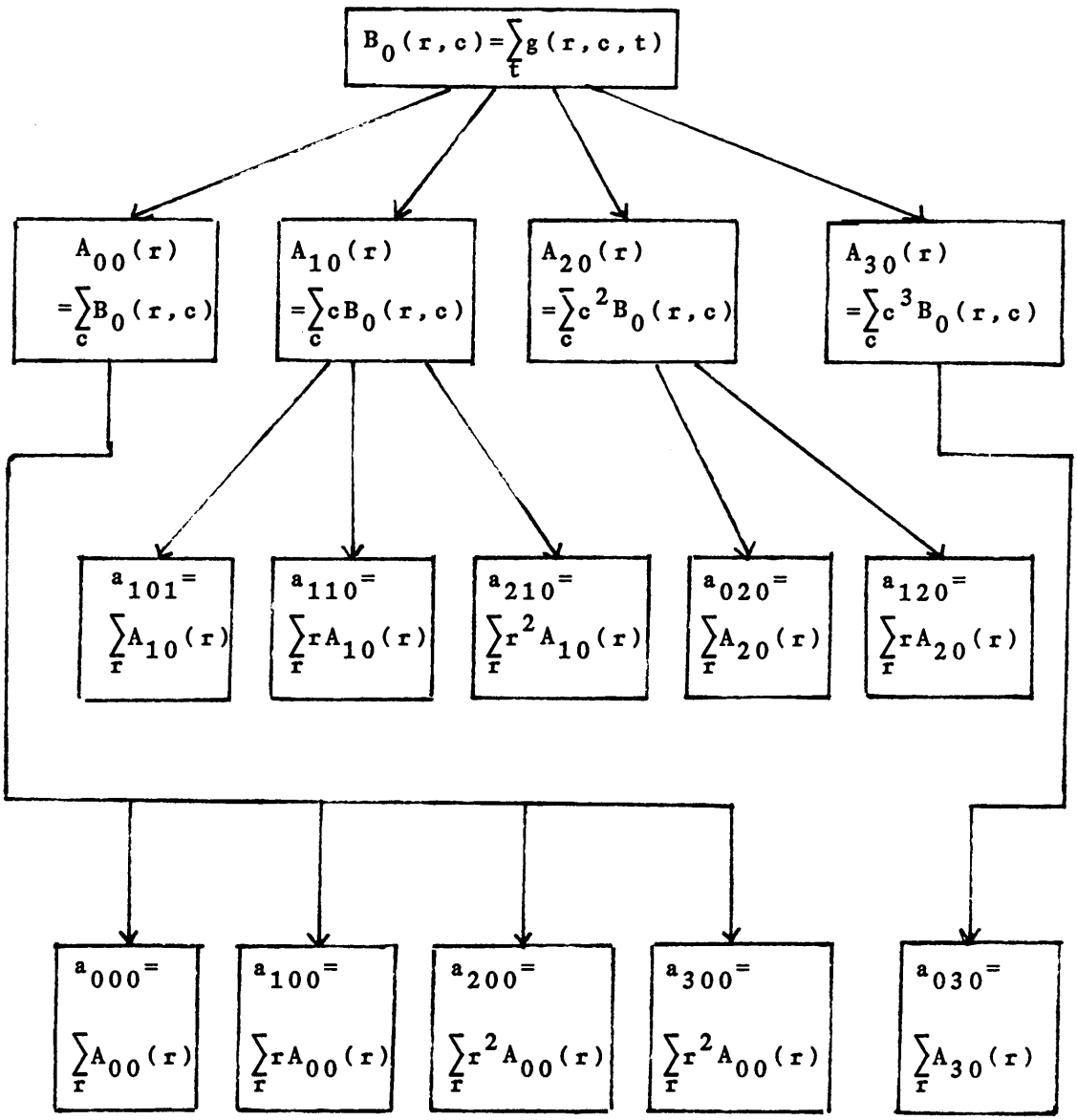

Fig 3.4 Determination of Fitting Coefficients
Over 3D Neighborhood

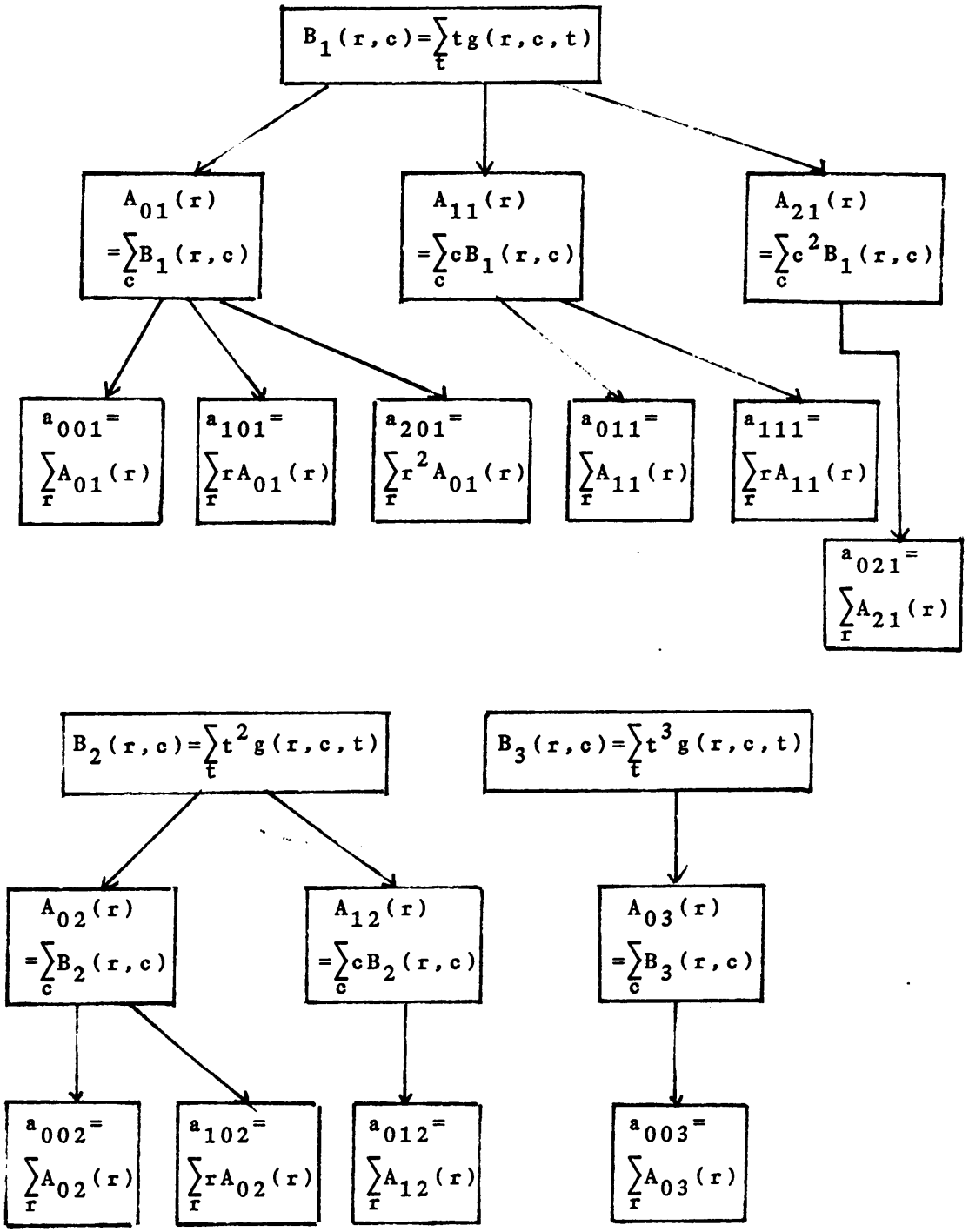

Fig 3.4 Continued

3.3 Computed Optic Flow Images

In this section, we compute optic flow from an underlying function estimated by the technique described in the last section for synthesized image sequences and a real image time sequence, and show the results comparing with the Horn and Schunk's.

To confirm that the facet technique works, we first test the algorithmn on 3 kinds of synthesized image sequences. The image sequences describe the movement of a brightness ellipsoid first in translation in a plane parallel to the image plane, second in contraction of the brightness ellipsoid , and third in rotation about the optic axis. The time interval between two consecutive images in a sequence corresponds to one pixel difference in an image. Next, we apply the facet technique to a real image sequence. The image sequence shows a car turning with unknown velocity at a cross section. In all cases, we compare the facet derived optic flow with the Horn and Schunk optic flow.

To compute an optic flow vector of a pixel on the image at t = 0, we determine the underlying function over its 3D neighborhood using a 3D cubic discrete orthogonal polynomial basis, and, next, derive the 4 constraining equations (3.14) on the row and column components of the optic flow vector at the center of the pixel. To solve the over-constrained equations, we, first, obtain two singular values using the

Singular Value Decomposition routine of the Linpack routines [Dongarra et al. 79], and, next, determine the least square solution from the singular values.

Using a 5x5x5 neighborhood on the time sequence of an ellipsoid moving with the velocity of $x/t = -.8$ and $z/t = -1$, shown in Fig 3.5, we obtain the optic flow image shown in Fig 3.6. At the pixels on or near the boundary of the ellipsoid, the optic flow vector does not show the correct movement of the ellipsoid because these neighborhoods contain a mixture of stationary background and moving ellipsoid, thereby providing inconsistent information for fitting. The reason for the inconsistency is that the center pixel may be in the stationary background but it has neighbors which are not. These neighbors generate an estimated surface which has some curvature for the center pixel.

To reject an optic flow vector obtained from such a neighborhood, we compute the ratio of the smaller to the larger of the two principal curvatures from the underlying gray tone intensity surface determined at $t = 0$. From the histogram of this curvature ratio over all the neighborhoods in the image sequence, shown in Fig 3.7, we notice a dominant peak at about .025 which corresponds to the majority of pixels having correct optic flow directions. Thus, we can determine a threshold value for the ratio at

about .05. Pixels with a ratio greater than the threshold are omitted. Fig 3.8 illustrates this result.

The pixels which still have incorrect directions correspond to neighborhoods with large fitting errors over the center pixel. Fig 3.9 illustrates a histogram of the center pixel residual fitting errors for those pixels surviving the curvature ratio test. Again, there is a dominant peak at a small fitting error corresponding to the majority of pixels having correct optic flow directions. We will reject pixels having a too large neighborhood fitting error. Thresholding the original optic flow image with the curvature ratio of .05 and rejecting the optic flow vectors obtained from the underlying function having relative fitting error of more than 1, we have the optic flow image shown in Fig 3.10. Rejecting the vectors having fitting error of more than .01, we have the optic flow image shown in Fig 3.11. We compare this optic flow image with the ideal optic flow image by computing the absolute error norm at each pixel. Fig 3.12 shows this absolute error norm which has the average error of .08.

For the time sequence of the brightness ellipsoid contracting with the magnification factor .95 shown in Fig 3.13, we obtain the optic flow image shown in Fig 3.14 where we thresholded the original optic flow image with the ratio .05 and rejected the vectors obtained from underlying

function having fitting error of more than 1. In the same way, for the time sequence of the ellipsoid rotating clockwise around the optic axis with the angular velocity .1 radian/sec shown in Fig 3.15, we obtain the optic flow image shown in Fig 3.16. We compare this optic flow image with the ideal optic flow image by computing the absolute error norm at each pixle. Fig 3.17 shows this error norm which has the average error of .192.

For the time sequence of real images shown in Fig 3.18, we obtain optic flow image shown in Fig 3.19 where we thresholded the original optic flow image with the two singular value ratio of .05 and rejected the vectors obtained from underlying function having fitting error of more than .05. In Fig 3.19, we show the approximate boundary of the moving car.

For comparison, we obtain optic flow images from the above image sequences using the algorithm suggested by Horn and Schunk 81. Using 64 iterations, we obtain in Fig 3.20 the optic flow image for the translation sequence of Fig 3.5, the optic flow image in Fig 3.21 for the contraction sequence of Fig 3.13, the optic flow image in Fig 3.22 for clockwise rotation of Fig 3.15, and the optic flow image in Fig 3.23 for the real image sequence of Fig 3.18. In Fig 3.23, we show the approximate boundary of the moving car.

The Horn and Schunk optic flow images have vectors varying smoothly in its length and directions because of the imposed smoothness constraint in the algorithm while the optic flow images obtained by the facet approach have irregular vectors at the pixels near the boundary of the ellipsoid. The facet approach must reject these pixels on the basis of the fitting error and the curvature ratio of the fitting surface at the pixels. Notice also that the optic flow image obtained by Horn and Schunk's method for the ellipsoid in uniform rotational motion does not show the correct movement of the ellipsoid because the method the technique uses to estimate the partial derivatives, especially with respect to time, is not appropriate for the smooth surface of the ellipsoid in uniform rotation.

In terms of the computational complexity, the Horn and Schunk's algorithm computes the optic flow iteratively until the largest uniform region, whose size is not known in advance, is filled. However, the facet approach computes the optic flow based on the underlying fitting function which can be estimated with known computational complexity beforehand when the 3D neighborhood size is given. The number of operations per iteration needed for the Horn and Schunk's method is 60 operations, i.e. 24 operations for estimating the partial derivatives, 18 operations for estimating the Laplacian of the flow velocities, and 18 operations for updating the flow velocities, while that

needed for the facet technique is 250 operations for each convolution plus 80 operations needed to solve the 4x2 linear system using the Singular Value Decomposition per each pixel when a 5x5x5 neighborhood is used. Supposing 64 iterations are needed for the Horn and Schunk's method, then the Horn and Schunk's method needs approximately 11 times more operations than the facet approach needs.

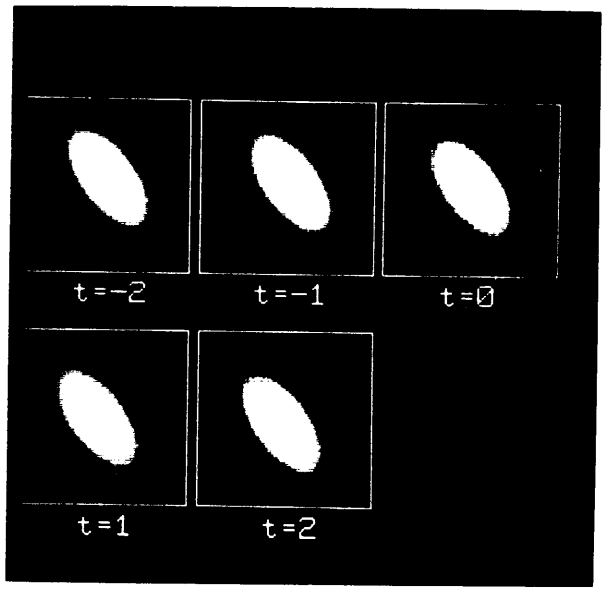

Fig 3.5 Time sequence of an ellipsoid in translation in a plane parallel to the image plane. The ellipsoid is moving to the left at a velocity of .8 pixels per frame and downward at a velocity of 1 pixel per frame.

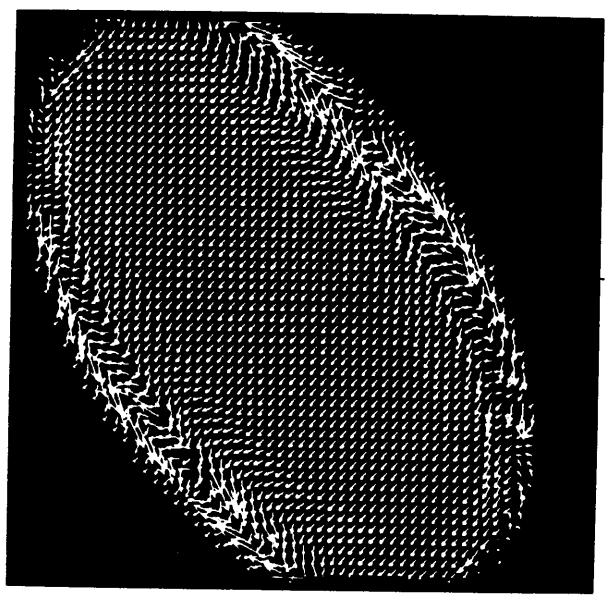

Fig 3.6 Raw optic flow image for the translation sequence of Fig 3.5 using the facet approach.

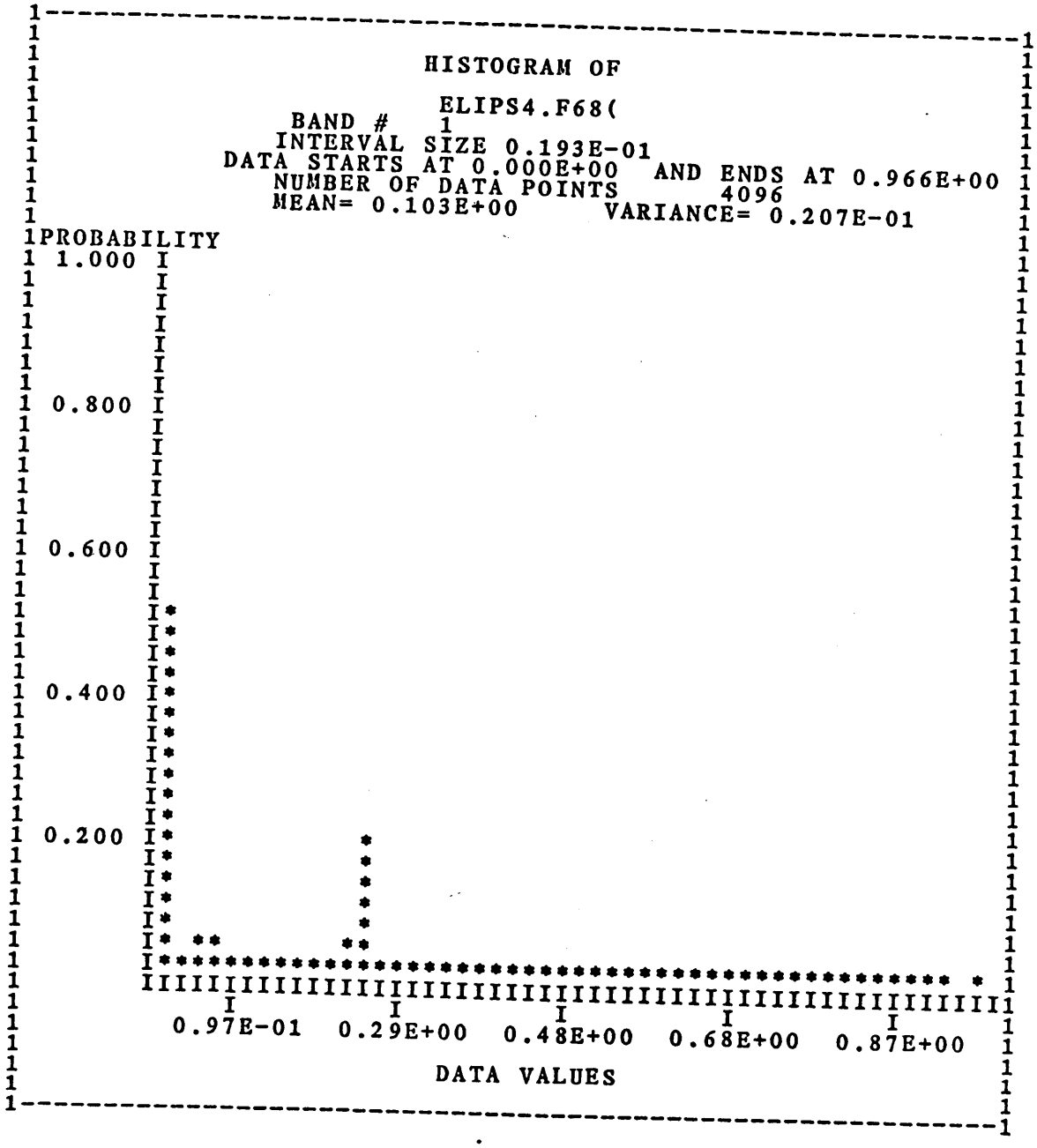

Fig 3.7 Histogram of ratio of smaller to larger principal curvatures of all surface fits at t=0.

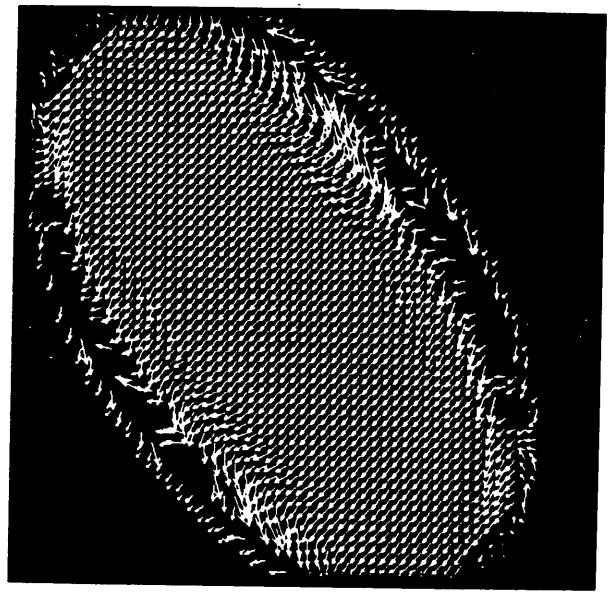

Fig 3.8 Facet approach optic flow image using only those pixels having a smaller to larger principal curvature ratio of less than .05 from the translation sequence of Fig 3.5.

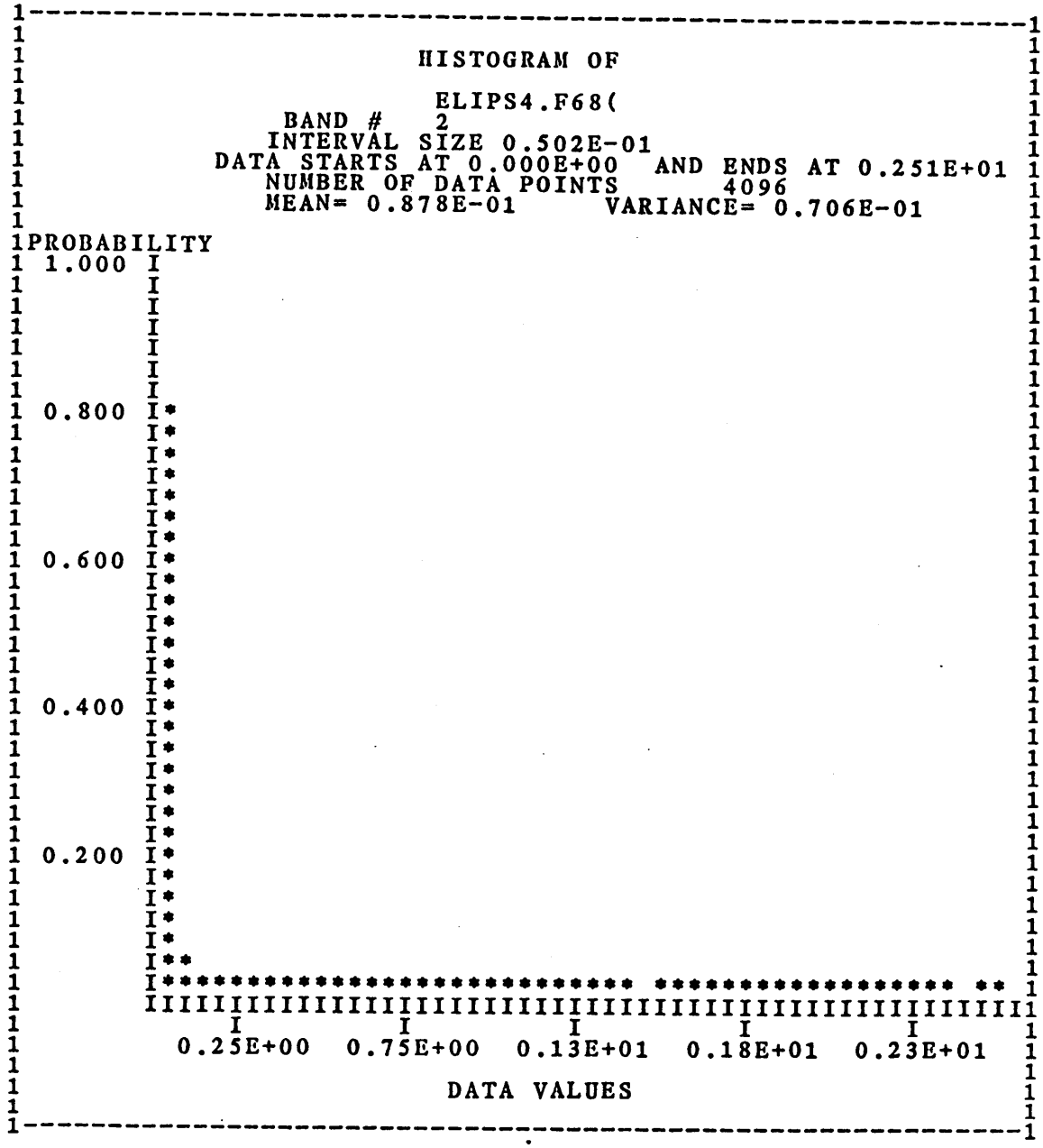

Fig 3.9 Histogram of neighborhood fitting error for all pixels

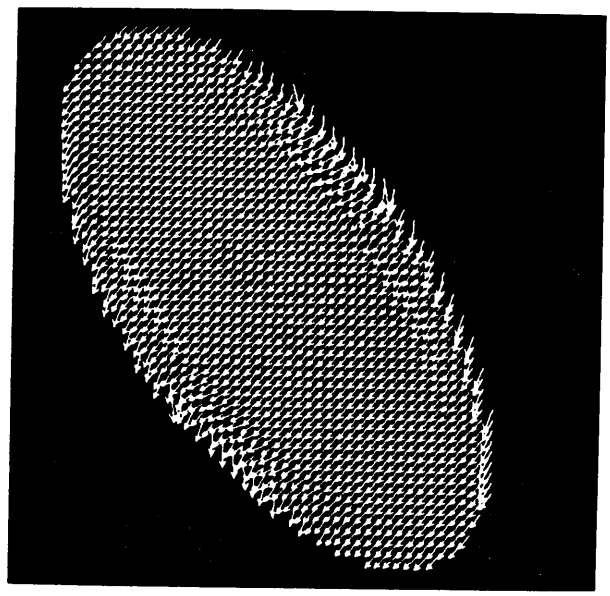

Fig 3.10 Facet approach optic flow image from the translation sequence of Fig 3.5 using only those pixels having a smaller to larger principal curvature ratio of less than .05 and a fitting error of less than 1.

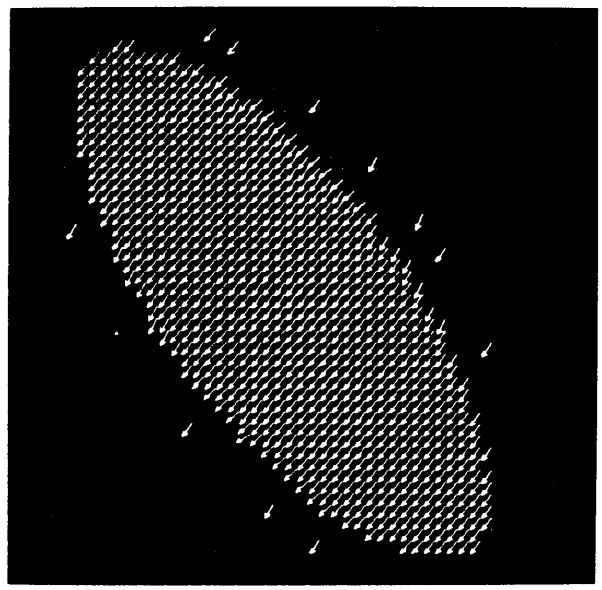

Fig 3.11 Facet approach optic flow image from the translation sequence of Fig 3.5 using only those pixels having a smaller to larger principal curvature ratio of less than .05 and a fitting error of less than .01.

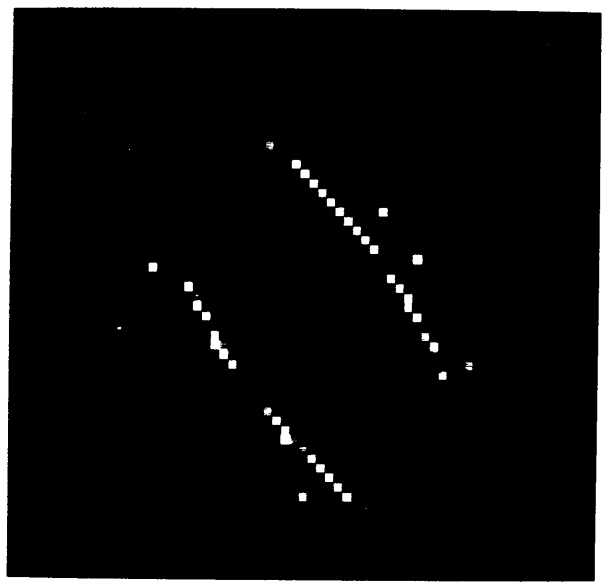

Fig 3.12 Absolute Error Norms Computed from the Optic Flow Image in Fig 3.11 and Its Ideal Optic Flow Image.

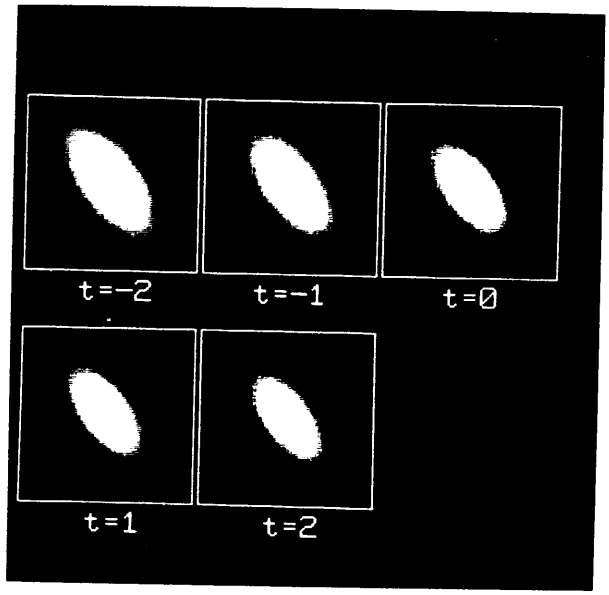

Fig 3.13 Time sequence of an ellipsoid contracting the size of the ellipsoid decrease at a rate of .95 pixels per frame.

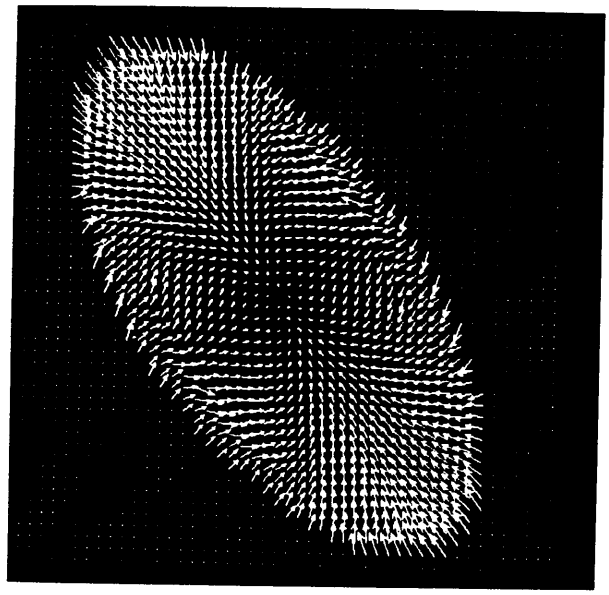

Fig 3.14 Facet approach optic flow image from the contracting ellipsoid of Fig 3.13.

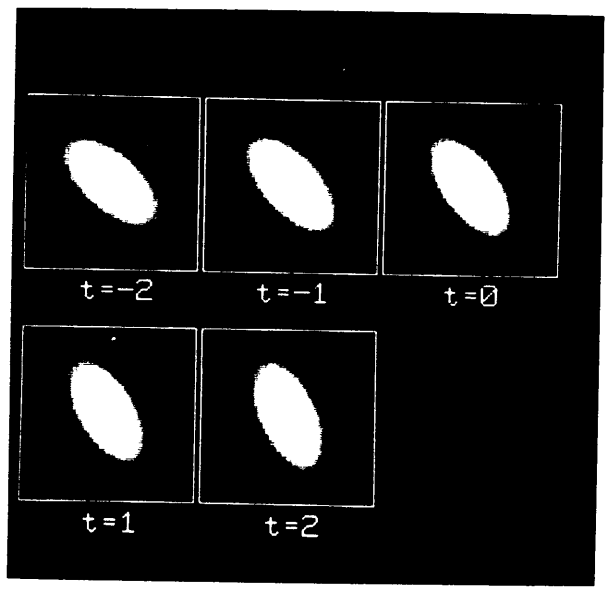

Fig 3.15 Time sequence of an ellipsoid moving in rotation about the optic axis with a clockwise velocity of .1 radians per frame.

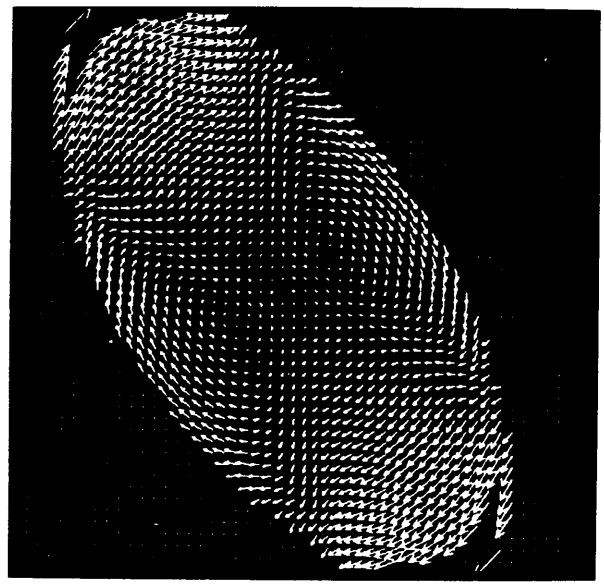

Fig 3.16 Facet approach optic flow image from the rotation sequence of Fig 3.15.

Fig 3.17 Absolute Error Norms Computed from the Optic Flow Image in Fig 3.16 and Its Ideal Optic Flow Image.

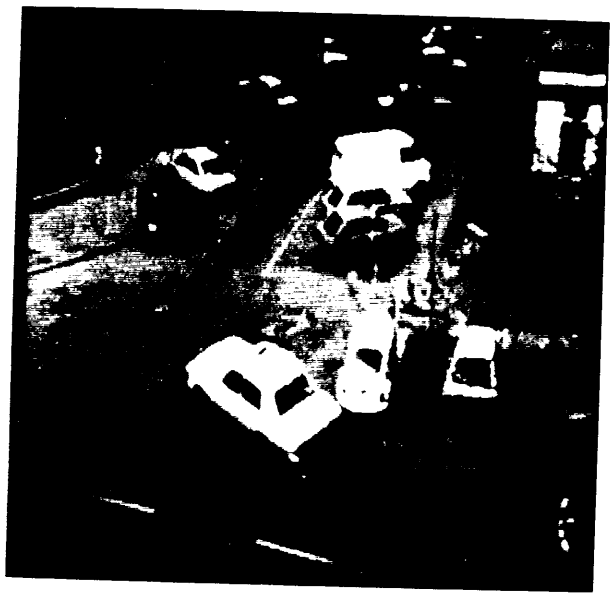

Fig 3.18a Real Image Sequence (t=-2)

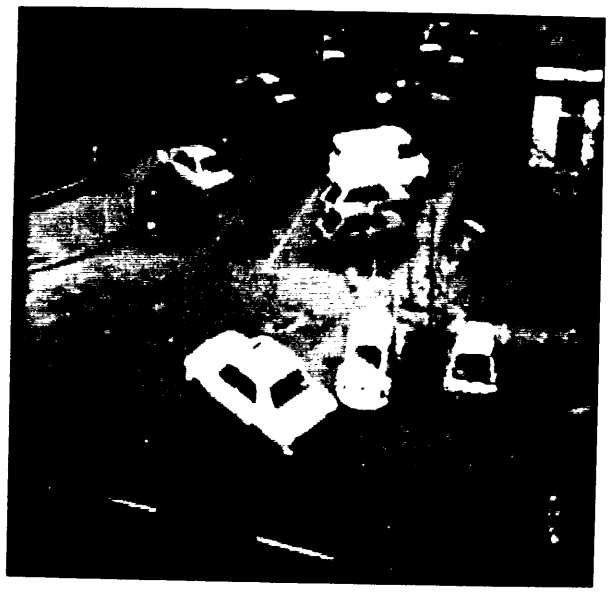

Fig 3.18b Real Image Sequence (t=-1)

Fig 3.18c Real Image Sequence (t=0)

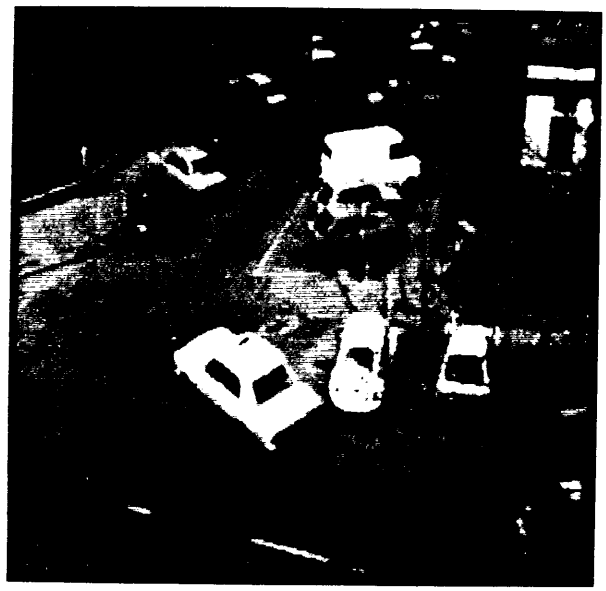

Fig 3.18d Real Image Sequence (t=1)

Fig 3.18e Real Image Sequence (t=2)

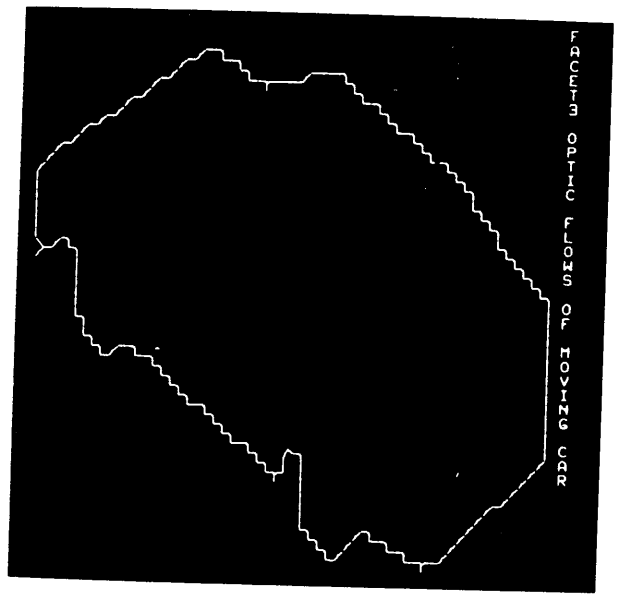

Fig 3.19 Facet approach optic flow image from the part inside the square marked at 3rd image of the real image sequence of Fig 3.18.

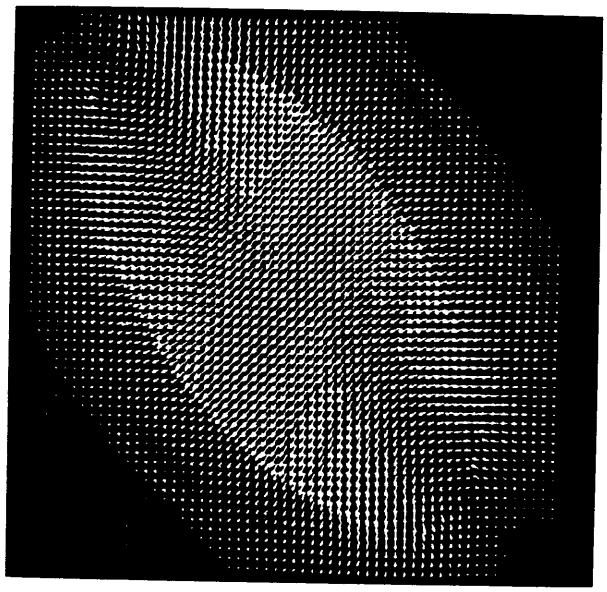

Fig 3.20 Horn and Schunk optic flow image from the ellipsoid translation sequence of Fig 3.5.

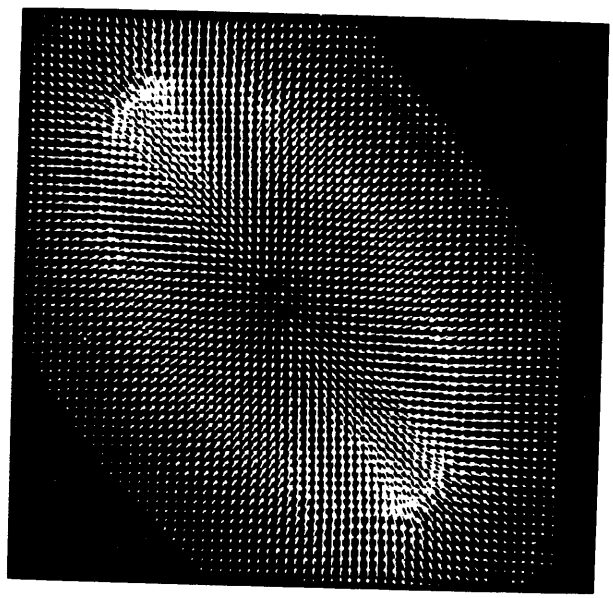

Fig 3.21 Horn and Schunk optic flow image from the ellipsoid contraction sequence of Fig 3.13.

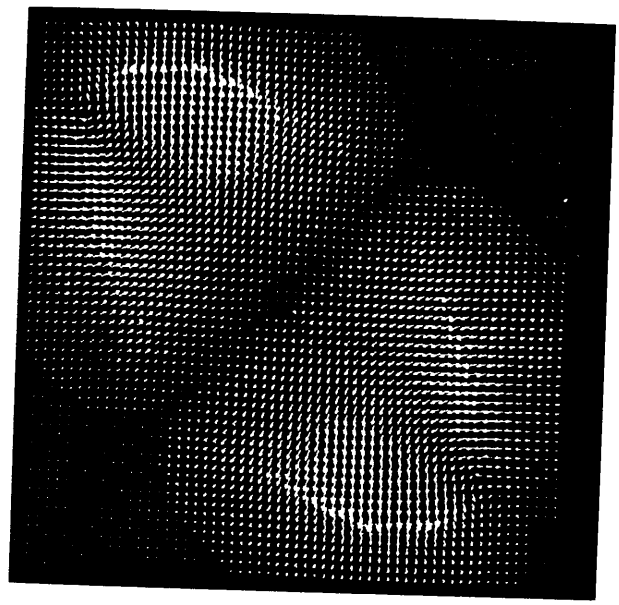

Fig 3.22 Horn and Schunk optic flow image from the ellipsoid rotation sequence of Fig 3.15. Notice that the optic flow field is not correct.

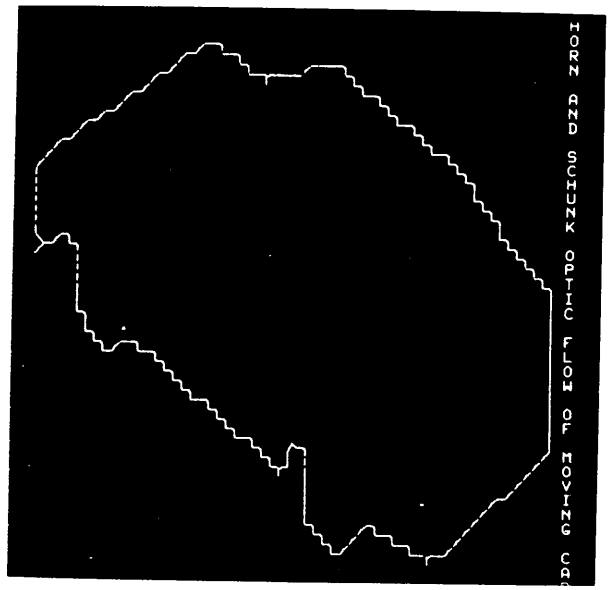

Fig 3.23 Horn and Schunk optic flow image from the part inside the square marked at 3rd image of the real image sequence of Fig 3.18.

CHAPTER IV

ITERATIVE MOTION AND DEPTH RECOVERY

In this chapter we consider the case of rigid objects moving with a possibly combined translational and rotational motion and a stationary camera. In section 4.1, we discuss the motion equations for rigid bodies. In section 4.2 we derive the fundamental optic flow equations for rigid body motion and in section 4.3 show how from some subset of the optic flow field it is possible to compute the object translational and rotational velocity parameters and the depth. Of course, the translational velocity and the depth are only computable to within an arbitrary scale factor if no absolute distance or velocity information is available for one point on each object. In section 4.4 we present results.

4.1 Rigid Body Motion

In rigid body motion, there is no internal motion of points in or on the rigid body. The points must always maintain a fixed position relative to one another. All its points move with the body as a whole. Hence, the moving position of each point in or on the moving rigid body can be

represented by the same rotational and translational transformation of the point from its initial position. This implies that there exists a rotation matrix R(t) and translation vector T(t) such that for all points P in or on the rigid body

$$P(t) = R(t)P(0) + T(t) \tag{4.1}$$

Here, P(0) represents the initial position of the given point. R(0) = I and T(0) = 0.

The motion of each point in or on the rigid body is described by its velocity vector which is just the time derivative of its position. Thus upon taking the time derivative of (4.1), we obtain

$$\dot{P}(t) = \dot{R}(t)P(0) + \dot{T}(t) \tag{4.2}$$

We can reexpress $\dot{P}$ of equation (4.2) in terms of its current position rather than initial position by solving (4.1) for P(0) and substituting $R^{-1}(t)(P(t) - T(t))$ for P(0) in (4.2). This yields

$$\dot{P}(t) = \dot{R}(t)R^{-1}(t)P(t) + \dot{T}(t) - \dot{R}(t)R^{-1}(t)T(t) \tag{4.3}$$

To simplify (4.3), we let

$$S(t) = \dot{R}(t)R^{-1}(t) = \dot{R}(t)R'(t) \tag{4.4}$$

and $$k(t) = \dot{T}(t) - S(t)T(t) \tag{4.5}$$

to obtain

$$\dot{P}(t) = S(t)P(t) + k(t) \qquad (4.6)$$

The system of first order ordinary linear differential equations represented by equation (4.6) can be uniquely solved for P(t) in terms of the initial position P(0)

$$P(t) = \exp(\int_0^t S(u)du)P(0) + \int_0^t \exp(\int_v^t S(u)du)(k(v))dv \qquad (4.7)$$

Equation (4.7) says that the description of motion in equation (4.6) is equivalent, in the sense of having the identical information, to the description of point position in equation (4.1).

From equation (4.4),

$$\dot{R}(t) - S(t)R(t) = 0$$

which implies that

$$R(t) = \exp(\int_0^t S(u)du) \qquad (4.8)$$

since R(0) = I. From equation (4.5)

$$T(t) = \int_0^t \exp(\int_v^t S(u)du)(k(v))dv \qquad (4.9)$$

since T(0) = 0. Hence the information in the motion description (S(t), k(t)) is sufficient to recover the rotation and translation transformations as well as the position description. We will find it convenient to use the

motion description (S(t), k(t)) instead of the motion description (R(t), T(t)) since (S(t), k(t)) ties the current velocity with the current position.

Before relating the optic flow with the velocity of points in the rigid body, it is appropriate to further understand the meaning of equation (4.6). Reexpressing k(t) in terms of S(t) and T(t) we have

$$\dot{P}(t) = S(t)(P(t) - T(t)) + \dot{T}(t) \qquad (4.10)$$

If there were no rotational component, $\dot{P}(t)$ would be exactly $\dot{T}(t)$. This suggests that S(t)(P(t) - T(t)) must be tied to the velocity of the motion due to angular rotation. P(t) - T(t) is just the position of the point relative to the frame whose origin is at T(t) and S(t)(P(t) - T(t)) must therefore be the same as
$\Omega(t) \times (P(t) - T(t))$ where $\Omega(t)$ is the angular velocity of the rigid body.

This can be understood in a more formal way by first showing that S(t) is skew symmetric, S(t) = -S(t)', and then relating the action of a skew symmetric matrix on a given vector with the cross product of a vector whose components are the unique entries in the skew symmetric matrix and the given vector. Differentiating

$I = R(t)R'(t)$ with respect to time yields

$$0 = R(t)\dot{R}'(t) + \dot{R}(t)R'(t)$$

$$= R(t)\dot{R}'(t) + S(t)$$

$$= (\dot{R}(t)R'(t))' + S(t)$$

$$= S(t)' + S(t) \qquad (4.11)$$

Hence, S(t) must have the form

$$S(t) = \begin{bmatrix} 0 & -\omega_z(t) & \omega_y(t) \\ \omega_z(t) & 0 & -\omega_x(t) \\ -\omega_y(t) & \omega_x(t) & 0 \end{bmatrix}$$

Now notice that

$$(S(t)P(t))' = (-\omega_z(t)P_y(t)+\omega_y(t)P_z(t),$$

$$\omega_z(t)P_x(t)-\omega_x(t)P_z(t),\ -\omega_y(t)P_x(t)+\omega_x P_y(t).)$$

where $P(t)' = (P_x(t),\ P_y(t),\ P_z(t))$.

This expression is exactly the same as the cross product

$$\Omega(t) \times P(t)$$

where $\Omega(t)' = (\omega_x(t),\ \omega_y(t),\ \omega_z(t))$.

Thus we can describe the rigid body motion given by equation (4.10) by

$$\dot{P}(t) = \Omega(t) \times P(t) + k(t) \qquad (4.12)$$

4.2 The Fundamental Optic Flow Equations

The point $P' = (P_x, P_y, P_z)$ on the moving rigid body has perspective projection (x,z) on the image plane which we take to be a distance f in front of the camera lens which is the origin. The motion of P (that is, its velocity) causes motion of its perspective projection (x,z) on the image. We denote by (u,v) the velocity of the point (x,z) as shown in Fig 4.1. The optic flow image is the image in which each pixel (x,z) has its own velocity (u,v) as its value.

The fundamental optic flow depth equation relates the motion of the 3D point P with the perspective projection (x,z) of P and the motion (u,v) of (x,z). By the geometry of the perspective projection we have

$$(x,f,z) = \frac{f}{P_y}(P_x, P_y, P_z) = \frac{fP'}{P_y} \qquad (4.13)$$

To change equation (4.13) into the optic flow, we take time derivatives of both sides of (4.13).

$$(x,o,z) = \frac{f}{P_y^2}[P_y\dot{P}' - \dot{P}_yP'] \qquad (4.14)$$

For $\dot{P}$ we substitute $\Omega \times P + k$ (from (4.12)) and for (x,z) we substitute (u,v). This results in

$$(u,o,v) = \frac{f}{P_y}(\Omega \times P)' + \frac{f}{P_y}k' - \frac{f\dot{P}_Y}{P_y^2}P' \qquad (4.15)$$

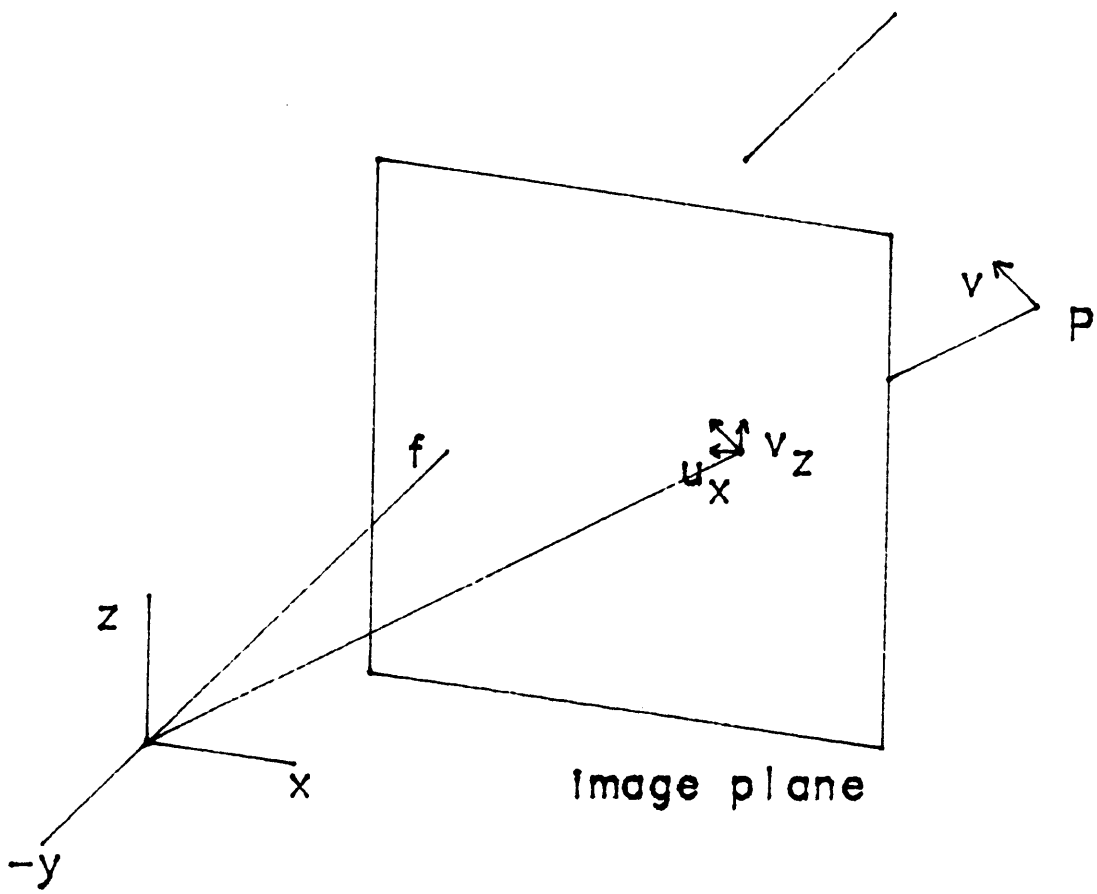

Fig 4.1 Geometry of optic flow vector (u,v).

To get as many terms as possible in the known image coordinates rather than the 3D point coordinate, we use (4.13) and substitute

$\frac{P_y}{f}(x,f,z)$ for P' in (4.15) to obtain

$$(u,o,v) = (\Omega \times (x,f,z)')' + \frac{f}{P_y} k' - \frac{\dot{P}_y}{P_y}(x,f,z)' \quad (4.16)$$

Equation (4.16) is the first fundamental optic flow equation. From (4.16), it follows

$$P_y[(u,o,v) - (\Omega \times (x,f,z)')'] + \dot{P}_y(x,f,z)' = fk'$$

Multiplying both sides by k x (x,f,z)', we obtain

$$P_y[(u,o,v) - (\Omega \times (x,f,z)')'] \; k \times (x,f,z)' = 0 \quad (4.17)$$

Since $P_y \neq 0$, we obtain the second fundamental optic flow equation

$$(u,o,v)\left[k \times \begin{bmatrix} x \\ f \\ z \end{bmatrix}\right] = \left[k \times \begin{bmatrix} x \\ f \\ z \end{bmatrix}\right]' \left[\Omega \times \begin{bmatrix} x \\ f \\ z \end{bmatrix}\right] \quad (4.18)$$

Equation (4.18) is concise and important because it does not involve any depth information. Based on it, a unified and stable linear scheme can be developed to compute motion parameters and other related information. This is done in chapter 5. However, in this section we develop a technique to simultaneously recover the motion parameters and the depth information from equation (4.16) directly.

There are three special cases of (4.16) which it is appropriate to examine further. The first case arises when there is no angular velocity; $\Omega = 0$. The second case arises when the combined rotational and translational motion makes $k = 0$. The third case is the general case.

If $\Omega = 0$, then from equation (4.12) we have $\dot{P} = k$ so that $\dot{P}_y = k_y$. In this case, the first fundamental optic flow equation (4.12) becomes

$$(u,o,v) = f(k_x,k_y,k_z)/P_y - k_y(x,f,z)/P_y \qquad (4.19)$$

We can rewrite (4.19) as

$$\begin{bmatrix} u \\ \\ v \end{bmatrix} = \frac{1}{P_y} \begin{bmatrix} f & -x & 0 \\ & & \\ 0 & -z & f \end{bmatrix} \begin{bmatrix} k_x \\ k_y \\ k_z \end{bmatrix} \qquad (4.20)$$

Equation (4.20) has general solution

$$\begin{bmatrix} k_x \\ k_y \\ k_z \end{bmatrix} = \lambda \begin{bmatrix} x \\ f \\ z \end{bmatrix} + \frac{P_y}{f} \begin{bmatrix} u \\ 0 \\ v \end{bmatrix} \qquad (4.21)$$

where λ is an arbitrary constant. Equation (4.21) shows that $(k_x,k_y,k_z)'$ must be in the plane determined by the line of sight ray $\lambda(x,f,z)'$ and the back projected velocity vector $(P_y/f)(u,o,v)'$. The arbitrariness of λ means that any information about the velocity component that the point has in the direction of the line of sight is lost in the perspective projection and cannot be recovered from the

observed (u,v).

If k=0 (the second case), from equation (4.12) we have $\dot{P} = \Omega \times P$ so that

$$\dot{P}_y = (-\omega_x P_z + \omega_z P_x) = (-\omega_x z + \omega_z x) P_y / f$$

where $\Omega = (\omega_x, \omega_y, \omega_z)$. Hence, equation (4.16) becomes

$$(u,0,v) = (-\omega_z f + \omega_y z, \omega_z x - \omega_x z, -\omega_y x + \omega_x f) - (-\omega_x z + \omega_z x)(x,f,z)/f$$

or

$$(u,v) = (-\omega_z f + \omega_y z + \omega_x z x/f - \omega_z x^2/f,\ -\omega_y x + \omega_x f + \omega_x z^2/f - \omega_z xz/f)$$

which can be rewritten

$$\begin{bmatrix} u \\ v \end{bmatrix} = \frac{1}{f} \begin{bmatrix} xz & fz & -(x^2+f^2) \\ z^2+f^2 & -fx & -xz \end{bmatrix} \begin{bmatrix} \omega_x \\ \omega_y \\ \omega_z \end{bmatrix} \qquad (4.22)$$

Equation (4.22) has general solution

$$\begin{bmatrix} \omega_x \\ \omega_y \\ \omega_z \end{bmatrix} = \lambda \begin{bmatrix} x \\ f \\ z \end{bmatrix} + \begin{bmatrix} -xzu + (x^2+f^2)v \\ 0 \\ -(z^2+f^2)u + xzv \end{bmatrix} \frac{1}{f(x^2+z^2+f^2)} \qquad (4.23)$$

where λ is an arbitrary constant. Equation (4.23) shows that $(\omega_x, \omega_y, \omega_z)'$ must be in the plane determined by the line of sight ray $(x,f,z)'$ and the back projected angular velocity vector $(-xzu + (x^2 + f^2)v,\ 0,\ -(z^2+f^2)u + xzv)/f(x^2+z^2+f^2)$. The arbitrariness of λ means that any information about the angular velocity component that the point has in the direction of the line of sight is lost in

the perspective projection and cannot be recovered from the observed (u,v).

In the general case,

$$\dot{P}_y = \frac{P_y}{f}(\omega_z x - \omega_x z) + k_y \qquad (4.24)$$

Substituting (4.24) into (4.16) and rearranging produces the linear equation

$$\begin{bmatrix} f/P_y & -x/P_y & 0 & xz/f & z & -(x^2+f^2)/f \\ 0 & -z/P_y & f/P_y & (z^2+f^2)/f & -x & -xz/f \end{bmatrix} \begin{bmatrix} k_x \\ k_y \\ k_z \\ \omega_x \\ \omega_y \\ \omega_z \end{bmatrix} = \begin{bmatrix} u \\ v \end{bmatrix} \qquad (4.25)$$

The kernel of

$$\begin{bmatrix} f/P_y & -x/P_y & 0 & xz/f & z & -(x^2+f^2)/f \\ 0 & -z/P_y & f/P_y & (z^2+f^2)/f & -x & -xz/f \end{bmatrix}$$

is spanned by the orthogonal vectors

$$\begin{bmatrix} x \\ f \\ z \\ 0 \\ 0 \\ 0 \end{bmatrix}, \begin{bmatrix} 0 \\ 0 \\ 0 \\ x \\ f \\ z \end{bmatrix}, \begin{bmatrix} xzP_y \\ zfP_y \\ -(x^2+f^2)P_y \\ f^2 \\ -xf \\ 0 \end{bmatrix}, \begin{bmatrix} -(x^2+f^2+z^2)P_y \\ x(x^2+f^2+z^2)P_y/f \\ 0 \\ xz \\ zf \\ -(x^2+f^2) \end{bmatrix}$$

The basis vectors of the kernel have a specific geometric interpretation. To understand this interpretation recall that k has three degrees of freedom and Ω has three

degrees of freedom. Fix a point (x,z) on the image. The line of sight direction is $(x,f,z)'$. A plane orthogonal to this line of sight is spanned by the orthogonal vectors $(xz,fz,-(x^2+f^2))'$ and $(-f,x,0)$. Thus any $(k_x,k_y,k_z)'$ could be represented as

$$\begin{bmatrix} k_x \\ k_y \\ k_z \end{bmatrix} = \alpha_k \begin{bmatrix} x \\ f \\ z \end{bmatrix} + \beta_k P_y \begin{bmatrix} xz \\ fz \\ -(x^2+f^2) \end{bmatrix} + \gamma_k \begin{bmatrix} -f \\ x \\ 0 \end{bmatrix} \frac{(x^2+f^2+z^2)P_y}{f}$$

Similarly any $\Omega = (\omega_x,\omega_y,\omega_z)'$ could be represented as

$$\begin{bmatrix} \omega_x \\ \omega_y \\ \omega_z \end{bmatrix} = \alpha_\Omega \begin{bmatrix} x \\ f \\ z \end{bmatrix} + \beta_\Omega \begin{bmatrix} xz \\ fz \\ -(f^2+x^2) \end{bmatrix} + \gamma_\Omega(-f) \begin{bmatrix} x \\ f \\ 0 \end{bmatrix}$$

The first basis vector $(x,f,z,0,0,0)'$ of the kernel of (4.25) indicates that any part of k in the line of sight direction $(x,f,z)'$ is lost in the projected motion on the image. That is, all projected motion due to a non-zero α_k results in zero motion on the projection. Similarly, the second basis vector $(0,0,0,x,f,z)'$ of the kernel of (4.25) indicates that any part of Ω in the line of sight direction $(x,f,z)'$ is lost in the projected motion on the image. That is, all projected motion due to a non-zero α_Ω results in zero motion on the projection.

Whereas the first two six dimensional basis vectors

indicate how motion due to k or Ω in the direction along the line of sight is lost in the projection, the second two basis vectors indicate in what ways the independent motions of k and Ω can cancel each other on the projection. The third basis vector indicates that any value β_k can take which would result in some projected motion on the image is precisely canceled by β_Ω taking the identical value. Likewise, the fourth basis vector indicates that any value γ_k can take which would result in some projected motion on the image is precisely canceled by γ_Ω taking the identical value. The observed projected motion is solely due to the difference between β_k and β_Ω and by the difference between γ_k and γ_Ω

A particular solution of (4.25) can be obtained from (4.21)

$$\begin{bmatrix} k_x \\ k_y \\ k_z \\ \omega_x \\ \omega_y \\ \omega_z \end{bmatrix} = \begin{bmatrix} u \\ 0 \\ \frac{p_y}{f} v \\ 0 \\ 0 \\ 0 \end{bmatrix}$$

Thus, the general solution to (4.25) is given by

$$\begin{bmatrix} k_x \\ k_y \\ k_z \\ \omega_x \\ \omega_y \\ \omega_z \end{bmatrix} = \lambda_1 \begin{bmatrix} x \\ f \\ z \\ 0 \\ 0 \\ 0 \end{bmatrix} + \lambda_2 \begin{bmatrix} 0 \\ 0 \\ 0 \\ x \\ f \\ z \end{bmatrix} + \lambda_3 \begin{bmatrix} xzP_y \\ zfP_y \\ -(x^2+f^2)P_y \\ f^2 \\ -xf \\ 0 \end{bmatrix} + \lambda_4 \begin{bmatrix} -(x^2+f^2+z^2)P_y \\ x(x^2+f^2+z^2)P_y/f \\ 0 \\ xz \\ zf \\ -(x^2+f^2) \end{bmatrix} + \begin{bmatrix} P_y \\ 0 \\ -- \\ v \\ f \\ 0 \end{bmatrix} \begin{bmatrix} u \\ 0 \end{bmatrix} \tag{4.26}$$

The algebraic meaning of (4.26) can be understood directly if we work out the general solution in terms of $(\alpha_k, \beta_k, \gamma_k, \alpha_\Omega, \beta_\Omega, \gamma_\Omega)$ instead of in terms of $(k_x, k_y, k_z, \omega_x, \omega_y, \omega_z)$. After performing the change of basis we obtain

$$\begin{bmatrix} \alpha_k \\ \beta_k \\ \gamma_k \\ \alpha_\Omega \\ \beta_\Omega \\ \gamma_\Omega \end{bmatrix} = \begin{bmatrix} \lambda_1 \\ \lambda_3 \\ \lambda_4 \\ \lambda_2 \\ \lambda_3 \\ \lambda_4 \end{bmatrix} + \frac{1}{(x^2+f^2)(x^2+f^2+z^2)} \begin{bmatrix} P_y(x^2+f^2)(ux+vz)/f \\ (xzu-(x^2+f^2)v)/f \\ -uf \\ 0 \\ 0 \\ 0 \end{bmatrix}$$

This equation says that since λ_1 and λ_2 are independent, α_k and α_Ω can be arbitrary. However, β_k and β_Ω are constrained since they are associated with the same λ_3 and γ_k and γ_Ω are constrained since they are associated with the same λ_4. Hence,

$$\beta_k = \beta_\Omega + \frac{xzu - (x^2+f^2)v}{(x^2+f^2)(x^2+f^2+z^2)f}$$

$$\gamma_k = \gamma_\Omega - \frac{uf}{(x^2+f^2)(x^2+f^2+z^2)}$$

4.3 Position and Motion Determination from Optic Flow

We assume a set $Q = \{(x_n, y_n)\}_{n=1...N}$ of pixels all of which arise from the perspective projection of the same moving rigid body and all of which have the observed corresponding optic flow $\{(u_n, v_n)\}_{n=1...N}$. The set Q does not have to correspond to the full set of pixels which are the perspective projection of an object. Now we want to use the observed optic flow to determine the motion of the rigid body. First we consider the case for translational motion only. Then we consider the case when k=0. Finally, we will consider the general case of rotational and translational motion.

Suppose $\Omega=0$. From equation (4.21), it is obvious that $\lambda=k_y/f$. Thus we seek to find k_x, k_y, k_z and P_y, P_y depending on x and z, which minimize the difference between the left and right hand sides of equation (4.21). Setting this up as a least squares problem, we seek to find k_x, k_y, k_z, and P_y, which minimizes

$$\varepsilon^2 = \sum_{n=1}^{N} \left\| \begin{bmatrix} k_x \\ k_z \end{bmatrix} - \frac{k_y}{f} \begin{bmatrix} x_n \\ z_n \end{bmatrix} - \frac{P_{yn}}{f} \begin{bmatrix} u_n \\ v_n \end{bmatrix} \right\|^2 \qquad (4.27)$$

Because the structure of (4.27) is special there is a nice least squares solution procedure which permits the solution for k_x, k_y, k_z to be obtained as the eigenvector having smallest eigenvalue of a 3x3 matrix and then the solution for P_{yn}, $n=1,\ldots,N$ to be obtained in terms of k_x, k_y, and k_z.

To see how this happens, note that multiplication by an orthonormal matrix does not change norms. Hence,

$$\varepsilon^2 = \sum_{n=1}^{N} \left\| \frac{1}{u_n^2+v_n^2} \begin{bmatrix} v_n & -u_n \\ u_n & v_n \end{bmatrix} \left(\begin{bmatrix} k_x \\ k_z \end{bmatrix} - \frac{k_y}{f} \begin{bmatrix} x_n \\ z_n \end{bmatrix} - \frac{P_{yn}}{f} \begin{bmatrix} u_n \\ v_n \end{bmatrix} \right) \right\|^2 \qquad (4.28)$$

Upon expanding (4.28) we have

$$\varepsilon^2 = \sum_{n=1}^{N} \left(\frac{1}{u_n^2+v_n^2} \right)^2 \left(v_n k_x + \frac{u_n z_n - x_n v_n}{f} k_y - u_n k_z \right)^2 + \qquad (4.29)$$

$$+ \left(u_n k_x - \frac{(x_n u_n + v_n z_n)}{f} k_y + v_n k_y - \frac{P_{yn}}{f} (u_n^2+v_n^2) \right)^2$$

Upon taking the partial derivative of (4.29) with respect to each P_{yn} and setting this partial to zero and solving for P_{yn} we obtain

$$P_{yn} = \frac{u_n k_x f - (x_n u_n + v_n z_n) k_y + v_n k_z f}{u_n^2 + v_n^2} \qquad (4.30)$$

Note that this value for P_{yn} makes the second term in (4.29) equal to zero. Hence

$$\min_{k_x,k_y,k_z,P_{yn}} \varepsilon^2 = \min_{k_x,k_y,k_z} \sum_{n=1}^{N} \frac{1}{(u_n^2+v_n^2)^2}\left(v_n k_x + \frac{u_n z_n - x_n v_n}{f} k_y - u_n k_z\right)^2 \tag{4.31}$$

Let

$$\varepsilon^* = \sum_{n=1}^{N} \frac{1}{u_n^2+v_n^2} \left[\left(v_n, \frac{u_n z_n - x_n v_n}{f}, -u_n \right) \begin{bmatrix} k_x \\ k_y \\ k_z \end{bmatrix} \right]^2$$

$$= \begin{bmatrix} k_x \\ k_y \\ k_z \end{bmatrix}^T \begin{bmatrix} \sum \frac{v_n^2}{(u_n^2+v_n^2)^2} & \sum \frac{v_n(u_n z_n - x_n v_n)}{f(u_n^2+v_n^2)^2} & \sum \frac{-u_n v_n}{(u_n^2+v_n^2)^2} \\ \sum \frac{v_n(u_n z_n - x_n v_n)}{f(u_n^2+v_n^2)^2} & \sum \frac{(u_n z_n - x_n v_n)^2}{f^2(u_n^2+v_n^2)^2} & \sum \frac{-u_n(u_n z_n - x_n v_n)}{f(u_n^2+v_n^2)^2} \\ \sum \frac{-u_n v_n}{(u_n^2+v_n^2)^2} & \sum \frac{-u_n(u_n z_n - x_n v_n)}{f(v_n^2+v_n^2)^2} & \sum \frac{u_n^2}{(u_n^2+v_n^2)^2} \end{bmatrix} \begin{bmatrix} k_x \\ k_y \\ k_z \end{bmatrix}$$

$$= \begin{bmatrix} k_x & k_y & k_z \end{bmatrix} A \begin{bmatrix} k_x \\ k_y \\ k_z \end{bmatrix} \tag{4.32}$$

From (4.32) it is obvious that the quadratic form for ε^* is minimized by the (k_x, k_y, k_z) which is the eigenvector of the matrix A having smallest eigenvalue.

Suppose k=0. From equation (4.23) it is obvious that

$\lambda = \omega_y/f$. Thus we seek to find ω_x, ω_y, and ω_z which minimize the difference between the left and right hand sides of equation (4.21). Setting this up as a least squares problem, we seek to find ω_x, ω_y, and ω_z which minimizes

$$\varepsilon^2 = \sum_{n=1}^{N} \left\| \begin{bmatrix} \omega_x \\ \omega_z \end{bmatrix} - \left(\frac{\omega_y}{f}\right) \begin{bmatrix} x_n \\ z_n \end{bmatrix} - \frac{1/f}{f^2+x_n^2+z_n^2} \begin{bmatrix} -x_n z_n u_n + (x_n^2 + f^2) v_n \\ -(z_n^2+f^2) u_n + x_n z_n u_n \end{bmatrix} \right\|^2$$

$$= \sum_{n=1}^{N} (\omega_x - \omega_y x_n/f + (x_n z_n u_n - (x_n^2+f^2) v_n)/(f^3+x_n^2 f+z_n^2 f))^2$$

$$+ (\omega_z - \omega_y z_n/f + ((z_n^2+f^2) u_n - x_n z_n v_n)/(f^3+x_n^2 f+z_n^2 f))^2 \qquad (4.33)$$

Taking the partial derivative of ε^2 with respect to ω_x, ω_y, and ω_z and setting them to zero results in

$$\begin{bmatrix} N & -\frac{\sum x_n}{f} & 0 \\ -\frac{\sum x_n}{f} & \frac{\sum x_n^2+z_n^2}{f^2} & -\frac{\sum z_n}{f} \\ 0 & -\frac{\sum z_n}{f} & N \end{bmatrix} \begin{bmatrix} \omega_x \\ \omega_y \\ \omega_z \end{bmatrix} = \begin{bmatrix} \frac{\sum((x_n v_n - z_n u_n) x_n + v_n f^2)}{(f^2+x_n^2+z_n^2)} \\ -\frac{1}{f} \sum (x_n v_n - z_n u_n) \\ \frac{\sum((x_n v_n - z_n u_n) z_n - u_n f^2)}{(f^2+x_n^2+z_n^2)} \end{bmatrix}$$

(4.34)

Solving (4.34) for ω_y we obtain

$$\omega_y = f \frac{N\sum(z_n u_n - x_n v_n) - \sum x_n \sum((z_n u_n - x_n v_n)x_n - v_n f^2)/(f^2+x_n^2+z_n^2) - \sum z_n \sum((z_n u_n - x_n v_n)z_n + u_n f^2)/(f^2+x_n^2+z_n^2)}{N\sum(x_n^2+z_n^2) - (\sum x_n)^2 - (\sum z_n)^2} \tag{4.35}$$

Then it quickly follows that

$$\omega_x = \frac{\omega_y \sum x_n/f - \sum((z_n u_n - x_n v_n)x_n - v_n f^2)/(f^3+x_n^2 f+z_n^2 f)}{N} \tag{4.36}$$

$$\omega_z = \frac{\omega_y \sum z_n/f - \sum((z_n u_n - x_n v_n)z_n + u_n f^2)/(f^3+x_n^2 f+z_n^2 f)}{N} \tag{4.37}$$

For the case of general translational and rotational motion we use equation (4.24) and seek to find values of k_x, k_y, k_z, ω_x, ω_y, ω_z and P_{yn} which minimize the squared error

$$\varepsilon^2 = \sum_n \left|\left| \begin{bmatrix} k_x \\ k_z \end{bmatrix} - \frac{k_y}{f}\begin{bmatrix} x_n \\ z_n \end{bmatrix} - \frac{P_{yn}}{f}\begin{bmatrix} u_n \\ v_n \end{bmatrix} + \frac{\omega_x P_{yn}}{f^2}\begin{bmatrix} x_n z_n \\ z_n^2+f^2 \end{bmatrix} + \frac{\omega_y P_{yn}}{f}\begin{bmatrix} z_n \\ -x_n \end{bmatrix} - \frac{\omega_z P_{yn}}{f^2}\begin{bmatrix} x_n^2+f^2 \\ x_n z_n \end{bmatrix} \right|\right|^2 \tag{4.38}$$

under the constraint that

$$\sum_n P_{yn} = I$$

where I is a given positive constant.

To find the minimizing value for the parameters, we let

$$\xi = \varepsilon^2 + \lambda \left(\sum_n P_{yn}^2 - I^2\right) \qquad (4.39)$$

Taking the partial derivative of ξ with respect to each of the parameters and setting the partial derivative to zero leads to

$$\begin{bmatrix} A & B \\ & \\ B' & C \end{bmatrix} \begin{bmatrix} k_x \\ k_y \\ k_z \\ \omega_x \\ \omega_y \\ \omega_z \end{bmatrix} = \sum_n \begin{bmatrix} P_{yn}u_n/f \\ -P_{yn}(v_n z_n + u_n x_n)/f^2 \\ P_{yn}v_n/f \\ P^2_{yn}(u_n x_n z_n + v_n(z_n^2+f^2))/f^3 \\ -P_{yn}^2(x_n v_n - u_n z_n)/f^2 \\ -P_{yn}^2(u_n(x_n^2+f^2)+v_n x_n z_n)/f^3 \end{bmatrix} \qquad (4.40)$$

where

$$A = \sum_n \begin{bmatrix} 1 & \frac{-x_n}{f} & 0 \\ -\frac{x_n}{f} & \frac{x_n^2+z_n^2}{f^2} & -\frac{z_n}{f} \\ 0 & \frac{-z_n}{f} & 1 \end{bmatrix}$$

$$B = \sum_n P_{yn} \begin{bmatrix} \frac{x_n z_n}{f^2} & \frac{z_n}{f} & -\frac{x_n^2+f^2}{f^2} \\ \frac{-(x_n^2+z_n^2+f^2)}{f^3} z_n & 0 & \frac{x_n^2+z_n^2+f^2}{f^3} x_n \\ \frac{z_n^2+f^2}{f^2} & \frac{-x_n}{f} & -\frac{x_n z_n}{f^2} \end{bmatrix}$$

$$C = \sum_n P_{yn}^2 \begin{bmatrix} \frac{x_n^2 z_n^2+(z_n^2+f^2)^2}{f^4} & -\frac{x_n}{f} & -\frac{x_n z_n (x_n^2+2f^2+z_n^2)}{f^4} \\ -\frac{x_n}{f} & \frac{x_n^2+z_n^2}{f^2} & -\frac{z_n}{f} \\ -\frac{x_n z_n (x_n^2+2f^2+z_n^2)}{f^4} & -\frac{z_n}{f} & \frac{(x_n^2+f^2)^2+x_n^2 z_n^2}{f^4} \end{bmatrix}$$

and

$$P_{yn} = \frac{\begin{array}{l}(-k_x+k_y x_n/f)(\omega_x x_n z_n + \omega_y z_n f - \omega_z (x_n^2+f^2) - u_n f) \\ + (-k_z+k_y z_n/f)(\omega_x (z_n^2+f^2) - \omega_y x_n f - \omega_z x_n z_n - v_n f) + \lambda f^2\end{array}}{\begin{array}{l}\left(\frac{\omega_x z_n x_n}{f} + \omega_y z_n - \frac{\omega_z (x_n^2+f^2)}{f} - u_n\right)^2 \\ + \left(\frac{\omega_x (z_n^2+f^2)}{f} - \omega_y x_n - \frac{\omega_z x_n z_n}{f} - v_n\right)^2\end{array}} \qquad (4.41)$$

Equation (4.40) and (4.41) can be solved iteratively. Set the initial $P_{yn} = I/N$ and use this value in (4.40) to solve for the motion parameters k_x, k_y, k_z, ω_x, ω_y, and ω_z.

Then substitute those values into (4.41) to solve for P_{yn}. Now, adjust λ to make $\sum P_{yn} = I$. Finally, use these values of P_{yn} in (4.40) and continue to iterate until the changes are small enough.

4.4 Convergence and Uniqueness

In this section we introduce convex functions and we use them to show that the iterative motion and relative depth recovery technique developed in the previous section guarantees a unique solution.

Let R^m be a m-dimensional real Euclidean space for any positive number m. Let θ be a numerical function defined on R^m. The function is said to be convex at $q_1 \varepsilon R^m$ if for any $q_2 \varepsilon R^m$ and $0 \leq \alpha \leq 1$

$$(1-\alpha)\theta(q_1) + \alpha\theta(q_2) \leq \theta((1-\alpha)q_1+\alpha q_2) \qquad (4.42)$$

The function θ is said to be convex if it is convex at each $q \varepsilon R^m$ [MANGASARIAN(1969)]. The function θ is strictly convex when the equality in (4.42) holds if and only if $q_1=q_2$. Concerning the minimization of a strictly convex function, we have the following useful result.

Lemma 4.1 When a function θ defined on R^m is strictly

convex, it has the unique minimum solution $q_a \varepsilon R^m$ such that

$$\theta(q_a) = \min_{q \varepsilon R^m} \theta(q).$$

Proof Let q_a be a minimum of θ. Suppose q_b, $q_b \neq q_a$, is another minimum such that $\theta(q_b) = \theta(q_a)$. Then, by the strict convexity of θ at q_a, we have

$$\theta((1-\alpha)q_a+\alpha q_b) < (1-\alpha)\theta(q_a) + \alpha\theta(q_b) = \theta(q_a)$$

for $0<\alpha<1$. This contradicts the assumption that $\theta(q_a)$ is a minimum, and, hence, q_b could not be another minimum solution.

Q.E.D.

Let h be the minimizing function ξ in (4.39) which can be expressed as

$$\begin{aligned} & h(k_x, k_y, k_z, \omega_x, \omega_y, \omega_z, P_{y1}, \ldots, P_{yN}) \\ &= \sum \{ k_x - (x_n/f)k_y - (u_n/f)P_{yn} + (x_n z_n/f^2)\omega_x P_{yn} \\ &\qquad + (z_n/f)\omega_y P_{yn} - (x_n^2/f^2+1)\omega_z P_{yn}\}^2 \\ &\quad + \sum \{ k_z - (z_n/f)k_y - (v_n/f)P_{yn} + (z_n^2/f^2+1)\omega_x P_{yn} \\ &\qquad - (x_n/f)\omega_y P_{yn} - (x_n z_n/f^2)\omega_z P_{yn}\}^2 \\ &\quad + \lambda \left(\sum P_{yn} - I \right) \end{aligned} \tag{4.43}$$

where λ is adjusted such that $\sum P_{yn}=I$. For the convergence of the technique, let

$$f(k_x, k_y, k_z, \omega_x, \omega_y, \omega_z;\ P_{y1}, \ldots, P_{yN}) \tag{4.44}$$

denote the function h in (4.43) defined on the manifold (subspace) specified by given P_{yn} $n=1\ldots N$ and let

$$g(P_{y1}, \ldots, P_{yN};\ k_x, k_y, k_z, \omega_x, \omega_y, \omega_z) \tag{4.45}$$

be h defined on the manifold by given k_x, k_y, k_z, ω_x, ω_y, and ω_z. The function f can be expressed as

$$\begin{aligned} f(k_x, k_y, k_z, \omega_x, \omega_y, \omega_z) &= \sum f_{1n}^2(k_x, k_y, k_z, \omega_x, \omega_y, \omega_z) \\ &+ \sum f_{2n}^2(k_x, k_y, k_z, \omega_x, \omega_y, \omega_z) \\ &+ \lambda \sum (P_{yn} - I) \end{aligned} \tag{4.46}$$

where

$$\begin{aligned} f_{1n}(k_x, k_y, k_z, \omega_x, \omega_y, \omega_z) &= k_x - (x_n/f)k_y - (u_n/f)P_{yn} \\ &+ (x_n z_n/f^2)\omega_x P_{yn} + (z_n/f)\omega_y P_{yn} - (x_n^2/f^2+1)\omega_z P_{yn} \end{aligned}$$

$$\begin{aligned} f_{2n}(k_x, k_y, k_z, \omega_x, \omega_y, \omega_z) &= k_z - (z_n/f)k_y - (v_n/f)P_{yn} \\ &+ (x_n^2/f^2+1)\omega_x P_{yn} - (x_n/f)\omega_y P_{yn} - (x_n z_n/f^2)\omega_z P_{yn} \end{aligned}$$

and the function g can be expressed as

$$\begin{aligned} g(P_{y1}, \ldots, P_{yN}) &= \sum g_{1n}^2(P_{yn}) + \sum g_{2n}^2(P_{yn}) \\ &+ \lambda (\sum P_{yn} - I) \end{aligned} \tag{4.47}$$

where

$$g_{1n}(P_{yn}) = (k_x - x_n k_y/f) + \{\omega_x x_n z_n + \omega_y z_n f - \omega_z(x_n^2 + f^2) - u_n f\} P_{yn}/f^2$$

$$g_{2n}(P_{yn})=(k_z-z_nk_y/f)+\{(\omega_x z_n^2+f^2)-\omega_y x_n f-\omega_z x_n z_n-v_n\}P_{yn}/f^2.$$

Then we have the following lemmas.

Lemma 4.2 The non-degenerate function f is strictly convex and, hence, f has the unique minimum solution.

Proof Let

$$q_a = (k_{xa},k_{ya},k_{za},\omega_{xa},\omega_{ya},\omega_{za}) \varepsilon R^6$$

and

$$q_b = (k_{xb},k_{yb},k_{zb},\omega_{xb},\omega_{yb},\omega_{zb}) \varepsilon R^6.$$

Then, for $0<\alpha<1$, we have from (4.46) that f_{1n} and f_{2n} are convex

$$f_{1n}((1-\alpha)q_a+\alpha q_b) = (1-\alpha)f_{1n}(q_a) + \alpha f_{1n}(q_b),$$

$$f_{2n}((1-\alpha)q_a+\alpha q_b) = (1-\alpha)f_{2n}(q_a) + \alpha f_{2n}(q_b),$$

and

$$f((1-\alpha)q_a+\alpha q_b) = \sum f_{1n}^2((1-\alpha)q_a+\alpha q_b) + \sum f_{2n}^2((1-\alpha)q_a+\alpha q_b)$$

$$+ \lambda (\sum P_{yn} - I)$$

$$= \sum\{(1-\alpha)^2 f_{1n}^2(q_a)+2(1-\alpha)\alpha f_{1n}(q_a)f_{1n}(q_b)+\alpha^2 f_{1n}^2(q_b)\}$$

$$+ \sum\{(1-\alpha)^2 f_{2n}^2(q_a)+2(1-\alpha)\alpha f_{2n}(q_a)f_{2n}(q_b)+\alpha^2 f_{2n}^2(q_b)\}$$

$$+ \lambda (\sum P_{yn} - I)$$

For the convexity of the function f, we compute

$$(1-\alpha)f(q_a) + \alpha f(q_b) - f((1-\alpha)q_a+\alpha q_b)$$
$$= (1-\alpha)\alpha \sum \{f_{1n}(q_a)-f_{1n}(q_b)\}^2$$
$$+ (1-\alpha)\alpha \sum \{f_{2n}(q_a)-f_{2n}(q_b)\}^2$$

which means that

$$(1-\alpha)f(q_a) + \alpha f(q_b) > f((1-\alpha)q_a+\alpha q_b)$$

when $0<\alpha<1$ and $q_a \neq q_b$. Thus the function f is strictly convex and by Lemma 4.1 f has the unique minimum solution.

Q.E.D.

In the similar way, we have

Lemma 4.3 The non-degenerate function g is strictly convex and, hence, has the unique minimum solution.

Proof The proof is similar to that used in Lemma 4.2.

Due to the strict convexity of the functions f and g, we can minimize the function h iteratively. Let k_x^i, k_y^i, k_z^i, ω_x^i, ω_y^i, and ω_z^i be the motion parameter values determined at the i-th iteration and let $P_{yn}^i, n=1...N$ be the relative depths determined at the same iteration. Let f^i and g^i be the function values such that

$$f^i = f(k_x^i, k_y^i, k_z^i, \omega_x^i, \omega_y^i, \omega_z^i; P^{i-1}_{y1}, \ldots, P^{i-1}_{yN})$$

and

$$g^i = g(P^i_{yn},\ldots,P^i_{yN};\ k^i_x,k^i_y,k^i_z,\omega^i_x,\omega^i_y,\omega^i_z)$$

where $P^0_{yn}{}_{n=1\ldots N}$ are given initial depths. Then we have the following theorem.

Theorem 4.1 A minimum solution of the function h in (4.43) can be obtained iteratively.

Proof The iterative technique developed in the previous section determine k^i_x, k^i_y, k^i_z, ω^i_x, ω^i_y, and ω^i_z uniquely such that

$$f^i = \min f(k_x,k_y,k_z,\omega_x,\omega_y,\omega_z;\ P^{i-1}_{yn}{}_{n=1\ldots N}) \qquad (4.48)$$

by solving the linear system (4.40) because the function f is strictly convex for given $P^{i-1}_{yn}{}_{n=1\ldots N}$ and, hence, has the unique minimum solution at the critical point where the gradient vector of f is zero. Because the function g is also strictly convex for given k^i_x, k^i_y, k^i_z, ω^i_x, ω^i_y, and ω^i_z, we can determine $P_{yn}{}_{n=1,\ldots,N}$ uniquely from (4.41) such that

$$g^i = \min g(P_{y1},\ldots,P_{yN};\ k^i_x,k^i_y,k^i_z,\omega^i_x,\omega^i_y,\omega^i_z) \qquad (4.49)$$

at the same iteration.

Let

$$\langle\ (k^i_x,k^i_y,k^i_z,\omega^i_x,\omega^i_y,\omega^i_z,P^i_{y1},\ldots,P^i_{yN})\ |\ i=1,\ldots,\ \rangle$$

be the sequence computed iteratively. For the sequence to

converge, the sequence of its objective function values must converge. Specifically, the value g^{i+1} (or f^{i+1}) computed at the (i+1)-th iteration must be less than or equal to the value g^i (f^i) computed at the i-th iteration. In the following we will derive this relationship from (4.48) and (4.49). Because f and g are the functions obtained from the same function h, we have

$$\begin{aligned} g^i &= g(P^i_{y1},\ldots,P^i_{yN};\ k^i_x,k^i_y,k^i_z,\omega^i_x,\omega^i_y,\omega^i_z) \\ &= f(k^i_x,k^i_y,k^i_z,\omega^i_x,\omega^i_y,\omega^i_z;\ P^i_{yn}n=1\ldots N) \\ &\geq f(k^{i+1}_x,k^{i+1}_y,k^{i+1}_z,\omega^{i+1}_x,\omega^{i+1}_y,\omega^{i+1}_z;\ P^i_{yn}n=1\ldots N) \\ &= g(P^i_{yn}n=1\ldots N;\ k^{i+1}_x,k^{i+1}_y,k^{i+1}_z,\omega^{i+1}_x,\omega^{i+1}_y,\omega^{i+1}_z) \\ &\geq g(P^{i+1}_{yn}n=1\ldots N;\ k^{i+1}_x,k^{i+1}_y,k^{i+1}_z,\omega^{i+1}_x,\omega^{i+1}_y,\omega^{i+1}_z) \\ &= g^{i+1} \end{aligned} \tag{4.50}$$

However, the function g is nonnegative since $\sum P_{yn}=I$ and, hence, the function g has the same value as that of ε^2 in (4.38) at each iteration. Thus, we have

$$g^1 \geq g^2 \geq\cdots\geq g^i \geq g^{i+1}\ldots\geq g^\infty \geq 0 \tag{4.51}$$

which means that the sequence

$$\langle\ (k^i_x,k^i_y,k^i_z,\omega^i_x,\omega^i_y,\omega^i_z,P^i_{y1},\ldots,P^i_{yN})\ \mid\ i=1,\ldots,\ \rangle$$

converges to

$$(k_x^\infty,\ k_y^\infty,\ k_z^\infty,\ \omega_x^\infty,\ \omega_y^\infty,\ \omega_z^\infty,\ P_{yn}^\infty n=1...N)$$

Q.E.D.

Is the minimum solution unique? Or is there any other local minimum? In the following, we will answer the question using the following lemma.

Lemma 4.4 Let $q \varepsilon R^m$ and let θ be a quadratic function such that

$$\theta(q) = q'Bq + v'q + s \tag{4.52}$$

where B, v, and s are given matrix, vector, and scalar, respectively. If the function θ has the critical point q^*, the function can be represented by

$$\theta(q) = (q-q^*)B(q-q^*) + d \tag{4.53}$$

where d is a scalar given by $s-q^{*\prime}Bq^*$.

Proof At the critical point q^*, we have

$$\frac{\partial \theta}{\partial q}(q^*) = 2Bq^* + v = 0 \tag{4.54}$$

Multiplying (4.54) by q with a trivial addition, we have

$$2q'Bq^* + q'v + q^{*\prime}Bq^* - q^{*\prime}Bq^* = 0 \tag{4.55}$$

Subtracting (4.55) from (4.52), we have (4.53)

Q.E.D.

Theorem 4.2 A minimum solution of the function h in (4.43) is unique.

Proof Let (q_a, p_a) be the minimum solution of h obtained by the iterative method. Suppose we have another local minimum solution (q_b, p_b). Let the manifolds M_{p_a} and M_{p_b} be subspaces of (q,p) for given p_a and p_b, respectively, and let L_{q_a} and L_{q_b} be subspaces of (p,q) for given q_a and q_b, respectively, as in Fig 4.2. Then, we have

$$(q_a, p_a) \in M_{p_a} \cap L_{q_a}$$
$$(q_b, p_b) \in M_{p_b} \cap L_{q_b}$$
$$(q_a, p_b) \in M_{p_b} \cap L_{q_a}$$
$$(q_b, p_a) \in M_{p_a} \cap L_{q_b}.$$

Let f_a and f_b be the function f in (4.46) defined on M_{p_a} and M_{p_b}, respectively, and let g_a and g_b be the function g in (4.47) defined on L_{q_a} and L_{q_b}, respectively. Because (q_a, p_a) and (q_b, p_b) must be the critical points for the local minimum, by Lemma 4.4 we can represent f_a and f_b by

$$f_a(q) = (q-q_a)'A_a(q-q_a) + d_a \qquad (4.56)$$

$$f_b(q) = (q-q_b)'A_b(q-q_b) + d_b \qquad (4.57)$$

where A_a and A_b are 6x6 Hessian matrices obtained from (4.43) for given p_a and p_b, respectively. Since f_a and g_a have the same numerical value at (q_a, p_a) and f_b and g_b have the same numerical value at (q_b, p_b), we can represent g_a and

g_b by

$$g_a(p) = (p-p_a)'B_b(p-p_a) + d_a \qquad (4.58)$$

$$g_b(p) = (p-p_b)'B_b(p-p_b) + d_b \qquad (4.59)$$

where B_a and B_b are NxN Hessian matrices obtained from (4.43) for given q_a and q_b, respectively. Since $f_a(q_b)=g_b(p_a)$ and $f_b(q_a)=g_a(p_b)$, we have

$$(q_b-q_a)'A_a(q_b-q_a)+d_a = (p_a-p_b)'B_b(p_a-p_b)+d_b \qquad (4.60)$$

$$(q_a-q_b)'A_b(q_a-q_b)+d_b = (p_b-p_a)'B_a(p_b-p_a)+d_a \qquad (4.61)$$

Adding (4.60) and (4.61), we have

$$(q_b-q_a)'(A_a+A_b)(q_b-q_a) = (p_b-p_a)'(B_a+B_b)(p_b-p_a) \qquad (4.62)$$

Let

$$q_b = q_a + \Delta q_a$$

Then, for given p_b, (4.62) holds for

$$q_b' = q_a - \Delta q_a$$

which means that there are two local minimums of f_b as shown in Fig 4.2. This contradicts to Lemma 4.2 that f has the unique minimum solution. Thus, we must have $q_b = q_a$. By the same argument, we have $p_b = p_a$

Q.E.D.

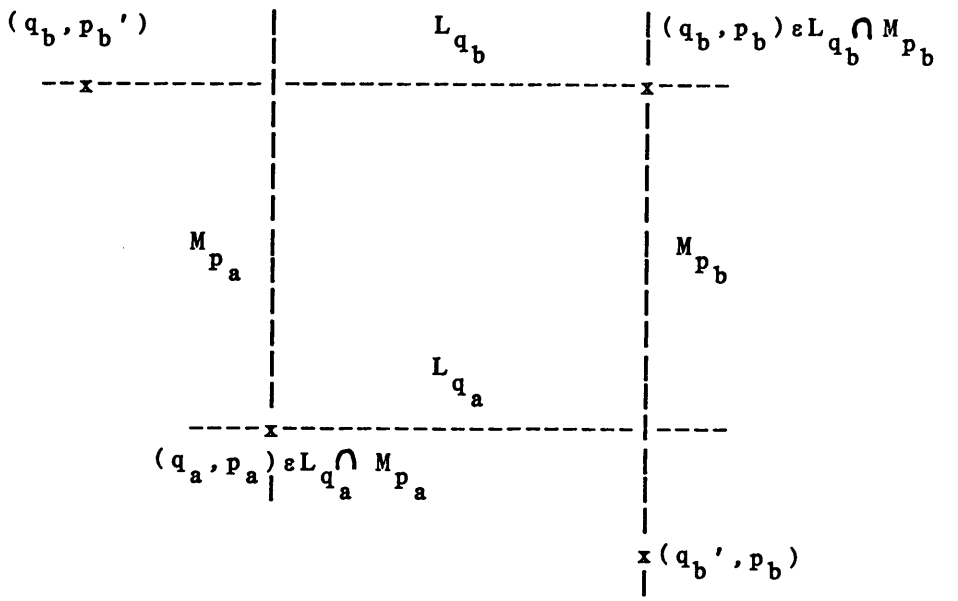

Fig 4.2 Manifolds L_{q_a}, L_{q_b}, M_{p_a}, and M_{p_b} where (q_a, p_a) is the computed minimum solution of the function h defined on $(q,p) \varepsilon R^{N+6}$. Hypothesizing another local minimum solution (q_b, p_b), we have two local minimum solutions (q_b, p_b) and (q_b', p_b) of the function h defined on the manifold M_{p_b}. This contradicts to the strict convex function h defined on M_{p_b}.

4.5 Error Analysis of Small Noise Perturbation

In this section we analyze noise perturbation of the optic flow image and estimate error bounds on both the motion parameter values and the relative depths determined.

Although we minimized the function h in (4.43) for the given set of optic flow vectors $\{(u_n, v_n)\}_{n=1,\ldots,N}$ in the previous sections, in this section we consider them as variables to investigate their effects on the minimum solution. Let q, p, u, and v be the vectors such that

$$q = (k_x, k_y, k_z, \omega_x, \omega_y, \omega_z)',$$

$$p = (P_1, P_2, \ldots, P_N)'$$

$$u = (u_1, u_2, \ldots, u_N)',$$

and $v = (v_1, v_2, \ldots, v_N)'$.

Then, k_x, k_y, k_z, ω_x, ω_y, and ω_z, which are determined by solving (4.40), are the implicit functions of p, u, and v, and P_{yn} is the explicit function of q, u_n, and v_n, as shown in (4.41).

Let a rigid object having the relative depths of $\{[(x_n, z_n), P^*_{yn}]\}_{n=1,\ldots,N}$ move with motion $k=(k^*_x, k^*_y, k^*_z)'$ and

$\Omega=(\omega_x^*,\omega_y^*,\omega_z^*)'$ and generate the optic flow image $\{[(x_n,z_n),(u_n^*,v_n^*)]\}_{n=1,\ldots,N}$. Let the optic flow image experience a small noise perturbation and become $\{[(x_n,z_n),(\bar{u}_n^*,\bar{v}_n^*)]\}_{n=1,\ldots,N}$. Suppose that the iterative technique recovers motion parameters $k=(\bar{k}_x^*,\bar{k}_y^*,\bar{k}_z^*)'$ and $\Omega=(\bar{\omega}_x^*,\bar{\omega}_y^*,\bar{\omega}_z^*)'$, and the relative depths $\{[(x_n,z_n),(\bar{u}_n^*,\bar{v}_n^*)]\}_{n=1,\ldots,N}$ from the perturbed optic flow image. Then for the small perturbation of the optic flow vectors, we have

$$k_x^* \simeq \bar{k}_x^* + \sum_{i=1}^{N} \frac{\partial k_x(\bar{p}^*,\bar{u}^*,\bar{v}^*)}{\partial u_i}(u_i^*-\bar{u}_i^*) + \sum_{i=1}^{N} \frac{\partial k_x(\bar{p}^*,\bar{u}^*,\bar{v}^*)}{\partial v_i}(v_i^*-\bar{v}_i^*) \tag{4.63a}$$

$$k_y^* \simeq \bar{k}_y^* + \sum_{i=1}^{N} \frac{\partial k_y(\bar{p}^*,\bar{u}^*,\bar{v}^*)}{\partial u_i}(u_i^*-\bar{u}_i^*) + \sum_{i=1}^{N} \frac{\partial k_y(\bar{p}^*,\bar{u}^*,\bar{v}^*)}{\partial v_i}(v_i^*-\bar{v}_i^*) \tag{4.63b}$$

$$k_z^* \simeq \bar{k}_z^* + \sum_{i=1}^{N} \frac{\partial k_z(\bar{p}^*,\bar{u}^*,\bar{v}^*)}{\partial u_i}(u_i^*-\bar{u}_i^*) + \sum_{i=1}^{N} \frac{\partial k_z(\bar{p}^*,\bar{u}^*,\bar{v}^*)}{\partial v_i}(v_i^*-\bar{v}_i^*) \tag{4.63c}$$

$$\omega_x^* \simeq \bar{\omega}_x^* + \sum_{i=1}^{N} \frac{\partial \omega_x(\bar{p}^*,\bar{u}^*,\bar{v}^*)}{\partial u_i}(u_i^*-\bar{u}_i^*) + \sum_{i=1}^{N} \frac{\partial \omega_x(\bar{p}^*,\bar{u}^*,\bar{v}^*)}{\partial v_i}(v_i^*-\bar{v}_i^*) \tag{4.63d}$$

$$\omega_y^* \simeq \bar{\omega}_y^* + \sum_{i=1}^{N} \frac{\partial \omega_y(\bar{p}^*,\bar{u}^*,\bar{v}^*)}{\partial u_i}(u_i^*-\bar{u}_i^*) + \sum_{i=1}^{N} \frac{\partial \omega_y(\bar{p}^*,\bar{u}^*,\bar{v}^*)}{\partial v_i}(v_i^*-\bar{v}_i^*) \tag{6.63e}$$

$$\omega_z^* \simeq \bar{\omega}_z^* + \sum_{i=1}^{N} \frac{\partial \omega_z(\bar{p}^*,\bar{u}^*,\bar{v}^*)}{\partial u_i}(u_i^*-\bar{u}_i^*) + \sum_{i=1}^{N} \frac{\partial \omega_z(\bar{p}^*,\bar{u}^*,\bar{v}^*)}{\partial v_i}(v_i^*-\bar{v}_i^*) \tag{6.63f}$$

and

$$P^*_{yj} \simeq \bar{P}^*_{yj} + \frac{\partial P_{yn}(\bar{p}^*,\bar{u}^*,\bar{v}^*)}{\partial u_j}(u^*_j-\bar{u}^*_j) + \frac{\partial P_{yn}(\bar{p}^*,\bar{u}^*,\bar{v}^*)}{\partial v_j}(v^*_j-\bar{v}^*_j) \tag{6.63g}$$

In the above, the true parameter values are approximated by the first order Taylor series expansions of the u and v components.

Let

$$|u^*_i-\bar{u}^*_i| \leq \delta/2 \text{ and } |v^*_i-\bar{v}^*_i| \leq \delta/2$$

for i = 1,...,N. Then a simple algebraic manipulation of (4.63) leads to

$$|k^*_x-\bar{k}^*_x| \leq \delta\{\sum_{i=1}^{N}\left|\frac{\partial k_x(\bar{p}^*,\bar{u}^*,\bar{v}^*)}{\partial u_i}\right| + \sum_{i=1}^{N}\left|\frac{\partial k_x(\bar{p}^*,\bar{u}^*,\bar{v}^*)}{\partial v_i}\right|\} \tag{6.64a}$$

$$|k^*_y-\bar{k}^*_y| \leq \delta\{\sum_{i=1}^{N}\left|\frac{\partial k_y(\bar{p}^*,\bar{u}^*,\bar{v}^*)}{\partial u_i}\right| + \sum_{i=1}^{N}\left|\frac{\partial k_y(\bar{p}^*,\bar{u}^*,\bar{v}^*)}{\partial v_i}\right|\} \tag{6.64b}$$

$$|k^*_z-\bar{k}^*_z| \leq \delta\{\sum_{i=1}^{N}\left|\frac{\partial k_z(\bar{p}^*,\bar{u}^*,\bar{v}^*)}{\partial u_i}\right| + \sum_{i=1}^{N}\left|\frac{\partial k_z(\bar{p}^*,\bar{u}^*,\bar{v}^*)}{\partial v_i}\right|\} \tag{6.64c}$$

$$|\omega^*_x-\bar{\omega}^*_x| \leq \delta\{\sum_{i=1}^{N}\left|\frac{\partial \omega_x(\bar{p}^*,\bar{u}^*,\bar{v}^*)}{\partial u_i}\right| + \sum_{i=1}^{N}\left|\frac{\partial \omega_x(\bar{p}^*,\bar{u}^*,\bar{v}^*)}{\partial v_i}\right|\} \tag{4.64d}$$

$$|\omega^*_y-\bar{\omega}^*_y| \leq \delta\{\sum_{i=1}^{N}\left|\frac{\partial \omega_y(\bar{p}^*,\bar{u}^*,\bar{v}^*)}{\partial u_i}\right| + \sum_{i=1}^{N}\left|\frac{\partial \omega_y(\bar{p}^*,\bar{u}^*,\bar{v}^*)}{\partial v_i}\right|\} \tag{6.64e}$$

$$|\omega^*_z-\bar{\omega}^*_z| \leq \delta\{\sum_{i=1}^{N}\left|\frac{\partial \omega_z(\bar{p}^*,\bar{u}^*,\bar{v}^*)}{\partial u_i}\right| + \sum_{i=1}^{N}\left|\frac{\partial \omega_z(\bar{p}^*,\bar{u}^*,\bar{v}^*)}{\partial v_i}\right|\} \tag{6.64f}$$

and

$$|P^*_{yj}-\bar{P}^*_{yj}| \leq \delta\{\left|\frac{\partial P_{yn}(\bar{p}^*,\bar{u}^*,\bar{v}^*)}{\partial u_j}\right| + \left|\frac{\partial P_{yn}(\bar{p}^*,\bar{u}^*,\bar{v}^*)}{\partial v_j}\right|\} \tag{6.64g}$$

For the determination of the partial derivatives in (4.64), let s be the vector such that

$$s = (k_x, k_y, k_z, \omega_x, \omega_y, \omega_z, P_{y1}, \ldots P_{yN})'$$

and η be the function of s, u, and v such that

$$\begin{aligned}\eta(s,u,v) &= \sum\{ k_x - (x_n/f)k_y - (u_n/f)P_{yn} + (x_n z_n/f^2)\omega_x P_{yn} \\ &\quad + (z_n/f)\omega_y P_{yn} - (x_n^2/f^2+1)\omega_z P_{yn}\}^2 \\ &\quad + \sum\{ k_z - (z_n/f)k_y - (v_n/f)P_{yn} + (z_n^2/f^2+1)\omega_x P_{yn} \\ &\quad - (x_n/f)\omega_y P_{yn} - (x_n z_n/f^2)\omega_z P_{yn}\}^2 \\ &\quad + \lambda (\sum P_{yn} - I). \end{aligned} \tag{4.65}$$

Let $\bar{s}^*$, $\bar{u}^*$, and $\bar{v}^*$ be the vectors such that

$$\bar{s}^* = (\bar{k}^*_x, \bar{k}^*_y, \bar{k}^*_z, \bar{\omega}^*_x, \bar{\omega}^*_y, \bar{\omega}^*_z, \bar{P}^*_{y1}, \ldots, \bar{P}^*_{yN})'$$

$$\bar{u}^* = (\bar{u}^*_1, \ldots, \bar{u}^*_N)'$$

and $\bar{v}^* = (\bar{v}^*_1, \ldots, \bar{v}^*_N)'$.

Then we have

$$\frac{\partial \eta(\bar{s}^*,\bar{u}^*,\bar{v}^*)}{\partial s_i} = 0 \quad \text{for } i=1,\ldots,N+6. \tag{4.66}$$

because the minimum solution $\bar{s}^*$ is the critical point of the function η. Differentiating (4.66) with respect to u_j and v_j, we have for $i=1,\ldots,N+6$

$$\sum_{k=1}^{N+6} \left\{\frac{\partial^2 \eta(\bar{s}^*,\bar{u}^*,\bar{v}^*)}{\partial s_k \partial s_i} \frac{\partial s_k(\bar{s}^*,\bar{u}^*,\bar{v}^*)}{\partial u_j}\right\} + \frac{\partial \eta(\bar{s}^*,\bar{u}^*,\bar{v}^*)}{\partial u_j} = 0 \tag{4.67}$$

and

$$\sum_{k=1}^{N+6} \left\{\frac{\partial^2 \eta(\bar{s}^*,\bar{u}^*,\bar{v}^*)}{\partial s_k \partial s_i} \frac{\partial s_k(\bar{s}^*,\bar{u}^*,\bar{v}^*)}{\partial v_j}\right\} + \frac{\partial \eta(\bar{s}^*,\bar{u}^*,\bar{v}^*)}{\partial v_j} = 0 \tag{4.68}$$

Although we can solve the $(N+6)\times(N+6)$ systems of (4.67) and (4.68) for the partial derivatives, we observe that

$$\frac{\partial s_k(\bar{s}^*,\bar{u}^*,\bar{v}^*)}{\partial u_j} = \frac{\partial s_k(\bar{s}^*,\bar{u}^*,\bar{v}^*)}{\partial v_j} = 0 \quad \text{if } k>6 \text{ and } k-6\neq j,$$

because P_{yk}, which is s_{k+6}, is the function of q and u_k, and v_k only. Thus, we have

$$\sum_{k=1}^{6} \left\{\frac{\partial^2 \eta(\bar{s}^*,\bar{u}^*,\bar{v}^*)}{\partial s_k \partial s_i} \frac{\partial s_k(\bar{s}^*,\bar{u}^*,\bar{v}^*)}{\partial u_j}\right\} + \frac{\partial^2 \eta(\bar{s}^*,\bar{u}^*,\bar{v}^*)}{\partial s_{j+6} \partial s_i} \frac{\partial s_{j+6}(\bar{s}^*,\bar{u}^*,\bar{v}^*)}{\partial u_j} + \frac{\partial \eta(\bar{s}^*,\bar{u}^*,\bar{v}^*)}{\partial u_j} = 0 \tag{4.69}$$

and

$$\sum_{k=1}^{6} \left\{\frac{\partial^2 \eta(\bar{s}^*,\bar{u}^*,\bar{v}^*)}{\partial s_k \partial s_i} \frac{\partial s_k(\bar{s}^*,\bar{u}^*,\bar{v}^*)}{\partial v_j}\right\}$$

$$+ \frac{\partial^2 \eta(\bar{s}^*, \bar{u}^*, \bar{v}^*)}{\partial s_{j+6} \partial s_i} \frac{\partial s_{j+6}(\bar{s}^*, \bar{u}^*, \bar{v}^*)}{\partial v_j} + \frac{\partial \eta(\bar{s}^*, \bar{u}^*, \bar{v}^*)}{\partial v_j} = 0 \tag{4.70}$$

Computing the first and second partial derivatives of the function η and plugging them in (4.69) and (4.70), we have for u_j

$$\begin{bmatrix} A & B & b \\ B' & C & c \\ b' & c' & a_{77} \end{bmatrix} \begin{bmatrix} \frac{\partial k_x(\bar{s}^*, \bar{u}^*, \bar{v}^*)}{\partial u_j} \\ \frac{\partial k_y(\bar{s}^*, \bar{u}^*, \bar{v}^*)}{\partial u_j} \\ \frac{\partial k_z(\bar{s}^*, \bar{u}^*, \bar{v}^*)}{\partial u_j} \\ \frac{\partial \omega_x(\bar{s}^*, \bar{u}^*, \bar{v}^*)}{\partial u_j} \\ \frac{\partial \omega_y(\bar{s}^*, \bar{u}^*, \bar{v}^*)}{\partial u_j} \\ \frac{\partial \omega_z(\bar{s}^*, \bar{u}^*, \bar{v}^*)}{\partial u_j} \\ \frac{\partial p_{yj}(\bar{s}^*, \bar{u}^*, \bar{v}^*)}{\partial u_j} \end{bmatrix} = \begin{bmatrix} \sum \frac{P_{yn}}{f} \\ -\sum \frac{x_n}{f} P_{yn} \\ 0 \\ \sum \frac{x_n z_n}{f^3} P_{yn}^2 \\ \sum \frac{z_n}{f^2} P_{yn}^2 \\ -\sum \frac{x_n^2 + f^2}{f^3} P_{yn}^2 \\ -\frac{P^*_{yj}}{f} a_{1j} \end{bmatrix} \tag{4.71}$$

where

$$A = \sum_n \begin{bmatrix} 1 & \frac{-x_n}{f} & 0 \\ \frac{-x_n}{f} & \frac{x_n^2+z_n^2}{f^2} & \frac{-z_n}{f} \\ 0 & \frac{-z_n}{f} & 1 \end{bmatrix} \qquad (4.72)$$

$$B = \sum_n P_{yn} \begin{bmatrix} \frac{x_n z_n}{f^2} & \frac{z_n}{f} & \frac{-(x_n^2+f^2)}{f^2} \\ \frac{-z_n(x_n^2+z_n^2+f^2)}{f^3} & 0 & \frac{x_n(x_n^2+z_n^2+f^2)}{f^3} \\ \frac{z_n^2+f^2}{f^2} & \frac{-x_n}{f} & \frac{-x_n z_n}{f^2} \end{bmatrix} \qquad (4.73)$$

$$C = \sum_n P_{yn}^2 \begin{bmatrix} \frac{x_n z_n+(z_n^2+f^2)^2}{f^4} & \frac{-x_n}{f} & \frac{-x_n z_n(x_n^2+z_n^2+2f^2)}{f^4} \\ \frac{-x_n}{f} & \frac{z_n^2+f^2}{f^2} & \frac{-z_n}{f} \\ \frac{-x_n z_n(x_n^2+z_n^2+2f^2)}{f^4} & \frac{-z_n}{f} & \frac{(x_n^2+f^2)^2+x_n^2 z_n^2}{f^4} \end{bmatrix} \qquad (4.74)$$

$$b = \begin{bmatrix} \frac{x_j z_j}{f^2}\bar{\omega}_x^* + \frac{z_j}{f}\bar{\omega}_y^* - \frac{x_j^2+f^2}{f^2}\bar{\omega}_z^* - \frac{\bar{u}_j^*}{f} \\ -\frac{z_j(x_j^2+f^2+z_j^2)}{f^3}\bar{\omega}_x^* - \frac{x_j(x_j^2+f^2+z_j^2)}{f^3}\bar{\omega}_z^* - \frac{x_j\bar{u}_j^*+z_j\bar{v}_j^*}{f^2} \\ \frac{z_j^2+f^2}{f^2}\bar{\omega}_x^* - \frac{x_j}{f}\bar{\omega}_y^* - \frac{x_j z_j}{f^2}\bar{\omega}_z^* - \frac{\bar{v}_j^*}{f} \end{bmatrix} \quad (4.75)$$

$$c = \begin{bmatrix} \frac{x_j z_j}{f^2}(\varepsilon_{1j}+\bar{P}_{yj}^*\alpha_{1j}) + \frac{z_j^2+f^2}{f^2}(\varepsilon_{2j}+\bar{P}_{yj}^*\alpha_{1j}) \\ \frac{z_j}{f}(\varepsilon_{1j}+\bar{P}_{yj}^*\alpha_{1j}) - \frac{x_j}{f}(\varepsilon_{2j}+\bar{P}_{yj}^*\alpha_{1j}) \\ -\frac{x_j^2+f^2}{f^2}(\varepsilon_{1j}+\bar{P}_{yj}^*\alpha_{1j}) - \frac{x_j z_j}{f^2}(\varepsilon_{2j}+\bar{P}_{yj}^*\alpha_{1j}) \end{bmatrix} \quad (4.76)$$

and

$$a_{77} = \alpha_{1j}^2 + \alpha_{1j}^2. \quad (4.77)$$

In the above ε_{1j}, ε_{2j}, α_{1j}, and α_{1j} are computed from

$$\varepsilon_{1j} = \bar{k}_x^* - \frac{x_j}{f}\bar{k}_y^* - \frac{\bar{u}_j^*}{f}\bar{P}_{yj}^* + \frac{x_j z_j}{f^2}\bar{P}_{yj}^*\bar{\omega}_x^* + \frac{z_j}{f}\bar{P}_{yj}^*\bar{\omega}_y^* - \frac{x_j^2+f^2}{f^2}\bar{P}_{yj}^*\bar{\omega}_z^* \quad (4.78)$$

$$\varepsilon_{2j} = \bar{k}_z^* - \frac{z_j}{f}\bar{k}_y^* - \frac{\bar{v}_j^*}{f}\bar{P}_{yj}^* + \frac{z_j+f^2}{f^2}\bar{P}_{yj}^*\bar{\omega}_x^* - \frac{x_j}{f}\bar{P}_{yj}^*\bar{\omega}_y^* - \frac{x_j z_j}{f^2}\bar{P}_{yj}^*\bar{\omega}_z^* \quad (4.79)$$

$$\alpha_{1j} = -\frac{x_j z_j}{f^2}\bar{\omega}_x^* + \frac{z_j}{f}\bar{\omega}_y^* - \frac{x_j^2+f^2}{f^2}\bar{\omega}_z^* - \frac{\bar{u}_j}{f} \qquad (4.80)$$

$$\alpha_{1j} = \frac{z_j^2+f^2}{f^2}\bar{\omega}_x^* - \frac{x_j}{f}\bar{\omega}_y^* - \frac{x_j z_j}{f^2}\bar{\omega}_z^* - \frac{\bar{v}_j}{f} \qquad (4.81)$$

Similarly we have for v_j

$$\begin{bmatrix} A & B & b \\ B' & C & c \\ b' & c' & a_{77} \end{bmatrix} \begin{bmatrix} \frac{\partial k_x(\bar{s}^*,\bar{u}^*,\bar{v}^*)}{\partial v_j} \\ \frac{\partial k_y(\bar{s}^*,\bar{u}^*,\bar{v}^*)}{\partial v_j} \\ \frac{\partial k_z(\bar{s}^*,\bar{u}^*,\bar{v}^*)}{\partial v_j} \\ \frac{\partial \omega_x(\bar{s}^*,\bar{u}^*,\bar{v}^*)}{\partial v_j} \\ \frac{\partial \omega_y(\bar{s}^*,\bar{u}^*,\bar{v}^*)}{\partial v_j} \\ \frac{\partial \omega_z(\bar{s}^*,\bar{u}^*,\bar{v}^*)}{\partial v_j} \\ \frac{\partial p_{yj}(\bar{s}^*,\bar{u}^*,\bar{v}^*)}{\partial v_j} \end{bmatrix} = \begin{bmatrix} 0 \\ -\sum \frac{z_n}{f} P_{yn} \\ -\sum \frac{P_{yn}}{f} \\ -\sum \frac{z_n^2+f^2}{f^3} P_{yn}^2 \\ -\sum \frac{x_n}{f^2} P_{yn}^2 \\ -\sum \frac{x_n z_n}{f^3} P_{yn}^2 \\ -\frac{P_{yj}^*}{f}\alpha_{1j} \end{bmatrix} \qquad (4.82)$$

where A, B, C, b, c, a_{77}, ε_{1j}, ε_{2j}, α_{1j}, and α_{1j} are the same as those in (4.72)-(4.81)

Solving (4.71) and (4.82) for u_j and v_j, j=1...N, we can determine the partial derivatives of the motion parameters

and relative depths with respect to the two optic flow vectors, u and v. Substituting these partial derivatives in (4.65), we can compute the error bounds of the estimated motion parameters and relative depths.

4.6 Motion Parameters Estimation

In this section we apply the algorithm developed in this chapter to optic flow images computed in chapter 3 to estimate the motion parameters of moving ellipsoids and the turning car.

For the optic flow images from the pure translational sequence, we estimate the translational velocity direction by the eigenvector of the matrix in equation (4.31) having smallest eigenvalue. Using the EISPACK routines to compute eigenvalues and corresponding vectors, we obtain the translational velocity direction

(-.62647755E+00, .29356266E-04, -.77943946E+00)'

for the Facet approach optic flow image of Fig 3.11 and

(-.79385524E+00, .20142616E-01, -.60777309E+00)'

for the Horn and Schunk optic flow image of Fig 3.20. Comparing with the ideal translational direction (-.8, 0., -1.)', i.e. (-.62470, 0., -.78087)' when normalized, we compute almost the ideal direction from the facet approach optic flow image Fig 3.11, but we could not from the Horn and Schunk optic flow image Fig 3.20. In fact, there is about 14.0 degree error in the direction of translational velocity vector for the Horn and Schunk

procedure. Removing the optic flow vectors propagated into the background in Fig 3.20, we have the optic flow image in Fig 4.3. For this optic flow image, we estimate the translational velocity direction

(-.7127596E+00, .5564735E-2, -.70138632E+00)'

which is about a 6.8 degree error in the direction.

When the nonzero translational motion components are determined, we can compute the relative depth of optic flow image points using equation (4.30). The optic flow images in Fig 3.11 and Fig 4.3 are obtained from the brightness moving on the image plane normal to the optical axis. This implies that the ideal relative depth is zero. However, from the facet optic flow image in Fig 3.11 and the translational components determined, we compute the relative depth between .1548 and .421 which are shown in Fig 4.4. From the Horn and Schunk optic flow image in Fig 4.3, we have the relative depth between .0049 and 1.426 which are shown in Fig 4.4. We observe that the computed relative depth image in Fig 4.4 shows some smoothness in the variation of the depth. In fact, this smoothness comes from the imposed smoothness constraint in computing the optic flow vector. The contraction of the brightness ellipsoid in the image sequence of Fig 3.13 seem to show the backward motion of the ellipsoid. However, the contraction of the brightness ellipsoid does not account for the perspective

transformation of the ellipsoid moving backward. Thus, the optic flow images in Fig 3.14 and Fig 3.21 shows the contraction of the brightness ellipsoid, not the backward motion of the ellipsoid. We will show an ideal optic flow image of the ellipsoid moving backward in Fig 4.6.

For the optic flow images from the pure rotational sequence, we compute the angular velocity $(\omega_x, \omega_y, \omega_z)'$ directly by equation (4.34), (4.35) and (4.36), and we have

(-.33591593E-09, .91833494E-01, .19956943E-08)'

for the Facet approach optic flow image of Fig 3.14 and

(.6778587E-03, .66410548E-02, -.57151997E-03)'

for the Horn and Schunk optic flow image of Fig 3.22. From the facet model optic flow image, we recover the rotational motion components with the 10 percent error. However, from the Horn and Schunk optic flow image, we recover the rotational motion components far from the the true values. In the case of pure rotational motion, it is not possible to recover relative depth from the optic flow image.

For the optic flow images from the general motion sequence, we determine motion parameters iteratively using equation (4.38) and (4.39). Suppose an ellipsoid moves with the translational velocity (1,1,1)' and the rotational

angular velocity (.1,.2,.5)'. Let the ellipse be positioned such that the relative depth is shown in Fig 4.7. Computing 3D optic flow vectors on the surface of this ellipsoid and projecting the vectors on the image plane in perspective, we have the optic flow image superimposed on the depth image in Fig 4.8. Computing the motion parameters and the depths iteratively from the optic flow image, we have Table 4.1 showing the motion parameter values converging to the ideal and the recovered depth image on Fig 4.9. For the ellipsoid moving with $k=(-1,-1,-1)'$ and $\Omega=(.1,-.2,.5)'$, we have the optic flow image shown in Fig 4.9. Computing the motion parameters and depths iteratively from Fig 4.10, we have Table 4.2 showing the converging motion parameter values and the recovered depth image in Fig 4.11.

The computed optic flow image in Fig 3.19 has some optic flow vectors which do not show the motion of the car. To analyze the optic flow image, we construct a histogram of the row and column components of the flow vectors. In Fig 4.12 we have the histogram of the row components and in Fig 4.13 we have for the column components. From the histogram in Fig 4.12, we observe that most row component values are in the range of -2 and .04 and from Fig 4.13, we observe that most column component values are in the range of -2 and .34. Applying the iterative technique to the optic flows in Fig 3.19 whose row and column component values are in the above range, we obtain Table 4.3 showing the

converging motion parameters of the car. This table show that the car moves with $k=(-89.6,-.14,72.7)'$, which shows the direction we observe from the image sequence in Fig 3.18. Also, the car rotates with $\Omega=(-.00032,-.0016,-.00046)'$ which shows the clockwise rotation of the car, mainly about the y axis.

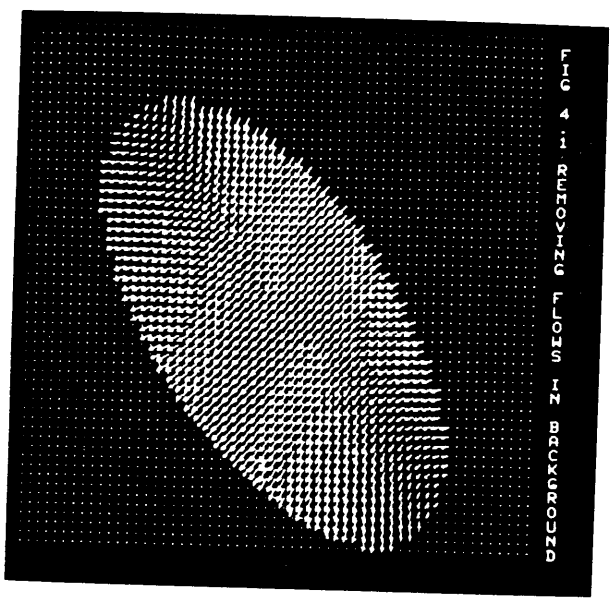

Fig 4.3 Horn and Schunk optic flow image from ellipsoid translation sequence of Fig 3.5 with optic flow set to zero for background pixles.

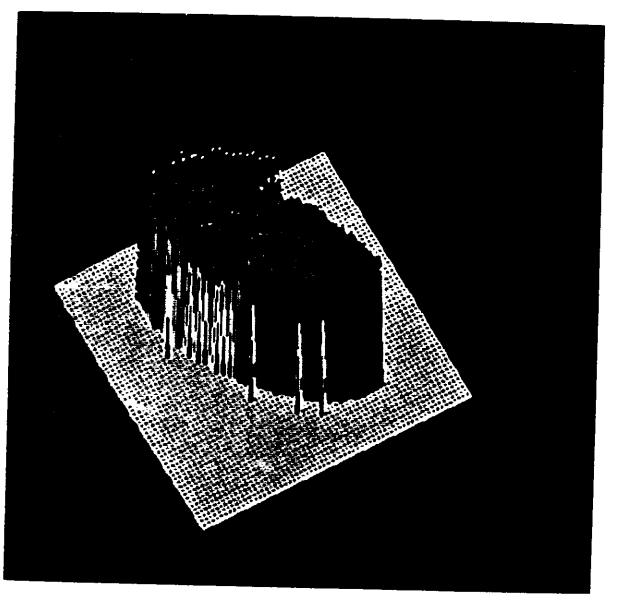

Fig 4.4 Recovered Depth Image using the Facet Model to Compute the the Optic Flow Field shown in Fig 3.11

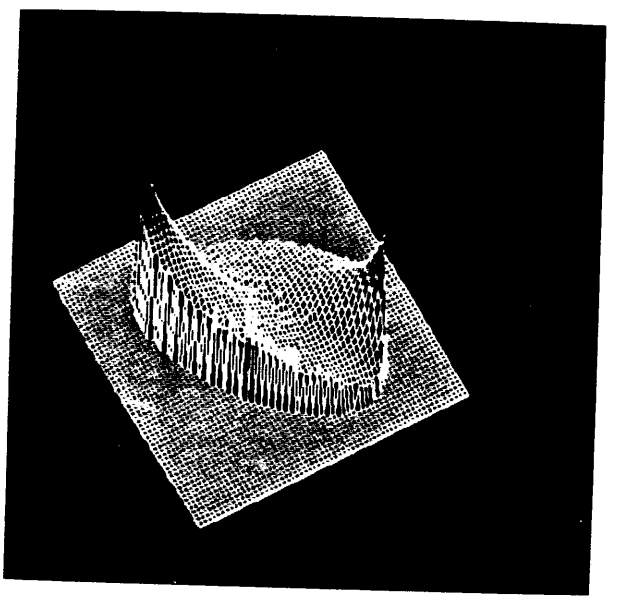

Fig 4.5 Recovered Depth Image using the Horn and Schunk Method to Compute the Optic Flow Field in Fig 4.2

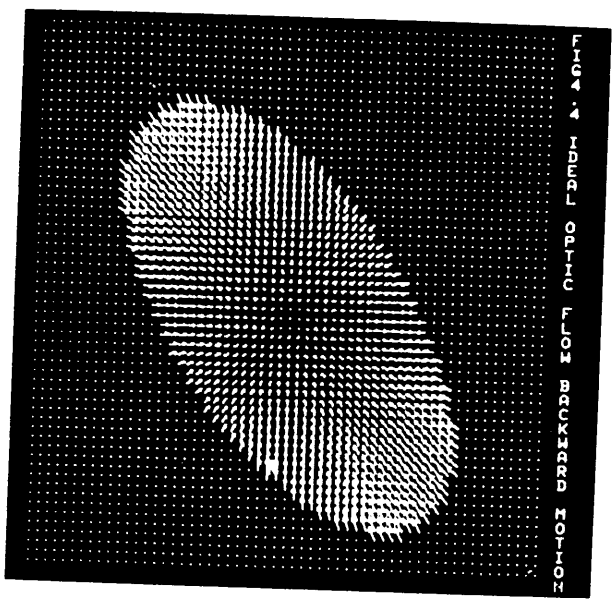

Fig 4.6 Synthesized Optic Flow Image of the Ellipsoid Moving Backward.

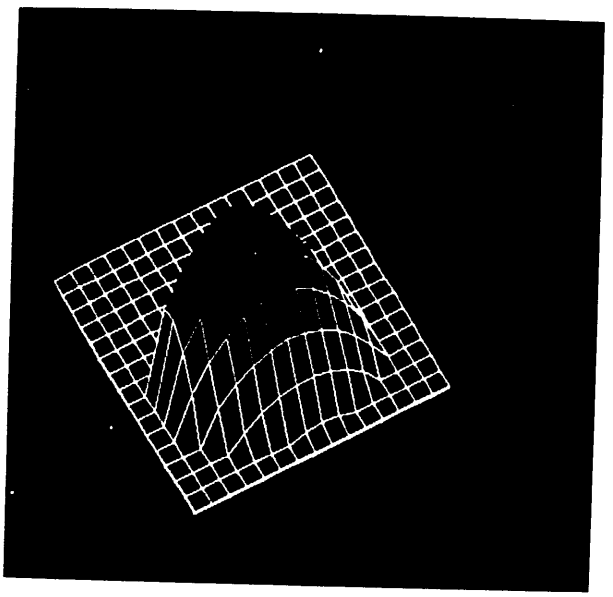

Fig 4.7 Ideal Depth Image of an Ellipsoid

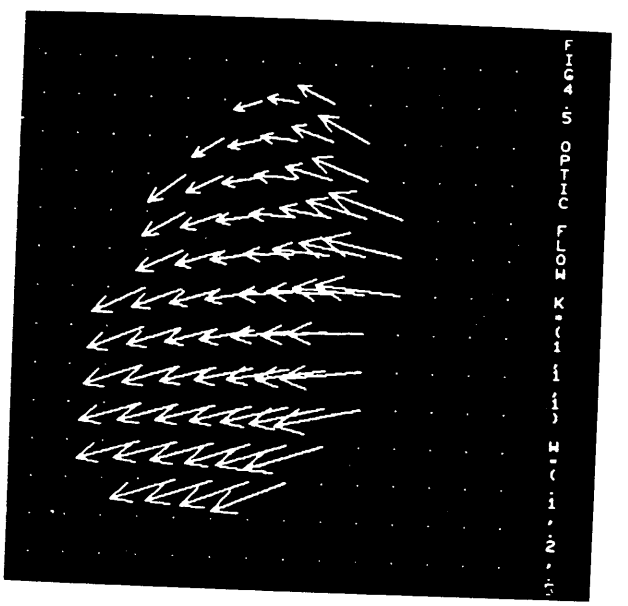

Fig 4.8 Synthesized Optic Flow Image of the Ellipsoid in Fig 4.6 Moving with $k=(1,1,1)'$ and $\Omega=(.1,.2,.5)'$

ITERATIVE SOLUTION FROM OPTIC FLOWS k=(1,1,1)',Ω=(.1,.2,.5)'

ITER	kx	ky	kz	Ωx	Ωy	Ωz
1	0.2999E+01	0.3611E+01	0.2998E+01	0.1053E+00	0.1959E+00	0.4943E+00
2	0.3073E+01	0.3717E+01	0.3218E+01	0.1039E+00	0.1982E+00	0.4945E+00
3	0.3247E+01	0.3759E+01	0.3311E+01	0.1033E+00	0.1991E+00	0.4958E+00
4	0.3397E+01	0.3775E+01	0.3368E+01	0.1028E+00	0.1994E+00	0.4970E+00
5	0.3497E+01	0.3779E+01	0.3413E+01	0.1025E+00	0.1996E+00	0.4979E+00
6	0.3559E+01	0.3778E+01	0.3454E+01	0.1022E+00	0.1997E+00	0.4984E+00
7	0.3599E+01	0.3774E+01	0.3491E+01	0.1019E+00	0.1997E+00	0.4988E+00
8	0.3625E+01	0.3770E+01	0.3524E+01	0.1016E+00	0.1998E+00	0.4990E+00
9	0.3645E+01	0.3765E+01	0.3553E+01	0.1014E+00	0.1998E+00	0.4992E+00
10	0.3659E+01	0.3761E+01	0.3578E+01	0.1012E+00	0.1998E+00	0.4993E+00
11	0.3671E+01	0.3757E+01	0.3600E+01	0.1010E+00	0.1998E+00	0.4994E+00
12	0.3680E+01	0.3753E+01	0.3619E+01	0.1009E+00	0.1999E+00	0.4995E+00
13	0.3688E+01	0.3750E+01	0.3635E+01	0.1008E+00	0.1999E+00	0.4996E+00
14	0.3695E+01	0.3747E+01	0.3649E+01	0.1006E+00	0.1999E+00	0.4997E+00
15	0.3700E+01	0.3744E+01	0.3660E+01	0.1006E+00	0.1999E+00	0.4997E+00
16	0.3705E+01	0.3742E+01	0.3670E+01	0.1005E+00	0.1999E+00	0.4998E+00
17	0.3708E+01	0.3740E+01	0.3679E+01	0.1004E+00	0.1999E+00	0.4998E+00
18	0.3711E+01	0.3739E+01	0.3686E+01	0.1003E+00	0.1999E+00	0.4998E+00
19	0.3714E+01	0.3737E+01	0.3692E+01	0.1003E+00	0.1999E+00	0.4999E+00
20	0.3716E+01	0.3736E+01	0.3698E+01	0.1002E+00	0.2000E+00	0.4999E+00
21	0.3718E+01	0.3735E+01	0.3702E+01	0.1002E+00	0.2000E+00	0.4999E+00
22	0.3720E+01	0.3734E+01	0.3706E+01	0.1002E+00	0.2000E+00	0.4999E+00
23	0.3721E+01	0.3733E+01	0.3709E+01	0.1002E+00	0.2000E+00	0.4999E+00
24	0.3722E+01	0.3732E+01	0.3712E+01	0.1001E+00	0.2000E+00	0.4999E+00
25	0.3723E+01	0.3732E+01	0.3715E+01	0.1001E+00	0.2000E+00	0.4999E+00
26	0.3724E+01	0.3731E+01	0.3717E+01	0.1001E+00	0.2000E+00	0.5000E+00
27	0.3725E+01	0.3731E+01	0.3718E+01	0.1001E+00	0.2000E+00	0.5000E+00
28	0.3725E+01	0.3730E+01	0.3720E+01	0.1001E+00	0.2000E+00	0.5000E+00
29	0.3726E+01	0.3730E+01	0.3721E+01	0.1001E+00	0.2000E+00	0.5000E+00
30	0.3726E+01	0.3730E+01	0.3722E+01	0.1000E+00	0.2000E+00	0.5000E+00
31	0.3726E+01	0.3730E+01	0.3723E+01	0.1000E+00	0.2000E+00	0.5000E+00
32	0.3727E+01	0.3729E+01	0.3724E+01	0.1000E+00	0.2000E+00	0.5000E+00
33	0.3727E+01	0.3729E+01	0.3725E+01	0.1000E+00	0.2000E+00	0.5000E+00
34	0.3727E+01	0.3729E+01	0.3725E+01	0.1000E+00	0.2000E+00	0.5000E+00
35	0.3727E+01	0.3729E+01	0.3726E+01	0.1000E+00	0.2000E+00	0.5000E+00
36	0.3727E+01	0.3729E+01	0.3726E+01	0.1000E+00	0.2000E+00	0.5000E+00
37	0.3728E+01	0.3729E+01	0.3726E+01	0.1000E+00	0.2000E+00	0.5000E+00
38	0.3728E+01	0.3729E+01	0.3727E+01	0.1000E+00	0.2000E+00	0.5000E+00
39	0.3728E+01	0.3729E+01	0.3727E+01	0.1000E+00	0.2000E+00	0.5000E+00
40	0.3728E+01	0.3729E+01	0.3727E+01	0.1000E+00	0.2000E+00	0.5000E+00
41	0.3728E+01	0.3729E+01	0.3727E+01	0.1000E+00	0.2000E+00	0.5000E+00
42	0.3728E+01	0.3729E+01	0.3727E+01	0.1000E+00	0.2000E+00	0.5000E+00
43	0.3728E+01	0.3728E+01	0.3728E+01	0.1000E+00	0.2000E+00	0.5000E+00

Table 4.1 Iteratively Converging Motion Estimation from the Synthesized Optic Flow Image in Fig 4.6

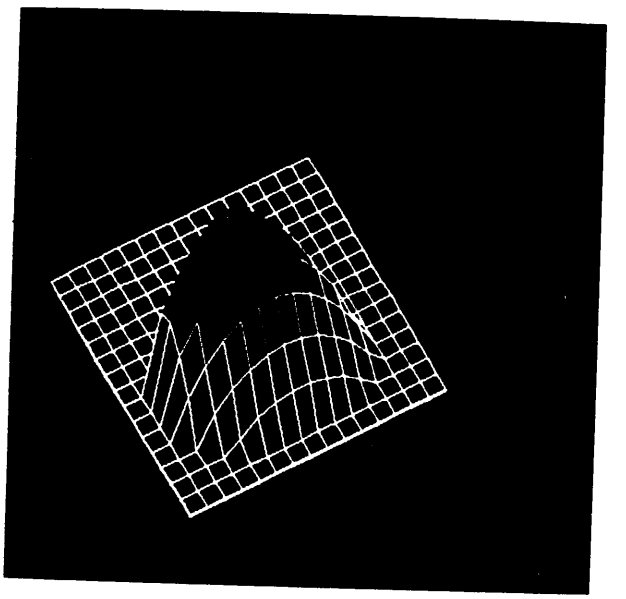

Fig 4.9 Recovered Depth Image from the Synthesized Optic Flow Image in Fig 4.7

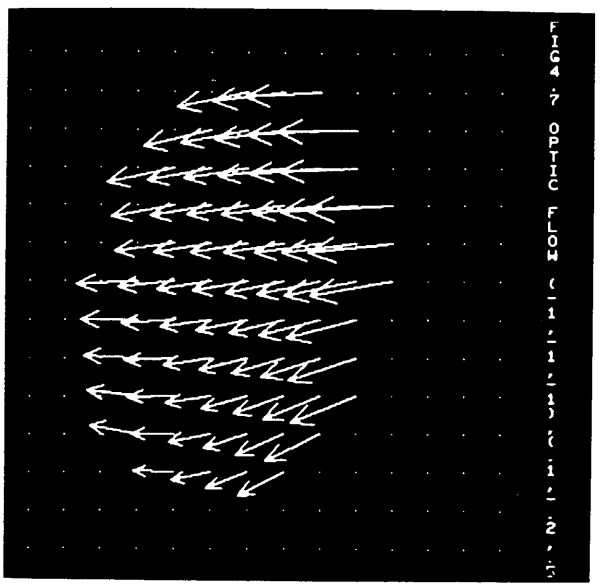

Fig 4.10 Synthesized Optic Flow Image of the Ellipsoid in Fig 4.6 Moving with $k=(-1,-1,-1)'$ and $\Omega=(.1,-.2,.5)'$

ITERATIVE SOLUTION FROM OPTIC FLOWS k=(-1,-1,-1)', Ω=(.1,-.2,.5)'

ITER	kx	ky	kz	Ωx	Ωy	Ωz
1	-0.2999E+01	-0.3611E+01	-0.2998E+01	0.9473E-01	-0.1959E+00	0.5057E+00
2	-0.3073E+01	-0.3717E+01	-0.3218E+01	0.9606E-01	-0.1982E+00	0.5055E+00
3	-0.3247E+01	-0.3759E+01	-0.3311E+01	0.9673E-01	-0.1991E+00	0.5042E+00
4	-0.3397E+01	-0.3775E+01	-0.3368E+01	0.9715E-01	-0.1994E+00	0.5030E+00
5	-0.3497E+01	-0.3779E+01	-0.3413E+01	0.9750E-01	-0.1996E+00	0.5021E+00
6	-0.3559E+01	-0.3778E+01	-0.3454E+01	0.9781E-01	-0.1997E+00	0.5016E+00
7	-0.3599E+01	-0.3774E+01	-0.3491E+01	0.9810E-01	-0.1997E+00	0.5012E+00
8	-0.3625E+01	-0.3770E+01	-0.3524E+01	0.9836E-01	-0.1998E+00	0.5010E+00
9	-0.3645E+01	-0.3765E+01	-0.3553E+01	0.9859E-01	-0.1998E+00	0.5008E+00
10	-0.3659E+01	-0.3761E+01	-0.3578E+01	0.9879E-01	-0.1998E+00	0.5007E+00
11	-0.3671E+01	-0.3757E+01	-0.3600E+01	0.9896E-01	-0.1998E+00	0.5006E+00
12	-0.3680E+01	-0.3753E+01	-0.3619E+01	0.9911E-01	-0.1999E+00	0.5005E+00
13	-0.3688E+01	-0.3750E+01	-0.3635E+01	0.9924E-01	-0.1999E+00	0.5004E+00
14	-0.3695E+01	-0.3747E+01	-0.3649E+01	0.9935E-01	-0.1999E+00	0.5003E+00
15	-0.3700E+01	-0.3744E+01	-0.3660E+01	0.9945E-01	-0.1999E+00	0.5003E+00
16	-0.3705E+01	-0.3742E+01	-0.3670E+01	0.9953E-01	-0.1999E+00	0.5002E+00
17	-0.3708E+01	-0.3740E+01	-0.3679E+01	0.9960E-01	-0.1999E+00	0.5002E+00
18	-0.3711E+01	-0.3739E+01	-0.3686E+01	0.9966E-01	-0.1999E+00	0.5002E+00
19	-0.3714E+01	-0.3737E+01	-0.3692E+01	0.9971E-01	-0.1999E+00	0.5001E+00
20	-0.3716E+01	-0.3736E+01	-0.3698E+01	0.9975E-01	-0.2000E+00	0.5001E+00
21	-0.3718E+01	-0.3735E+01	-0.3702E+01	0.9979E-01	-0.2000E+00	0.5001E+00
22	-0.3720E+01	-0.3734E+01	-0.3706E+01	0.9982E-01	-0.2000E+00	0.5001E+00
23	-0.3721E+01	-0.3733E+01	-0.3709E+01	0.9985E-01	-0.2000E+00	0.5001E+00
24	-0.3722E+01	-0.3732E+01	-0.3712E+01	0.9987E-01	-0.2000E+00	0.5001E+00
25	-0.3723E+01	-0.3732E+01	-0.3715E+01	0.9989E-01	-0.2000E+00	0.5001E+00
26	-0.3724E+01	-0.3731E+01	-0.3717E+01	0.9991E-01	-0.2000E+00	0.5000E+00
27	-0.3725E+01	-0.3731E+01	-0.3718E+01	0.9992E-01	-0.2000E+00	0.5000E+00
28	-0.3725E+01	-0.3730E+01	-0.3720E+01	0.9993E-01	-0.2000E+00	0.5000E+00
29	-0.3726E+01	-0.3730E+01	-0.3721E+01	0.9994E-01	-0.2000E+00	0.5000E+00
30	-0.3726E+01	-0.3730E+01	-0.3722E+01	0.9995E-01	-0.2000E+00	0.5000E+00
31	-0.3726E+01	-0.3730E+01	-0.3723E+01	0.9996E-01	-0.2000E+00	0.5000E+00
32	-0.3727E+01	-0.3729E+01	-0.3724E+01	0.9996E-01	-0.2000E+00	0.5000E+00
33	-0.3727E+01	-0.3729E+01	-0.3725E+01	0.9997E-01	-0.2000E+00	0.5000E+00
34	-0.3727E+01	-0.3729E+01	-0.3725E+01	0.9997E-01	-0.2000E+00	0.5000E+00
35	-0.3727E+01	-0.3729E+01	-0.3726E+01	0.9998E-01	-0.2000E+00	0.5000E+00
36	-0.3727E+01	-0.3729E+01	-0.3726E+01	0.9998E-01	-0.2000E+00	0.5000E+00
37	-0.3728E+01	-0.3729E+01	-0.3726E+01	0.9998E-01	-0.2000E+00	0.5000E+00
38	-0.3728E+01	-0.3729E+01	-0.3727E+01	0.9999E-01	-0.2000E+00	0.5000E+00
39	-0.3728E+01	-0.3729E+01	-0.3727E+01	0.9999E-01	-0.2000E+00	0.5000E+00
40	-0.3728E+01	-0.3729E+01	-0.3727E+01	0.9999E-01	-0.2000E+00	0.5000E+00
41	-0.3728E+01	-0.3729E+01	-0.3727E+01	0.9999E-01	-0.2000E+00	0.5000E+00
42	-0.3728E+01	-0.3729E+01	-0.3727E+01	0.9999E-01	-0.2000E+00	0.5000E+00
43	-0.3728E+01	-0.3728E+01	-0.3728E+01	0.9999E-01	-0.2000E+00	0.5000E+00
44	-0.3728E+01	-0.3728E+01	-0.3728E+01	0.9999E-01	-0.2000E+00	0.5000E+00
45	-0.3728E+01	-0.3728E+01	-0.3728E+01	0.1000E+00	-0.2000E+00	0.5000E+00

Table 4.2 Iterative Motion Estimation from the Synthesized Optic Flow Image in Fig 4.9. The table shows the motion parameter values converging the true motion k=(-1,-1,-1)' and Ω=(.1,-.2,.5)'.

Table 4.2 Iteratively Converging Motion Estimation from the Synthesized Optic Flow Image in Fig 4.9

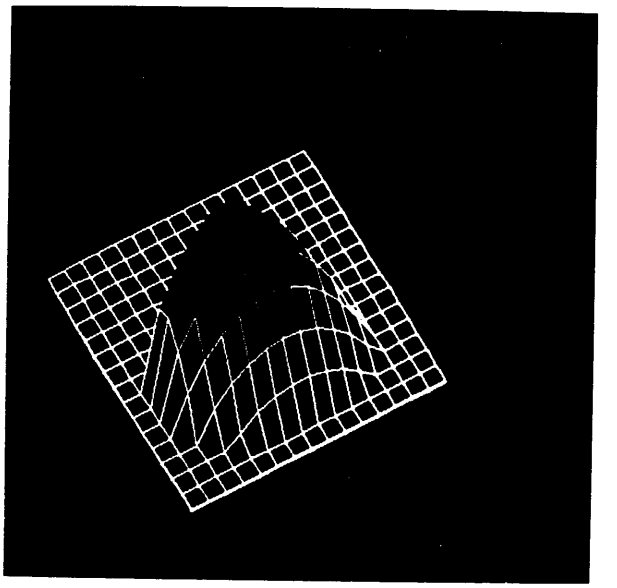

Fig 4.11 Recovered Depth Image from the Synthesized Optic Flow Image in Fig 4.9

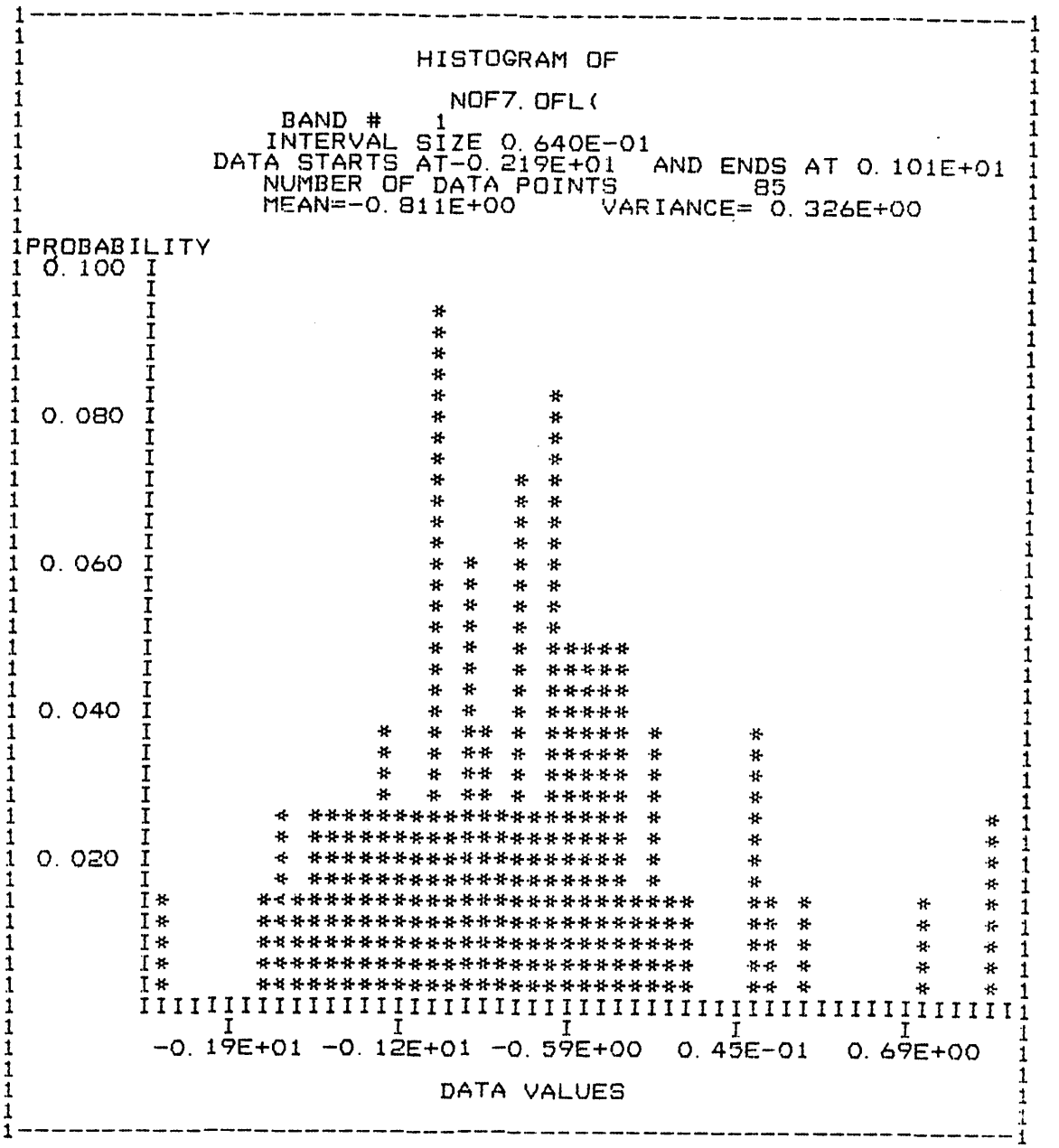

Fig 4.12 Histogram of row optic flow components in the Optic Flow Image of Fig 3.19.

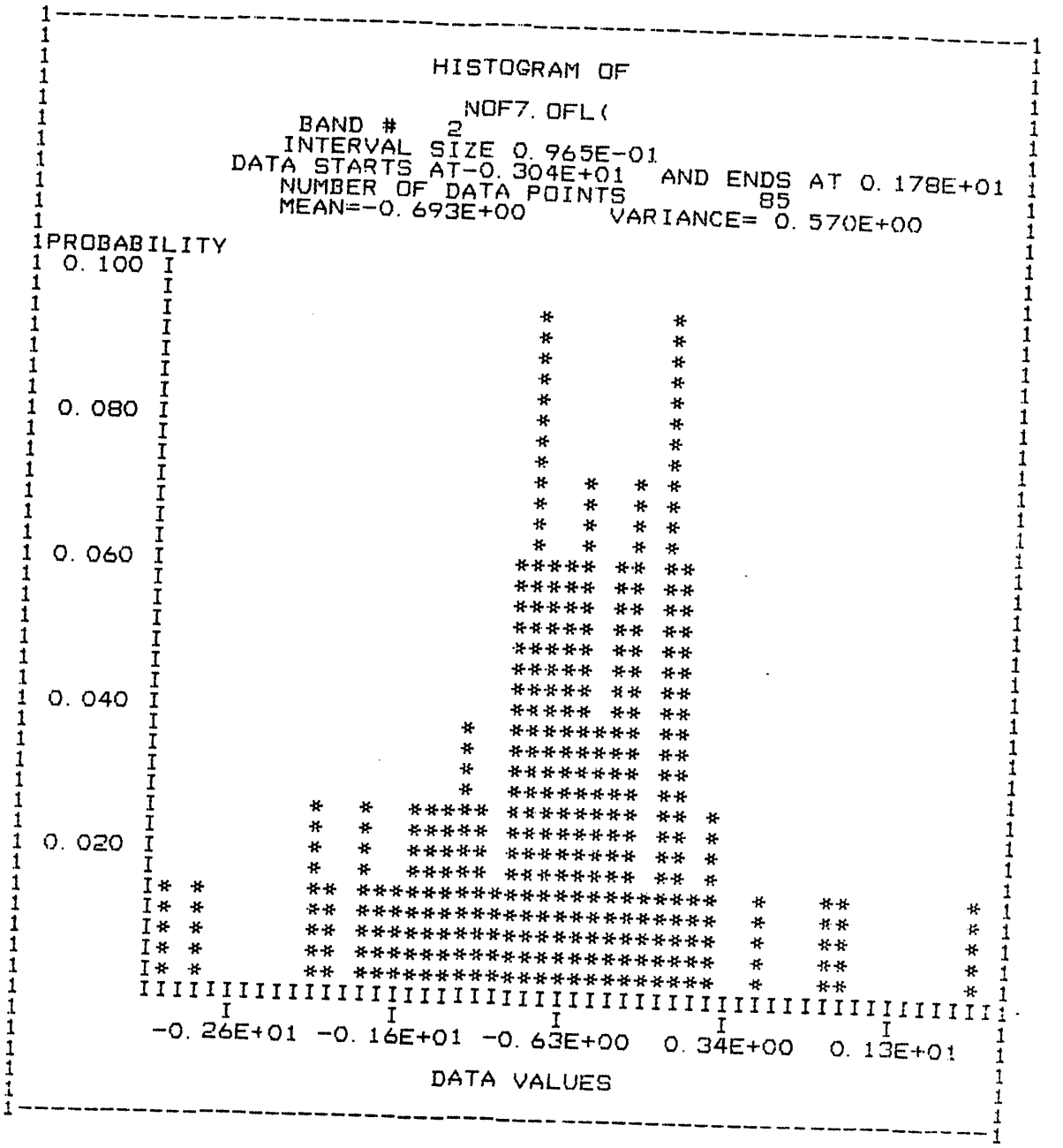

Fig 4.13 Histogram of column optic flow components in the Optic Flow Image of Fig 3.19.

ITERATIVE MOTION RECOVERY OF THE MOVING CAR

ITER	kx	ky	kz	Ωx	Ωy	Ωz
1	-0.9203E+02	-0.8477E+00	0.9617E+02	-0.1215E-03	-0.1765E-02	-0.3982E-03
2	-0.8459E+02	-0.1033E+01	0.9488E+02	-0.2869E-03	-0.4501E-02	-0.5534E-03
3	-0.8806E+02	-0.8313E+00	0.9137E+02	-0.3275E-03	-0.4584E-02	-0.5655E-03
4	-0.9119E+02	-0.6506E+00	0.8853E+02	-0.3422E-03	-0.4468E-02	-0.5579E-03
5	-0.9327E+02	-0.5161E+00	0.8633E+02	-0.3496E-03	-0.4327E-02	-0.5484E-03
6	-0.9454E+02	-0.4188E+00	0.8460E+02	-0.3533E-03	-0.4171E-02	-0.5396E-03
7	-0.9525E+02	-0.3486E+00	0.8319E+02	-0.3547E-03	-0.4008E-02	-0.5318E-03
8	-0.9557E+02	-0.2979E+00	0.8202E+02	-0.3546E-03	-0.3843E-02	-0.5249E-03
9	-0.9564E+02	-0.2612E+00	0.8104E+02	-0.3536E-03	-0.3681E-02	-0.5188E-03
10	-0.9553E+02	-0.2343E+00	0.8020E+02	-0.3520E-03	-0.3524E-02	-0.5134E-03
11	-0.9532E+02	-0.2145E+00	0.7946E+02	-0.3501E-03	-0.3375E-02	-0.5086E-03
12	-0.9504E+02	-0.1998E+00	0.7882E+02	-0.3479E-03	-0.3235E-02	-0.5043E-03
13	-0.9472E+02	-0.1886E+00	0.7825E+02	-0.3458E-03	-0.3104E-02	-0.5004E-03
14	-0.9440E+02	-0.1801E+00	0.7774E+02	-0.3436E-03	-0.2982E-02	-0.4969E-03
15	-0.9407E+02	-0.1735E+00	0.7729E+02	-0.3415E-03	-0.2869E-02	-0.4937E-03
16	-0.9374E+02	-0.1683E+00	0.7687E+02	-0.3395E-03	-0.2763E-02	-0.4908E-03
17	-0.9343E+02	-0.1641E+00	0.7650E+02	-0.3376E-03	-0.2666E-02	-0.4882E-03
18	-0.9313E+02	-0.1607E+00	0.7616E+02	-0.3358E-03	-0.2576E-02	-0.4857E-03
19	-0.9284E+02	-0.1580E+00	0.7584E+02	-0.3341E-03	-0.2493E-02	-0.4835E-03
20	-0.9257E+02	-0.1557E+00	0.7556E+02	-0.3325E-03	-0.2416E-02	-0.4815E-03
21	-0.9232E+02	-0.1538E+00	0.7529E+02	-0.3310E-03	-0.2346E-02	-0.4796E-03
22	-0.9209E+02	-0.1521E+00	0.7505E+02	-0.3296E-03	-0.2280E-02	-0.4779E-03
23	-0.9187E+02	-0.1508E+00	0.7483E+02	-0.3283E-03	-0.2220E-02	-0.4764E-03
24	-0.9166E+02	-0.1496E+00	0.7462E+02	-0.3271E-03	-0.2164E-02	-0.4749E-03
25	-0.9147E+02	-0.1485E+00	0.7444E+02	-0.3259E-03	-0.2112E-02	-0.4736E-03
26	-0.9129E+02	-0.1476E+00	0.7426E+02	-0.3249E-03	-0.2064E-02	-0.4724E-03
27	-0.9113E+02	-0.1469E+00	0.7410E+02	-0.3239E-03	-0.2020E-02	-0.4712E-03
28	-0.9097E+02	-0.1462E+00	0.7395E+02	-0.3230E-03	-0.1979E-02	-0.4702E-03
29	-0.9083E+02	-0.1456E+00	0.7381E+02	-0.3222E-03	-0.1941E-02	-0.4692E-03
30	-0.9070E+02	-0.1450E+00	0.7369E+02	-0.3214E-03	-0.1906E-02	-0.4683E-03
31	-0.9057E+02	-0.1446E+00	0.7357E+02	-0.3206E-03	-0.1873E-02	-0.4675E-03
32	-0.9046E+02	-0.1442E+00	0.7346E+02	-0.3200E-03	-0.1843E-02	-0.4667E-03
33	-0.9035E+02	-0.1438E+00	0.7336E+02	-0.3193E-03	-0.1815E-02	-0.4660E-03
34	-0.9025E+02	-0.1435E+00	0.7327E+02	-0.3187E-03	-0.1790E-02	-0.4654E-03
35	-0.9016E+02	-0.1432E+00	0.7318E+02	-0.3182E-03	-0.1765E-02	-0.4648E-03
36	-0.9007E+02	-0.1429E+00	0.7310E+02	-0.3177E-03	-0.1743E-02	-0.4642E-03
37	-0.8999E+02	-0.1427E+00	0.7303E+02	-0.3172E-03	-0.1723E-02	-0.4637E-03
38	-0.8992E+02	-0.1425E+00	0.7296E+02	-0.3167E-03	-0.1703E-02	-0.4632E-03
39	-0.8985E+02	-0.1423E+00	0.7289E+02	-0.3163E-03	-0.1685E-02	-0.4627E-03
40	-0.8978E+02	-0.1421E+00	0.7283E+02	-0.3160E-03	-0.1669E-02	-0.4623E-03
41	-0.8972E+02	-0.1420E+00	0.7278E+02	-0.3156E-03	-0.1654E-02	-0.4619E-03
42	-0.8967E+02	-0.1418E+00	0.7273E+02	-0.3153E-03	-0.1639E-02	-0.4616E-03
43	-0.8961E+02	-0.1417E+00	0.7268E+02	-0.3150E-03	-0.1626E-02	-0.4613E-03

Table 4.3 Iterative Motion Estimation of the Car from the Facet Model Optic Flow Image in Fig 3.20

Table 4.3 Iterative Motion Estimation of the Car in TV Sequence of Fig 3.18 from the optic Flow Image in Fig 3.20

CHAPTER V

LINEAR ESTIMATION OF MOTION AND DEPTH

In this chapter, we use the second optic flow equation derived in the previous chapter for 3D motion and surface structure estimation. The second fundamental optic flow equation which relates an optic flow field to rigid body motion is a nonlinear (second order polynomial) equation in motion parameters. From this equation, we can derive a linear equation by assigning unique variables for nonlinear terms. Using the linear equation, we can develop a unified and stable scheme to compute motion parameters, relative depth, and other related information from the optic flow field. Furthermore, when the optic flow field experiences small noise perturbation, the scheme estimates the motion parameters and relative depth as well as their error bounds.

In section 5.1 we review the second fundamental optic flow equation from which we derive linear equations and solve the linear equations for the motion parameters. In section 5.2, we show that an optic flow image and one spatial point of an object describe the rigid body motion of the given object completely. For optic flow images perturbed by a small noise, we estimate rotational motion

and unsigned scaled translation in section 5.3. We determine the actual translational motion direction and estimate relative depth in section 5.4. In section 5.5, we recapitulate the motion estimation scheme and show some experimental results.

5.1 The second fundamental optic flow equation

In section 4.1, we derived the second fundamental optic flow equation (4.18). This equation can also be derived from the time derivative of a moving 3D object point and the rigid body motion equation (4.12). Let P(t) be a spatial point $(x(t),y(t),z(t))'$ of a moving object. Then we have

$$\begin{aligned}\dot{P}(t) &= \frac{d}{dt}\begin{bmatrix} x(t) \\ y(t) \\ z(t) \end{bmatrix} \\ &= \frac{d}{dt}\left\{y(t)\begin{bmatrix} X(t) \\ 1 \\ Z(t) \end{bmatrix}\right\} \\ &= \dot{y}(t)\begin{bmatrix} X(t) \\ 1 \\ Z(t) \end{bmatrix} + y(t)\begin{bmatrix} u(t) \\ 0 \\ v(t) \end{bmatrix} \end{aligned} \qquad (5.1a)$$

From the rigid body motion equation (4.12), we have

$$\dot{P}(t) = y(t)\Omega(t)x\begin{bmatrix} X(t) \\ 1 \\ Z(t) \end{bmatrix} + k(t) \qquad (5.1b)$$

Subtracting (5.1b) from (5.1a), we have

$$y(t)\left\{\begin{bmatrix} u(t) \\ 0 \\ v(t) \end{bmatrix} - \Omega(t)x\begin{bmatrix} X(t) \\ 1 \\ Z(t) \end{bmatrix}\right\} + \dot{y}(t)\begin{bmatrix} X(t) \\ 1 \\ Z(t) \end{bmatrix} - k(t) = 0 \quad (5.2)$$

The equality (5.2) necessarily implies a linear dependence among the three vectors

$$\left| \begin{bmatrix} u \\ 0 \\ v \end{bmatrix} - \Omega x \begin{bmatrix} X \\ 1 \\ Z \end{bmatrix}, \begin{bmatrix} X \\ 1 \\ Z \end{bmatrix}, k \right| = 0 \quad (5.3)$$

where the time variable t is omitted for the brevity. Since the cross product of three linearly dependent vectors is zero, we have

$$\left(k \times \begin{bmatrix} X \\ 1 \\ Z \end{bmatrix}\right)' \left(\begin{bmatrix} u \\ 0 \\ v \end{bmatrix} - \Omega x \begin{bmatrix} X \\ 1 \\ Z \end{bmatrix}\right) = 0 \quad (5.4)$$

or

$$[u,0,v]\left(k \times \begin{bmatrix} X \\ 1 \\ Z \end{bmatrix}\right) = \left(k \times \begin{bmatrix} X \\ 1 \\ Z \end{bmatrix}\right)'\left(\Omega \times \begin{bmatrix} X \\ 1 \\ Z \end{bmatrix}\right) \quad (5.5)$$

which is the same equation as (4.18).

Combining the rigid body motion equation with the time derivative of a moving 3D point, we can independently derive the same second fundamental optic flow equation which the motion parameters k,Ω satisfy. What about uniqueness? Suppose (k^*,Ω^*) is a solution to (5.5). That is

$$[u,0,v]\ (k^* \times \begin{bmatrix} X \\ 1 \\ Z \end{bmatrix}) = (k^* \times \begin{bmatrix} X \\ 1 \\ Z \end{bmatrix})'(\Omega^* \times \begin{bmatrix} X \\ 1 \\ Z \end{bmatrix}) \qquad (5.6)$$

What is the relationship between (k^*,Ω^*) and the motion parameters (k,Ω)? From (5.1a) and (5.1b), we have

$$y \begin{bmatrix} u \\ 0 \\ v \end{bmatrix} = y\Omega \times \begin{bmatrix} X \\ 1 \\ Z \end{bmatrix} - y \begin{bmatrix} \dot{X} \\ 1 \\ Z \end{bmatrix} + k \qquad (5.7)$$

which is the equation that the true motion parameters (k,Ω) have to satisfy. Combining (5.7) with (5.6), we could obtain an equation describing the relationship between (k^*,Ω^*) and the motion parameters (k,Ω). Replacing $[u,0,v]$ in (5.6) by (5.7), we have

$$(y\,\Omega \times \begin{bmatrix} X \\ 1 \\ Z \end{bmatrix} - y \begin{bmatrix} \dot{X} \\ 1 \\ Z \end{bmatrix} + k)'(yk^* \times \begin{bmatrix} X \\ 1 \\ Z \end{bmatrix}) = (yk^* \times \begin{bmatrix} X \\ 1 \\ Z \end{bmatrix})'(y\Omega^* \times \begin{bmatrix} X \\ 1 \\ Z \end{bmatrix})$$

Or

$$(\Omega \times P)'(k^* \times P) - \frac{\dot{y}}{y} P'(k^* \times P) + k'(k^* \times P) = (k^* \times P)'(\Omega^* \times P)$$

$$[(\Omega \times P)' - (\Omega^* \times P)'](k^* \times P) + k'(k^* \times P) = 0$$

$$[(\Omega - \Omega^*) \times P]'(k^* \times P) + k'(k^* \times P) = 0 \qquad (5.8)$$

Let

$$K(t) = \begin{bmatrix} 0 & -k_3(t) & k_2(t) \\ k_3(t) & 0 & -k_1(t) \\ -k_2(t) & k_1(t) & 0 \end{bmatrix}, \quad K^*(t) = \begin{bmatrix} 0 & -k_3^*(t) & k_2^*(t) \\ k_3^*(t) & 0 & -k_1^*(t) \\ -k_2^*(t) & k_1^*(t) & 0 \end{bmatrix}$$

$$\Omega^*(t) = \begin{bmatrix}\omega_1^*(t)\\ \omega_2^*(t)\\ \omega_3^*(t)\end{bmatrix}, \quad S^*(t) = \begin{bmatrix} 0 & -\omega_3^*(t) & \omega_2^*(t)\\ \omega_3^*(t) & 0 & -\omega_1^*(t)\\ -\omega_2^*(t) & \omega_1^*(t) & 0\end{bmatrix}$$

and remember

$$\Omega(t) = \begin{bmatrix}\omega_1(t)\\ \omega_2(t)\\ \omega_3(t)\end{bmatrix}, \quad S(t) = \begin{bmatrix} 0 & -\omega_3(t) & \omega_2(t)\\ \omega_3(t) & 0 & -\omega_1(t)\\ -\omega_2(t) & \omega_1(t) & 0\end{bmatrix}.$$

Then we can rewrite (5.8) as follows

$$[(S-S^*)P]'K^*P + k'K^*P = 0$$

or

$$P'(S'-S^{*\prime})K^*P + k'K^*P = 0$$

$$P'(S^*-S)K^*P + k'K^*P = 0 \tag{5.9}$$

Lemma 5.1. Assume that the part on the rigid body producing the optic flow image can not be contained in a quadratic surface containing the origin 0. Then, (k^*,Ω^*) is a solution of (5.5) iff

$$k'K^* = 0$$

and

$$(S^*-S)K^* + K^*(S^*-S) = 0 \tag{5.10}$$

Proof. From the previous reasoning, it is clear that (k^*,Ω^*) is a solution of (5.5) if and only if (k^*,Ω^*) satisfies (5.9) with (k,Ω) being the genuine motion parameters. Under the assumption, (k^*,Ω^*) satisfies (5.9)

for all the optic flow image points if and only if the coefficients of both the first term and the second term in (5.9) should be zero. That means

$$k' K^* = 0$$

and

$$(S^*-S)K^* + [(S^*-S)K^*]' = 0 \qquad (5.11)$$

The latter leads to (5.10).

Q.E.D.

Lemma 5.2. $k' K^* = 0$ if and only if $k^* = \alpha k$ with α any real number when $k \neq 0$ or any vector (where K^* is any skew-symmetric matrix) when $k=0$.

Proof. Because $k' K^* = (k \times k^*)'$, the conclusion is immediate.

Q.E.D.

Lemma 5.3. (5.10) holds if and only if $k^*=0$ or $K^* \neq 0$ and $S^* = S$.

Proof. (5.10) holds if and only if $(S^*-S)K^*$ is skew-symmetric.

$$\text{Let } S^*-S = \begin{bmatrix} 0 & -\omega_3 & \omega_2 \\ \omega_3 & 0 & -\omega_1 \\ -\omega_2 & \omega_1 & 0 \end{bmatrix}. \text{ Then}$$

$$(S^*-S)K^* = \begin{bmatrix} -\omega_3 k_3^* - \omega_2 k_2^* & \omega_2 k_1^* & \omega_3 k_1^* \\ \omega_1 k_2^* & -\omega_3 k_3^* - \omega_1 k_1^* & \omega_3 k_2^* \\ \omega_1 k_3^* & \omega_2 k_3^* & -\omega_2 k_2^* - \omega_1 k_1^* \end{bmatrix}$$

Thus

$(S^*-S)K^*$ is skew-symmetric if and only if

$$\omega_3 k_3^* + \omega_2 k_2^* = \omega_3 k_3^* + \omega_1 k_1^* = \omega_2 k_2^* + \omega_1 k_1^* = 0 \qquad (5.12)$$

$$\omega_2 k_1^* + \omega_1 k_2^* = \omega_1 k_3^* + \omega_3 k_1^* = \omega_2 k_3^* + \omega_3 k_2^* = 0 \qquad (5.13)$$

It is easy to see that (5.12) is equivalent to

$$\omega_1 k_1^* = \omega_2 k_2^* = \omega_3 k_3^* = 0 \qquad (5.14)$$

It is obvious that (5.13) and (5.14) hold if and only if $K^*=0$.

Suppose $k_1^* \neq 0$. Then (5.14) implies $\omega_1=0$ and the first two equalities in (5.13) lead to $\omega_2 = \omega_3 = 0$. Similar treatment can be applied to $k_2^* \neq 0$ or $k_3^* \neq 0$. Therefore, $(S^*-S)K^*$ is skew-symmetric if and only if $K^*=0$ or $K^* \neq 0$ and $S^*-S=0$.

Q.E.D.

Theorem 5.1. Under the same assumption as Lemma 5.1, the second fundamental optic flow equation (5.5) has the general solution $(\alpha k, S)$ (α any real number) when $k \neq 0$ or (k^*, S) (k^* any real vector) when $k = 0$.

Proof. Lemma 5.1 derives two necessary and sufficient conditions, $k'K^*=0$ and $(S^*-S)K^* + K^*(S^*-S) = 0$, for the solution of the second fundamental optic flow equation. Lemma 5.2 solves for the instantaneous translational motion from the first condition and Lemma 5.3 determines the

rotational motion from the second condition.

Q.E.D.

Rewrite (5.5) as follows:

$$[u,0,v]\ K \begin{bmatrix} X \\ 1 \\ Z \end{bmatrix} = [X,1,Z]\ K'S \begin{bmatrix} X \\ 1 \\ Z \end{bmatrix} \tag{5.15}$$

Suppose K^*, M^* satisfy

$$[u,0,v]\ K^* \begin{bmatrix} X \\ 1 \\ Z \end{bmatrix} = [X,1,Z]\ M^* \begin{bmatrix} X \\ 1 \\ Z \end{bmatrix} \tag{5.16}$$

for all optic flow image points $\{[(X,Z),(u,v)]\}$. What is the relationship between the motion (K,S) (i.e. (k,Ω)) and (K^*,M^*)? From an argument similar to the previous one in in lemma 5.1, it is clear that (5.16) holds if and only if

$$k'\ K^* = 0 \tag{5.17}$$

and

$$M^* + M^{*\prime} = -(S\ K^* + K^* S) \tag{5.18}$$

when the assumption in the Lemma 5.1 holds.

Theorem 5.2. Under the same assumption as Lemma 5.1, given a solution (K^*,M^*) of the equation (5.16) with $K^* \neq 0$, the rotation S is uniquely determined by (K^*,M^*) and the translation k is parallel to k^*.

Proof. Under the assumption of Theorem 5.2, the relations (5.17) and (5.18) hold. (5.17) implies that the translation

k is parallel to K^*. (5.18) is equivalent to

$$\begin{aligned} 2(\omega_3 k_3^* + \omega_2 k_2^*) &= 2\, m_{11}^* \\ 2(\omega_3 k_3^* + \omega_1 k_1^*) &= 2\, m_{22}^* \\ 2(\omega_2 k_2^* + \omega_1 k_1^*) &= 2\, m_{33}^* \end{aligned} \tag{5.19}$$

$$\begin{aligned} -\omega_2 k_1^* - \omega_1 k_2^* &= m_{12}^* + m_{21}^* \\ -\omega_1 k_3^* - \omega_3 k_1^* &= m_{13}^* + m_{31}^* \\ -\omega_2 k_3^* - \omega_3 k_2^* &= m_{23}^* + m_{32}^* \end{aligned} \tag{5.20}$$

It is easy to see that (5.19) is equivalent to

$$\begin{aligned} \omega_1 k_1^* &= \frac{m_{22}^* + m_{33}^* - m_{11}^*}{2} \\ \omega_2 k_2^* &= \frac{m_{11}^* + m_{33}^* - m_{22}^*}{2} \\ \omega_3 k_3^* &= \frac{m_{11}^* + m_{22}^* - m_{33}^*}{2} \end{aligned} \tag{5.21}$$

If $k_1^* \neq 0$, then

$$\omega_1 = \frac{m_{22}^* + m_{33}^* - m_{11}^*}{2k_1^*} \tag{5.22}$$

From (5.20) we obtain

$$\begin{aligned} \omega_2 &= \frac{-(m_{12}^* + m_{21}^*) - \omega_1 k_2^*}{k_1^*} \\ \omega_3 &= \frac{-(m_{13}^* + m_{31}^*) - \omega_1 k_3^*}{k_1^*} \end{aligned} \tag{5.23}$$

Furthermore, if $k_2^* \neq 0$, we can also use the following equation

derived from (5.19) to compute ω_2

$$\omega_2 = \frac{m_{11}^* + m_{33}^* - m_{22}^*}{2k_2^*} \tag{5.24}$$

which must be in agreement with ω_2 in (5.23) for the uniqueness. We will show that we can derive (5.24) from the equation for ω_2 in (5.23). Substituting (5.22) for ω_1 in (5.23), we have

$$\omega_2 = \frac{-(m_{12}^*+m_{21}^*) - k_2^* \frac{m_{22}^*+m_{33}^*-m_{11}^*}{2k_1^*}}{k_1^*}$$

$$= \frac{-2k_1^*(m_{12}^*+m_{21}^*) + (m_{11}^*-m_{22}^*-m_{33}^*)k_2^*}{2k_1^{*2}}$$

$$= \frac{2k_1^*(\omega_2 k_1^*+\omega_1 k_2^*) - 2m_{33}^* k_2^* + (m_{11}^*+m_{33}^*-m_{22}^*)k_2^*}{2k_1^{*2}}$$

Substituting (5.19) for m_{33}^* in the above equation and rearranging the result, we derive

$$\omega_2 = \frac{m_{11}^* + m_{33}^* - m_{22}^*}{2k_2^*}$$

which is the same as (5.24). In the same way, we can show the uniqueness of other solutions.

Q.E.D.

Because of Theorem 5.2, we attempt to solve the following equation (5.25) instead of (5.5) for (k^*, M^*)

$$[u,0,v]\begin{bmatrix} 0 & -k_3^* & k_2^* \\ k_3^* & 0 & -k_1^* \\ -k_2^* & k_1^* & 0 \end{bmatrix}\begin{bmatrix} X \\ 1 \\ Z \end{bmatrix} = [X,1,Z]\begin{bmatrix} m_{11}^* & m_{12}^* & m_{13}^* \\ m_{21}^* & m_{22}^* & m_{23}^* \\ m_{31}^* & m_{32}^* & m_{33}^* \end{bmatrix}\begin{bmatrix} X \\ 1 \\ Z \end{bmatrix} \quad (5.25)$$

Expanding and rearranging (5.25) leads to the following equation.

$$[X^2,1,Z^2,X,XZ,Z,-v,vX-uZ,u]\begin{bmatrix} m_{11}^* \\ m_{22}^* \\ m_{33}^* \\ m_{12}^*+m_{21}^* \\ m_{13}^*+m_{31}^* \\ m_{23}^*+m_{32}^* \\ k_1^* \\ k_2^* \\ k_3^* \end{bmatrix} = 0 \quad (5.26)$$

Let

$$B = [X^2,\ 1,\ Z^2,\ X,\ XZ,\ Z,\ -v,\ vX-uZ,\ u] \quad (5.27)$$

and

$$h = \begin{bmatrix} m_{11}^* \\ m_{22}^* \\ m_{33}^* \\ m_{12}^*+m_{21}^* \\ m_{13}^*+m_{31}^* \\ m_{23}^*+m_{32}^* \\ k_1^* \\ k_2^* \\ k_3^* \end{bmatrix} \tag{5.28}$$

It is obvious that

$$\{ \sum_{[(X,Z),(u,v)]} B' \; B \} \; h = 0 \tag{5.29}$$

Let

$$W = \sum_{[(X,Z),(u,v)]} B' \; B \tag{5.30}$$

It is clear that $W \geq 0$ and h is an eigenvector corresponding to the smallest eigenvalue (i.e. zero) of W.

From (5.19) and (5.20) it is clear that m_{11}^*, m_{22}^*, m_{33}^*, $m_{12}^*+m_{21}^*$, $m_{13}^*+m_{31}^*$, and $m_{23}^*+m_{32}^*$ are linear homogeneous functions of k_1^*, k_2^*, and k_3^*. Thus, relating to Theorem 5.1, we have

Theorem 5.3. The general solution h of (5.29) is one-parameter if and only if $k \neq 0$, is three-parameter iff $k = 0$.

And

$$\text{Rank } (W) = 8 \quad \text{if and only if } k \neq 0 \tag{5.31}$$

$$\text{Rank } (W) = 6 \quad \text{if and only if } k = 0 \tag{5.32}$$

Theorem 5.4. $k=0$ if and only if for two optic flow image points $\{[(X_i,Z_i),(u_i,v_i)]\ i=1,2\}$ there holds

$$-\begin{vmatrix} \omega_1 & \omega_3 \\ X_i & Z_i \end{vmatrix} \begin{bmatrix} X_i \\ Z_i \end{bmatrix} + \begin{bmatrix} u_i \\ v_i \end{bmatrix} = \begin{bmatrix} \begin{vmatrix} \omega_2 & \omega_3 \\ 1 & Z_i \end{vmatrix} \\ \begin{vmatrix} \omega_1 & \omega_2 \\ X_i & 1 \end{vmatrix} \end{bmatrix}, \quad i=1,2. \tag{5.33}$$

Proof.

From $\dot{y} \begin{bmatrix} X \\ 1 \\ Z \end{bmatrix} + y \begin{bmatrix} u \\ 0 \\ v \end{bmatrix} = y\,\Omega x \begin{bmatrix} X \\ 1 \\ Z \end{bmatrix} + k$, we have

$$\dot{y} = -y \begin{vmatrix} \omega_1 & \omega_3 \\ X & Z \end{vmatrix} + k_2 \tag{5.34}$$

and

$$-y \begin{vmatrix} \omega_1 & \omega_3 \\ X & Z \end{vmatrix} \begin{bmatrix} X \\ Z \end{bmatrix} + k_2 \begin{bmatrix} X \\ Z \end{bmatrix} + y \begin{bmatrix} u \\ v \end{bmatrix} = y \begin{bmatrix} \begin{vmatrix} \omega_2 & \omega_3 \\ 1 & Z \end{vmatrix} \\ \begin{vmatrix} \omega_1 & \omega_2 \\ X & 1 \end{vmatrix} \end{bmatrix} + \begin{bmatrix} k_1 \\ k_3 \end{bmatrix} \tag{5.35}$$

Noticing $y > 1$, it is clear that $k = 0$ if and only if for two optic flow image points $\{[(X_i,Z_i),(u_i,v_i)]\ i=1,2\}$ equation (5.33) holds.

Q.E.D.

Theorem 5.5. Keep the same assumption of Lemma 5.1. Assume

that (k^*,Ω) is a solution of (5.5) with $k^*\neq 0$ and $[X,Z]^t$ is linearly independent with $[k_1^*,k_3^*]^t$.

Then, the following equation (5.36) has a solution for α if and only if $k\neq 0$.

$$-\alpha\begin{vmatrix}\omega_1 & \omega_3\\ X & Z\end{vmatrix}\begin{bmatrix}X\\ Z\end{bmatrix}+k_2^*\begin{bmatrix}X\\ Z\end{bmatrix}+\alpha\begin{bmatrix}u\\ v\end{bmatrix}=\alpha\begin{vmatrix}\omega_2 & \omega_3\\ 1 & Z\\ \omega_1 & \omega_2\\ X & 1\end{vmatrix}+\begin{bmatrix}k_1^*\\ k_2^*\end{bmatrix} \tag{5.36}$$

Moreover, the solution α of (5.36) is unique and

$$\frac{k}{\|k\|}=\operatorname{sign}(\alpha)\,\frac{k^*}{\|k^*\|} \tag{5.37}$$

Proof. We prove that the necessary and sufficient condition for (5.36) to have a solution is $k\neq 0$. For the sufficiency, we have $k^*=\beta k$ with some real number β by Theorem 1. Thus, when $k\neq 0$, (5.36) becomes

$$-\alpha\begin{vmatrix}\omega_1 & \omega_3\\ X & Z\end{vmatrix}\begin{bmatrix}X\\ Z\end{bmatrix}+\beta k_2\begin{bmatrix}X\\ Z\end{bmatrix}+\alpha\begin{bmatrix}u\\ v\end{bmatrix}=\alpha\begin{vmatrix}\omega_2 & \omega_3\\ 1 & Z\\ \omega_1 & \omega_2\\ X & 1\end{vmatrix}+\beta\begin{bmatrix}k_1\\ k_3\end{bmatrix} \tag{5.38}$$

Multiplying both sides of (5.35) by β and subtracting the result from (5.38), we have

$$\alpha=y\beta \tag{5.39}$$

which is the solution of (5.36). To show this is a necessary condition, suppose that α is a solution of (5.36) and

negate the consequence such that k=0. Substituting (5.33) in (5.35), we have

$$k_2^* \begin{bmatrix} X \\ Z \end{bmatrix} = \begin{bmatrix} k_1^* \\ k_3^* \end{bmatrix} \tag{5.40}$$

which contradicts the assumption that $[X,Z]^t$ and $[k_1^*,k_3^*]^t$ are linearly independent. Thus, the necessary and sufficient condition is $k \neq 0$.

To prove the solution uniqueness of (5.36), we assume that there are two solutions α_1 and α_2 such that

$$-\alpha_1 \begin{vmatrix} \omega_1 & \omega_3 \\ X & Z \end{vmatrix} \begin{bmatrix} X \\ Z \end{bmatrix} + k_2^* \begin{bmatrix} X \\ Z \end{bmatrix} + \alpha_1 \begin{vmatrix} \omega_2 & \omega_3 \\ 1 & Z \\ \omega_1 & \omega_2 \\ X & 1 \end{vmatrix} + \begin{bmatrix} k_1^* \\ k_3^* \end{bmatrix} \tag{5.41a}$$

$$-\alpha_2 \begin{vmatrix} \omega_1 & \omega_3 \\ X & Z \end{vmatrix} \begin{bmatrix} X \\ Z \end{bmatrix} + k_2^* \begin{bmatrix} X \\ Z \end{bmatrix} + \alpha_2 \begin{vmatrix} \omega_2 & \omega_3 \\ 1 & Z \\ \omega_1 & \omega_2 \\ X & 1 \end{vmatrix} + \begin{bmatrix} k_1^* \\ k_3^* \end{bmatrix} \tag{5.41b}$$

Multiplying (5.41a) by α_2 and (5.41b) by α_1 and subtracting one result from the other, we have

$$(\alpha_1-\alpha_2) k_2^* \begin{bmatrix} X \\ Z \end{bmatrix} = (\alpha_1-\alpha_2) \begin{bmatrix} k_1^* \\ k_3^* \end{bmatrix} \tag{5.42}$$

which is a contradiction to the linear independence assumption.

Because $k^* = \beta k$ and $\alpha = y\beta$ $(y>1)$ when $k \neq 0$, we

derive (5.37) from

$$\frac{k^*}{\|k^*\|} = \text{sign}(\beta)\frac{k}{\|k\|} = \text{sign}(\alpha)\frac{k}{\|k\|}$$

Corollary. If $k \neq 0$ and $[X_i, Z_i]^t$ $(i=1,2)$ is linearly independent with $[k_1^*, k_3^*]^t$, then from (5.39), we have

$$\alpha_i = y_i \beta, \quad i = 1, 2$$

As a result, the relative depth of the two optic flow image points is given by

$$\frac{y_1}{y_2} = \frac{\alpha_1}{\alpha_2} \tag{5.43}$$

5.2 Optic Flow Image and One Spatial Point

In this section, we show that the rigid body motion of an object is completely described by the optic flow image and one spatial point of the object. Suppose $k_2=0$ (for instance, when $t \geq \tau$). Then, from (5.34), we have

$$\dot{y} = -y \begin{vmatrix} \omega_1 & \omega_3 \\ X & Z \end{vmatrix} \qquad (t \geq \tau)$$

and

$$y(t) = y(\tau) \exp\left(\int_\tau^t \begin{vmatrix} \omega_1(\xi) & \omega_3(\xi) \\ X(\xi) & Z(\xi) \end{vmatrix} d\xi\right) \tag{5.44}$$

That is, the depth $y(t)$ can be uniquely determined by the given depth $y(\tau)$ at the time τ. By the way,

$$P(t) = y(t)\begin{bmatrix} X(t) \\ 1 \\ Z(t) \end{bmatrix}$$

and

$$\dot{P}(t) = y(t)\begin{bmatrix} \omega_1(t) & \omega_3(t) \\ & \\ X(t) & Z(t) \end{bmatrix}\begin{bmatrix} X(t) \\ 1 \\ Z(t) \end{bmatrix} + y(t)\begin{bmatrix} u(t) \\ 0 \\ v(t) \end{bmatrix}$$

are uniquely determined. Thus, $k(t)$ is uniquely determined by

$$\dot{P}(t) - \Omega(t) \times P(t).$$

In general, we have

Theorem 5.6. A rigid body motion (k,Ω) is completely described by an optic flow image and the motion of one spatial point.

Proof. The optic flow image uniquely determines the rotation $\Omega(t)$. The rotation $\Omega(t)$ plus the motion of one spatial point $\{P(t),\dot{P}(t)\}$ uniquely determines the translation by

$$k(t) = \dot{P}(t) - \Omega(t) \times P(t)$$

Q.E.D.

In the following, we will consider two special cases of motion. Suppose $\Omega = 0$. Then (5.5) reduces to

$$[u,0,v]\ (k \times \begin{bmatrix} X \\ 1 \\ Z \end{bmatrix}) = 0 \tag{5.45}$$

or equivalently,

$$[u,v] \begin{vmatrix} k_2 & k_3 \\ 1 & Z \\ k_1 & k_2 \\ X & 1 \end{vmatrix} = 0 \tag{5.46}$$

which is equivalent to

$$u[k_2Z-k_3] + v[k_1-k_2X] = 0 \tag{5.47}$$

Lemma 5.4. Assume $\Omega = 0$. Then $k = 0$ if and only if $u = 0$ and $v = 0$ for all optic flow image points.

Proof. If $\Omega=0$, then (5.5) becomes (5.47). By theorem 5.1, we have $k=0$ if and only if any vector k^* satisfies

$$u[k_2^*Z-k_3^*] + v[k_1^*-k_2^*X] = 0 \tag{5.48}$$

Hence $u = 0$ and $v = 0$. Q.E.D.

Let $k_0^* = [k_{01}^*, k_{02}^*, k_{03}^*]^t$ and $k^* = [k_1^*, k_2^*, k_3^*]^t$. Suppose k_0^* is the solution of k^* such that

$$\min_{||k^*||=1} \sum [u(k_2^*Z-k_3^*) + v(k_1^*-k_2^*X)]^2$$

and α_0 is the solution of the following equation

$$k^*_{02}\begin{bmatrix}X_0\\ Z_0\end{bmatrix}+\alpha_0\begin{bmatrix}u_0\\ v_0\end{bmatrix}=\begin{bmatrix}k^*_{01}\\ k^*_{03}\end{bmatrix}$$

for some $\begin{bmatrix}X_0\\ Z_0\end{bmatrix}$ linearly independent with $\begin{bmatrix}k^*_{01}\\ k^*_{03}\end{bmatrix}$.

Then, $k\neq 0$ and $\dfrac{k}{||k||}=\text{sign}(\alpha_0)\dfrac{k^*_0}{||k^*_0||}$ by Theorem 5.5.

If the depth y_0 at (X_0,Z_0) is known, then k is determined from (5.39) and $k^*=\beta k$, and the depth y at any other optic flow image point $[(X,Z),(u,v)]$ is given by

$$y=\frac{\alpha}{\alpha_0}y_0 \tag{5.49}$$

where α is the solution of $k^*_{02}\begin{bmatrix}X\\ Z\end{bmatrix}+\alpha\begin{bmatrix}u\\ v\end{bmatrix}=\begin{bmatrix}k^*_{01}\\ k^*_{03}\end{bmatrix}$.

Suppose k = 0. From (5.34) and (5.35), we have

$$-\begin{vmatrix}\omega_1 & \omega_3\\ X & Z\end{vmatrix}\begin{bmatrix}X\\ Z\end{bmatrix}+\begin{bmatrix}u\\ v\end{bmatrix}=\begin{bmatrix}\begin{vmatrix}\omega_2 & \omega_3\\ 1 & Z\end{vmatrix}\\ \begin{vmatrix}\omega_1 & \omega_2\\ X & 1\end{vmatrix}\end{bmatrix} \tag{5.50}$$

and

$$\frac{\dot{y}}{y}=-\begin{vmatrix}\omega_1 & \omega_3\\ X & Z\end{vmatrix} \tag{5.51}$$

Therefore, when k=0, we see that it is impossible to

determine the relative depth using (5.51) alone.

The rigid body motion is uniquely determined by the optic flow image plus depth information of four noncoplanar spatial points[95]. Due to Theorem 5.5, the conditions can be reduced to the optic flow image plus depth information of one spatial point. This follows from the fact that the optic flow image determines the rotational components and the scaled translation, and depth information of one spatial point computes the translational scale factor and, thus, determines the true translational motion.

5.3 Motion Parameter Estimation

Suppose the optic flow image experiences a noise perturbation and becomes $\{[(X,Z),(\bar{u},\bar{v})]\}$. Correspondingly, B defined by (5.27) becomes

$$\bar{B} = [X^2, 1, Z^2, X, XZ, Z, -\bar{v}, \bar{v}X - \bar{u}Z, \bar{u}], \tag{5.52}$$

W defined by (5.30) becomes

$$\bar{W} = \sum_{[(X,Z),(\bar{u},\bar{v})]} \bar{B}'\bar{B} \tag{5.53}$$

and the equation (5.29) for h becomes

$$\bar{W}\cdot\bar{h} = 0 \tag{5.54}$$

From section 5.1, it is clear that the smallest

eigenvalue of W is zero and the eigenvector subspace corresponding to zero eigenvalue has a dimension 1 or 3 (when $k\neq 0$ or $k=0$ respectively). $\bar{W}$ is positive definite as we see from (5.53). Let the smallest eigenvalue of $\bar{W}$ be λ. We know $\lambda = \min h'\bar{W}h$ where $||h||=1$ and $\lambda \to 0$ as $\bar{W} \to W$ [FRANKLIN(1968),pp.191].

Lemma 5.5. Assume that

$$\bar{W}\cdot\bar{h} = \lambda\bar{h}, \quad ||\bar{h}|| = 1 \tag{5.55}$$

Then, there always is a $h(\lambda)$ such that

$$W\cdot h(\lambda) = 0 \tag{5.56}$$

and

$$\lim_{\bar{W}\to W} (\bar{h}(\lambda)-h(\lambda)) = 0 \tag{5.57}$$

Proof. Let h be an arbitrary 9x1 vector and

$$\Delta h = \bar{h} - h \tag{5.58}$$

$$\Delta W = \bar{W} - W \tag{5.59}$$

Then, it follows that $W\cdot h = 0$ if and only if $W\cdot\Delta h = W\cdot\bar{h}$ if and only if

$$W\cdot\Delta h = (\lambda I_9 - \Delta W)\bar{h} \tag{5.60}$$

where I_9 is 9x9 identity matrix

because $W\bar{h} = \lambda\bar{h}$. Since such h's and hence Δh's always

exist, it follows

$$\text{Rank}(W) = \text{Rank}([W, (\lambda I_9 - \Delta W)\bar{h}])$$

Without loss of generality, we could assume that

$$W = \begin{bmatrix} W_1 \\ W_2 \end{bmatrix}, \qquad W_1 = [W_{11}, W_{12}]$$

where W_{11} is a full rank square matrix and

$$\text{Rank}(W) = \text{Rank}(W_{11})$$

Let $\Delta h = [\Delta h_1, \Delta h_2]^t$ where the length of vector Δh_1 equals to $\text{Rank}(W_{11})$. Then, from(5.60), we have equivalently

$$W_{11}\Delta h_1 + W_{12}\Delta h_2 = (\lambda I_{11} - \Delta W_{11})\bar{h}_1 - \Delta W_{12}\bar{h}_2 \qquad (5.61)$$

where I_{11} is a corresponding identity matrix.

From (5.61) we have

$$\Delta h_1 = W_{11}^{-1}\{(\lambda I_{11} - \Delta W_{11})\bar{h}_1 - \Delta W_{12}\bar{h}_2 - W_{12}\Delta h_2\}$$

Set $\Delta h_2 = 0$. We have

$$\Delta h_1 \to 0 \quad (\Delta W \to 0)$$

since $\lambda \to 0$ ($\Delta W \to 0$) and $||\bar{h}|| = 1$.

Q.E.D.

Lemma 5.6. Assume that

$$W \cdot \bar{h} = \lambda \bar{h}, \quad ||\bar{h}|| = 1$$

Then, when $\bar{W}\to W$, all clustering points of $\bar{h}(\lambda)$ belong to the eigenvector subspace of W corresponding to zero eigenvalue.

Proof. Because of Lemma 5.5, there always is a $h(\lambda)$ such that

$$W\cdot h(\lambda) = 0$$

and

$$\lim_{\bar{W}\to W} (\bar{h}(\lambda)-h(\lambda)) = 0$$

Thus, $\bar{h}(\lambda)$ and $h(\lambda)$ have the same clustering points. And the clustering points of $h(\lambda)$ obviously belong to the eigenvector subspace of W corresponding to zero eigenvalue. Q.E.D.

Let $\Delta_1=\bar{u}-u$, $\Delta_2=\bar{v}-v$, $d=[X^2,1,Z^2,X,XZ,Z]$, $c=[-v,vX-uZ,u]$, $\Delta c=[-\Delta_2,\Delta_2 X-\Delta_1 Z,\Delta_1]$ and $\bar{c}=c+\Delta c$. Then, it is clear that B is equal to $[d,c]$ and $\bar{B}$ becomes $[d,\bar{c}]$. A direct computation leads to

$$\bar{B}^t\bar{B} = \begin{bmatrix} d^t d & d^t\bar{c} \\ \bar{c}^t d & \bar{c}^t\bar{c} \end{bmatrix}$$

$$= B^tB + \begin{bmatrix} 0_{6x6} & d^t\Delta c \\ \Delta c^t d & \Delta c^t c+c^t\Delta c+\Delta c^t\Delta c \end{bmatrix} \qquad (5.62)$$

where 0_{6x6} is the 6x6 matrix whose entries are all zero.

Thus, the nonnegative matrix W becomes another nonnegative matrix $\bar{W}$:

$$\bar{W} = W + \begin{bmatrix} 0_{6x6} & \sum d^t \Delta c \\ \sum \Delta c^t d & \sum \Delta c^t c + c^t \Delta c + \Delta c^t \Delta c \end{bmatrix} \tag{5.63}$$

In the following discussion, the l_1 vector and matrix norms are chosen because the l_1 norm denoted by $||\cdot||$ can be computed rapidly and because the subordinate matrix norm can be computed directly from the columns a_j by

$$||A|| = \max_j ||a_j||$$

$$||a_j|| = \sum_i |a_{ij}|$$

We denote the l_2 vector norm by $||\cdot||_2$.

From Theorem 5.2 and (5.28) it is clear that an eigenvector h corresponding to the zero eigenvalue of W implies the rotation Ω and the vector k^* with $kxk^*=0$ where k is the translation. Let

$$\lambda = \bar{h}^t \bar{W} \bar{h} = \min h^t W h, \quad ||h||_2=1 \tag{5.64}$$

There holds the estimation for λ:

$$\lambda = \bar{h}^t \bar{W} \bar{h} = \sum \bar{h}^t B^t B \bar{h}$$

$$= \sum (B\bar{h})^2 \leq \sum (Bh)^2 \quad \text{(with } Bh=0 \text{ and } ||h||_2=1\text{)}$$

$$= \sum(\Delta B \cdot h)^2 = \sum(\Delta c \cdot k^*)^2 \quad (\text{since } \Delta B=[0,0,0,0,0,0,\Delta c])$$

$$\leq \sum ||\Delta c||_2^2 \cdot ||k^*||_2^2$$

$$\leq \{\sum(|\Delta_1|+|\Delta_2|)^2(|X|+|Z|+1)^2\} \cdot ||k^*||_2^2 \qquad (5.65)$$

Because $||k^*||_2^2 \leq ||h||_2^2=1$, (5.65) becomes

$$\lambda \leq \sum(|\Delta_1|+|\Delta_2|)^2(|X|+|Z|+1)^2 \qquad (5.66)$$

When k=0, the rank of W equals 6 and the general solution of the linear equation $W \cdot h=0$ has three independent variables h_7, h_8, and h_9 (i.e. k_1^*, k_2^*, and k_3^*). This implies that the last three columns of W are linear combinations of the first six columns of W. Because of the symmetry of W, the last three rows are linear combinations of the first six rows of W too. Thus, the upper left 6x6 submatrix $W_1 (=\sum d^t d)$ has a rank 6.

Let $H=[h_1,\ldots,h_6]^t$ and $H=[\bar{h}_1,\ldots,\bar{h}_6]^t$. Then, we have

$$W_1 H + W_2 k^* = 0 \quad (W_2=\sum d^t c) \qquad (5.67)$$

and

$$W_1 \bar{H} + W_2 \bar{k}^* = \lambda H \qquad (5.68a)$$

$$W_1 (H+\Delta H) + (W_2+\Delta W_2)\bar{k}^* = \lambda H \qquad (5.68b)$$

since $W_1 = W_1$. Because of k=0, we can take $k^*=\bar{k}^*$ in (5.67), and substituting this in the left side of (5.68b), we derive the following equation.

$$W_1 \Delta H = \lambda \bar{H} - \Delta W_2 \cdot \bar{k}^* \tag{5.69}$$

where

$$\Delta W_2 = \begin{bmatrix} -\Delta v X^2 & \Delta v X^3 - \Delta u X^2 Z & \Delta u X^2 \\ -\Delta v & \Delta v X - \Delta u Z & \Delta u \\ -\Delta v Z^2 & \Delta v X Z^2 - \Delta u Z^3 & \Delta u Z^2 \\ -\Delta v X & \Delta v X^2 - \Delta u X Z & \Delta u X \\ -\Delta v X Z & \Delta v X^2 Z - \Delta u X Z^2 & \Delta u X Z \\ -\Delta v Z & \Delta v X Z - \Delta u Z^2 & \Delta u Z \end{bmatrix}$$

Since Δu and Δv are random noises the zero mean which are in $[-\Delta_1, \Delta_1]$ and $[-\Delta_2, \Delta_2]$, respectively, the expectation of ΔW_2 is zero as

$$E[\Delta W_2] = 0$$

Suppose that Δu and Δv are independent of each other and $E[H]=H$, then for the constants $\bar{k}_1^*$, $\bar{k}_2^*$, and $\bar{k}_3^*$, expectation of ΔH is given by

$$E[\Delta H] = \lambda W_1^{-1} H \tag{5.70}$$

Let $||\Delta H|| \leq \gamma_0 E[\Delta H]$ for a certain γ_0 $\gamma_0 \geq 1$ and $k^* = [\bar{k}_7, \bar{k}_8, \bar{k}_9]$. Let

$$\xi_0 = \frac{\gamma_0 E[\Delta H]}{||\bar{k}^*||} \tag{5.71}$$

Then we have

$$\frac{||\Delta H||}{||\bar{k}^*||} \leq \xi_0 \tag{5.72}$$

When $k \neq 0$, the rank of W is equal to 8 and the genreal solution of the linear equation $W \cdot h = 0$ has one degree of freedom; i.e. $h = [H, k^*]^t$ with $k^* = \alpha k$, α arbitrary. Thus, any nonzero component of k^* can be selected as an independent variable. Suppose $\bar{K}_3^* \neq 0$ which implies $k_3 \neq 0$. Let

$$W' = \begin{bmatrix} W_1 & \sum d^t [-v, vX-uZ] \\ \sum_{\lfloor vX-uZ \rfloor} d & \sum_{\lfloor vX-uZ \rfloor} \begin{bmatrix} -v \\ [-v, vX-uZ] \end{bmatrix} \end{bmatrix} \tag{5.73}$$

$$W'' = \begin{bmatrix} \sum d^t u \\ \sum_{\lfloor vX-uZ \rfloor} \begin{bmatrix} -v \\ u \end{bmatrix} \end{bmatrix} \tag{5.74}$$

Here, we notice that Rank(W') is 8 because W' is a submatrix (8x8) of W and Rank(w) is 8. Since Wh = 0, we have

$$W' \begin{bmatrix} H \\ k_1^* \\ k_2^* \end{bmatrix} + W'' k_3^* = 0 \tag{5.75}$$

and setting $\bar{W}\bar{h} = \lambda \bar{h}$, we have

$$W' \begin{bmatrix} H \\ k_1^* \\ k_2^* \end{bmatrix} + W'' \bar{k}_3^* = \lambda \begin{bmatrix} H \\ \bar{k}_1^* \\ \bar{k}_2^* \end{bmatrix} \tag{5.76}$$

Let $k_3^* = \bar{k}_3^*$, $\Delta W' = W'$, and $\Delta W'' = \bar{W}'' - W''$. For brief notation, let

$$g = \begin{bmatrix} H \\ k_1^* \\ k_2^* \end{bmatrix}, \quad \bar{g} = \begin{bmatrix} H \\ \bar{k}_1^* \\ \bar{k}_2^* \end{bmatrix}, \text{ and } \Delta g = \bar{g} - g.$$

Then (5.76) becomes

$$W' \cdot \Delta g = \lambda \bar{g} - \Delta W' \cdot g - \Delta W'' \cdot \bar{k}_3^* \tag{5.77}$$

With the same assumption as above and $E[\bar{g}] = \bar{g}$, for the constant k_3^* we have the expectation of Δg as

$$E[\Delta g] = \lambda W'^{-1} \bar{g} \tag{5.78}$$

Let $||\Delta g|| \leq \gamma_3 E[\Delta g]$ for a certain γ_3, $\gamma_3 \geq 1$ and let

$$\text{where } \xi_3 = \frac{\gamma_3 E[\Delta g]}{||\bar{k}_3^*||} \tag{5.79}$$

Then we have

$$\frac{||\Delta g||}{||\bar{k}_3^*||} \leq \xi_3 \tag{5.80}$$

When $k_1 \neq 0$, k_1^* can be set as an independent variable of the

linear homogeneous equation $W \cdot h = 0$. Let

$$U' = \begin{bmatrix} W_1 & \sum d^t[vX-uZ,u] \\ \left[\sum_{\lfloor\ u\ \rfloor}^{\lceil vX-uZ \rceil}\right]^d & \left[\sum_{\lfloor\ u\ \rfloor}^{\lceil vX-uZ \rceil}\right]^{[vX-uZ,u]} \end{bmatrix} \tag{5.81}$$

$$U'' = \begin{bmatrix} \sum d^t(-v) \\ \left[\sum_{\lfloor\ u\ \rfloor}^{\lceil vX-uZ \rceil}\right]^{(-v)} \end{bmatrix} \tag{5.82}$$

and let

$$e = \begin{bmatrix} H \\ k_2^* \\ k_3^* \end{bmatrix}, \quad \bar{e} = \begin{bmatrix} H \\ \bar{k}_2^* \\ \bar{k}_3^* \end{bmatrix}, \text{ and } \Delta e = \bar{e} - e \tag{5.83}$$

Then we have

$$U'e + U''k_1^* = 0, \tag{5.84}$$

$$\bar{U}'\bar{e} + \bar{U}''\bar{k}_1^* = \lambda\bar{e}, \tag{5.85}$$

and, thus

$$\bar{U}'\Delta e = \lambda\bar{e} - \Delta U'e - \Delta''U\bar{k}_1^* \tag{5.86}$$

$$E[\Delta e] = \lambda\bar{U}'^{-1}\bar{e} \tag{5.87}$$

Let, for some $\gamma_1 \geq 1$, $||\Delta e|| \leq \gamma_1[\Delta e]$ and set

$$\xi_1 = \frac{\gamma_1 E[\Delta e]}{||\bar{k}_1^*||} \tag{5.88}$$

Then we have

$$\frac{||\Delta e||}{||\bar{k}_1^*||} \leq \xi_1 \tag{5.89}$$

In the same way, for $k_2 \neq 0$ we let

$$V' = \begin{bmatrix} W_1 & \sum d^t[-v,u] \\ \sum_{\lfloor u \rfloor}^{\lceil -v \rceil} d & \sum_{\lfloor u \rfloor}^{\lceil -v \rceil} [-v,u] \end{bmatrix}, \tag{5.90}$$

$$V'' = \begin{bmatrix} \sum d^t(vX-uZ) \\ \sum_{\lfloor u \rfloor}^{\lceil -v \rceil} (vX-uZ) \end{bmatrix}, \tag{5.91}$$

$$f = \begin{bmatrix} H \\ k_1^* \\ k_3^* \end{bmatrix}, \quad \bar{f} = \begin{bmatrix} H \\ \bar{k}_1^* \\ \bar{k}_3^* \end{bmatrix}, \text{ and } \Delta f = \bar{f} - f.$$

Then we have

$$\bar{V}'\Delta f = \lambda \bar{f} - \Delta V' f - \Delta V'' \bar{k}_2^* \tag{5.92}$$

$$E[\Delta f] = \lambda \bar{V}'^{-1} \bar{f} \tag{5.93}$$

Suppose $||\Delta f|| \leq \gamma_2 E[\Delta f]$ for some $\gamma_2 \geq 1$ and let

$$\xi_2 = \frac{\gamma_2 E[\Delta f]}{||\bar{k}_2^*||} \tag{5.94}$$

Then we have

$$\frac{||\Delta f||}{||\bar{k}_2^*||} \leq \xi_2 \tag{5.95}$$

Because $\lambda \to 0$ when $\delta \to 0$ ($\bar{W} \to W$), (5.72), (5.80), (5.89), and (5.95) imply that

$$\lim_{\delta \to 0} ||\bar{h}-h|| = 0 \tag{5.96}$$

and

$$\lim_{\delta \to 0} ||\bar{h}||_2 = 1 \tag{5.97}$$

for any case of k.

Suppose that δ is so small that $|\bar{k}_1^*| \geq |\bar{k}_2^*|, |\bar{k}_3^*|$, or $|\bar{k}_2^*| \geq |\bar{k}_1^*|, |\bar{k}_3^*|$, or $|\bar{k}_3^*| \geq |\bar{k}_1^*|, |\bar{k}_2^*|$ implying $\bar{k}_1^* \neq 0$, or $\bar{k}_2^* \neq 0$, or $\bar{k}_3^* \neq 0$, respectively. In the following, we attempt to get an approximation of Ω. We assume $|\bar{k}_3^*| \geq |\bar{k}_1^*|, |\bar{k}_2^*|$ which implies $\bar{k}_3^* \neq 0$. From (5.28),(5.19), and (5.20), for any solution h of the linear equation $W \cdot h = 0$, we have

$$\begin{aligned}
h_1 &= \omega_3 k_3^* + \omega_2 k_2^* \\
h_2 &= \omega_3 k_3^* + \omega_1 k_1^* \\
h_3 &= \omega_2 k_2^* + \omega_1 k_1^* \\
h_4 &= -(\omega_2 k_1^* + \omega_1 k_2^*) \\
h_5 &= -(\omega_1 k_3^* + \omega_3 k_1^*) \\
h_6 &= -(\omega_2 k_3^* + \omega_3 k_2^*)
\end{aligned}$$

and hence, when $k_3^* \neq 0$,

$$\omega_1 = \frac{-h_5 - \omega_3 k_1^*}{k_3^*}$$

$$\omega_2 = \frac{-h_6 - \omega_3 k_2^*}{k_3^*} \qquad (5.98)$$

$$\omega_3 = \frac{h_1 + h_2 - h_3}{2k_3^*}$$

Let

$$\bar{\omega}_3 = \frac{\bar{h}_1 + \bar{h}_2 - \bar{h}_3}{2\bar{k}_3^*}$$

$$\bar{\omega}_1 = \frac{-\bar{h}_5 - \bar{\omega}_3 \bar{k}_1^*}{\bar{k}_3^*} \qquad (5.99)$$

$$\bar{\omega}_2 = \frac{-\bar{h}_6 - \bar{\omega}_3 \bar{k}_2^*}{\bar{k}_3^*}$$

and h be defined such that $||\Delta h||$ satifies (5.72) or (5.80) depending on whether k equals zero or not. In both cases $k_3^* = \bar{k}_3^*$ and it follows that:

$$|\bar{\omega}_3 - \omega_3| \leq \frac{|\bar{h}_1 - h_1| + |\bar{h}_2 - h_2| + |\bar{h}_3 - h_3|}{2|\bar{k}_3^*|}$$

If k=0, then k_1^* (k_2^*) equals to $\bar{k}_1^*$ ($\bar{k}_2^*$), too. Thus

$$|\bar{\omega}_1-\omega_1| \le \frac{|\bar{h}_5-h_5|+|\bar{\omega}_3-\omega_3|\cdot|\bar{k}_1^*|}{|\bar{k}_3^*|}$$

$$\le \frac{|\bar{h}_5-h_5|}{|\bar{k}_3^*|} + |\bar{\omega}_3-\omega_3| \quad (\text{since } |\bar{k}_1^*|<|\bar{k}_3^*|)$$

$$|\bar{\omega}_2-\omega_2| \le \frac{|\bar{h}_6-h_6|}{|\bar{k}_3^*|} + |\bar{\omega}_3-\omega_3| \quad (\text{since } |\bar{k}_2^*|<|\bar{k}_3^*|)$$

$$||\bar{\Omega}-\Omega|| \le \frac{|\bar{h}_1-h_1| + |\bar{h}_2-h_2| + |\bar{h}_3-h_3| + 2(|\bar{h}_5-h_5| + |\bar{h}_6-h_6|) + 2|\bar{\omega}_3-\omega_3|}{2|\bar{k}_3^*|}$$

$$\le \frac{3(|\bar{h}_1-h_1|+|\bar{h}_2-h_2|+|\bar{h}_3-h_3|)+2(|\bar{h}_5-h_5|+|\bar{h}_6-h_6|)}{2|\bar{k}_3^*|}$$

$$\le \frac{3(||\bar{h}-h||}{2|\bar{k}_3^*|} \le \frac{3||\bar{h}-h||}{(2/3)||\bar{k}^*||} \quad (\text{since } |\bar{k}_3^*|>|\bar{k}_1^*|,|\bar{k}_2^*|)$$

$$\le 4.5\xi_0 = \varepsilon_0 \qquad (5.100)$$

If $k\neq 0$, then $\bar{k}_3^*\neq 0$ implies $k_3\neq 0$ and

$$|\bar{\omega}_1-\omega_1| \le \frac{|\bar{h}_5-h_5|+|\bar{\omega}_3-\omega_3|\cdot|k_1^*|+|\bar{k}_1^*-k_1^*|\cdot|\bar{\omega}_3|}{|\bar{k}_3^*|}$$

$$\le \frac{|\bar{h}_5-h_5|+|\bar{\omega}_3-\omega_3|\cdot|\bar{k}_1^*|+|\bar{k}_1^*-k_1^*|(|\bar{\omega}_3|+|\bar{\omega}_3-\omega_3|)}{|\bar{k}_3^*|}$$

$$|\bar{\omega}_2-\omega_2| \le \frac{|\bar{h}_6-h_6|+|\bar{\omega}_3-\omega_3|\cdot|\bar{k}_2^*|+|\bar{k}_2^*-k_2^*|(|\bar{\omega}_3|+|\bar{\omega}_3-\omega_3|)}{|\bar{k}_3^*|}$$

Thus

$$||\bar{\Omega}-\Omega|| \leq \frac{3(|\bar{h}_1-h_1|+|\bar{h}_2-h_2|+|\bar{h}_3-h_3|)+2(|\bar{h}_5-h_5|+|\bar{h}_6-h_6|)}{2|\bar{k}_3^*|}$$

$$+ \frac{(|\bar{k}_1^*-k_1^*|+|\bar{k}_2^*-k_2^*|)(|\bar{\omega}_3|+\frac{|\bar{h}_1-h_1|+|\bar{h}_2-h_2|+|\bar{h}_3-h_3|}{2|\bar{k}_3^*|})}{|\bar{k}_3^*|}$$

$$= \frac{3(|\bar{h}_1-h_1|+|\bar{h}_2-h_2|+|\bar{h}_3-h_3|)+2(|\bar{h}_5-h_5|+|\bar{h}_6-h_6|)}{2|\bar{k}_3^*|}$$

$$+ \frac{2|\bar{\omega}_3|(|\bar{k}_1^*-k_1^*|+|\bar{k}_2^*-k_2^*|)}{2|\bar{k}_3^*|}$$

$$+ \frac{(|\bar{k}_1^*-k_1^*|+|\bar{k}_2^*-k_2^*|)(|\bar{h}_1-h_1|+|\bar{h}_2-h_2|+|\bar{h}_3-h_3|)}{2|\bar{k}_3^*|^2}$$

$$\leq \frac{\max\{3,2|\bar{\omega}_3|\}\ ||\bar{h}-h||}{2|\bar{k}_3^*|} + \frac{\xi_3^2}{2}$$

$$\leq \xi_3(\max\{1.5,|\bar{\omega}_3|\}+0.5\xi_3)$$

$$= \varepsilon_3 \qquad (5.101)$$

Now we turn to the case: $|\bar{k}_1^*| \geq |\bar{k}_2^*|, |\bar{k}_3^*|$, which implies $\bar{k}_1^* \neq 0$. For any solution h of the linear equation $W \cdot h = 0$, we have

$$\omega_1 = \frac{h_2+h_3-h_1}{2k_1^*}$$

$$\omega_2 = \frac{-h_4 - \omega_1 k_2^*}{k_1^*} \qquad (5.102)$$

$$\omega_3 = \frac{-h_5 - \omega_1 k_3^*}{k_1^*}$$

instead of (5.98). Set

$$\bar{\omega}_1 = \frac{\bar{h}_2+\bar{h}_3-\bar{h}_1}{2\bar{k}_1^*}$$

$$\bar{\omega}_2 = \frac{-\bar{h}_4 - \bar{\omega}_1 \bar{k}_2^*}{\bar{k}_1^*} \qquad (5.103)$$

$$\bar{\omega}_3 = \frac{-\bar{h}_5 - \bar{\omega}_1 \bar{k}_3^*}{\bar{k}_1^*}$$

and h be defined such that $||\Delta h||$ satisfies (5.72) or (5.89) depending whether k equals zero or not. In any case, it is certain that $k_1^*=\bar{k}_1^*$. It is easy to see

$$|\bar{\omega}_1-\omega_1| \leq \frac{|\bar{h}_1-h_1|+|\bar{h}_2-h_2|+|\bar{h}_3-h_3|}{2|\bar{k}_1^*|}$$

If k=0, then $k_2^*(k_3^*)$ equals to $\bar{k}_2^*(\bar{k}_3^*)$, too. Thus

$$|\bar{\omega}_2-\omega_2| \leq \frac{|\bar{h}_4-h_4|+|\bar{\omega}_1-\omega_1|\cdot|\bar{k}_2^*|}{|\bar{k}_1^*|}$$

$$|\bar{\omega}_3-\omega_3| \leq \frac{|\bar{h}_5-h_5|+|\bar{\omega}_1-\omega_1|\cdot|\bar{k}_3^*|}{|\bar{k}_1^*|}$$

and

$$||\bar{\Omega}-\Omega|| \leq \varepsilon_0$$

If $k\neq 0$, then $k_1^*\neq 0$ implies $k_1\neq 0$ and

$$||\bar{\Omega}-\Omega|| \leq \xi_1 \left(\max\{1.5, |\bar{\omega}_1|\} + 0.5\xi_1 \right)$$

$$= \varepsilon_1 \qquad (5.104)$$

Similarly, when $|\bar{k}_2^*| \geq |\bar{k}_1^*|, |\bar{k}_3^*|$ we have either

$$||\bar{\Omega}-\Omega|| \leq \varepsilon_0 \quad (k=0)$$

or

$$||\bar{\Omega}-\Omega|| \leq \xi_2 \left(\max\{1.5, |\bar{\omega}_2|\} + 0.5\xi_2 \right)$$

$$= \varepsilon_2 \quad (k\neq 0) \qquad (5.105)$$

where

$$\bar{\omega}_2 = \frac{\bar{h}_1+\bar{h}_3-\bar{h}_2}{2\bar{k}_2^*}$$

$$\bar{\omega}_1 = \frac{-\bar{h}_4 - \bar{\omega}_2\bar{k}_1^*}{\bar{k}_2^*} \qquad (5.106)$$

$$\bar{\omega}_3 = \frac{-\bar{h}_6 - \bar{\omega}_2\bar{k}_3^*}{\bar{k}_2^*}$$

Theorem 5.7. Assume that the noise perturbation bound δ

is small enough, $\bar{h}^t\bar{W}\bar{h} = \min\ h^t\bar{W}h\ ||h||_2=1$ and $\bar{\Omega}$ is defined by (5.103) or (5.106) or (5.99) depending on which component is the largest among $|\bar{k}_1^*|$, $|\bar{k}_2^*|$ and $|\bar{k}_3^*|$. Then, there is a solution (Ω,k^*) of the basic equation (5.5) such that either

$$k^* = \bar{k}^*,\ ||\bar{\Omega}-\Omega|| \leq \varepsilon_0 \tag{5.107}$$

or

$$||k^*-\bar{k}^*|| \leq \xi_i||\bar{k}^*|| \quad (i=1,\ 2,\ \text{or}\ 3)$$

and (5.108)

$$||\bar{\Omega}-\Omega|| \leq \varepsilon_i \quad (i=1,\ 2,\ \text{or}\ 3)$$

5.4 Estimation of Translational Motion and Relative Depth

In the previous section the small perturbation is assumed and estimations $||\bar{\Omega}-\Omega||$ and $||\bar{k}-k^*||$ are obtained.

$$k^* = \bar{k}^*,\ ||\bar{\Omega}-\Omega|| \leq \varepsilon_0 \quad \text{if } k=0$$

$$||\bar{k}^*-k^*|| \leq \xi_1||\bar{k}^*||,\quad ||\bar{\Omega}-\Omega|| \leq \varepsilon_1 \quad \text{if } k\neq 0 \text{ and } |\bar{k}_1^*| \geq |\bar{k}_2^*|, |\bar{k}_3^*|$$

$$||\bar{k}^*-k^*|| \leq \xi_2||\bar{k}^*||,\quad ||\bar{\Omega}-\Omega|| \leq \varepsilon_2 \quad \text{if } k\neq 0 \text{ and } |\bar{k}_2^*| \geq |\bar{k}_1^*|, |\bar{k}_3^*|$$

$$||\bar{k}^*-k^*|| \leq \xi_3||\bar{k}^*|| \qquad \text{if } k\neq 0 \text{ and } |\bar{k}_3^*|\geq|\bar{k}_1^*|,|\bar{k}_2^*|$$
$$||\bar{\Omega}-\Omega|| \leq \varepsilon_3$$

When $k\neq 0$, the translational orientation $k/||k||$ is equal to $\pm k^*/||k^*||$ and the relative depth $z/||k||$ could be obtained from (Ω,k^*). In this section we consider how to judge $k\neq 0$ and to estimate $k/||k||$ and $z/||k||$ when $k\neq 0$ from an approximate solution $(\bar{\Omega},\bar{k}^*)$.

Lemma 5.7 Keep the same assumption as in Lemma 5.1. Assume that the instantaneous translation velocity k is not zero and (k^*,Ω) is a solution of the second fundamental optic flow equation (5.5) with $k^*\neq 0$. Then, either

$$a||b|| = b||a|| \tag{5.109}$$

or

$$a||b|| = -b||a|| \tag{5.110}$$

where

$$a = -\begin{vmatrix} \omega_1 & \omega_3 \\ X & Z \end{vmatrix}\begin{bmatrix} X \\ Z \end{bmatrix} + \begin{bmatrix} u \\ v \end{bmatrix} - \begin{vmatrix} \begin{vmatrix} \omega_2 & \omega_3 \\ 1 & Z \end{vmatrix} \\ \begin{vmatrix} \omega_1 & \omega_1 \\ Z & 1 \end{vmatrix} \end{vmatrix} \tag{5.111}$$

and

$$b = \begin{bmatrix} k_1^* \\ k_3^* \end{bmatrix} - k_2^*\begin{bmatrix} X \\ Z \end{bmatrix} \tag{5.112}$$

Proof. $k\neq 0$ implies $k^*=\beta k$ by Theorem 5.1. From (5.35) it is clear $(\beta y)a=b$ with $y>1$ and hence either (5.109) or (5.110) holds.

Q.E.D.

Corollary 1. (5.109) implies $k/||k|| = k^*/||k^*||$ and (5.110) implies $k/||k|| = -k^*/||k^*||$.

Proof. (5.37) implies $k/||k|| = \text{sign}\ (\beta y)k^*/||k^*||$ and (5.109) implies $\beta>0$ and (5.110) implies $\beta<0$. Thus, we have the conclusion.

Q.E.D.

Corollary 2. (5.109) ((5.110)), $(\beta y)a=b$ with $y>1$, and $k^*=\beta k$ imply

$$\beta y||a|| = ||b|| \quad (-||b||) \tag{5.113}$$

$$\frac{y}{||k||} = \frac{1}{||k^*||} \cdot \frac{||b||}{||a||} \tag{5.114}$$

Corollary 3. For at most one image point $a=0$ and for at most one image point $b=0$.

From Theorem 5.4 it is clear that $k=0$ iff $a=0$.

Let

$$\bar{a} = \begin{vmatrix} \bar{\omega}_1 & \bar{\omega}_3 \\ X & Z \end{vmatrix} \begin{bmatrix} X \\ Z \end{bmatrix} + \begin{bmatrix} \bar{u} \\ \bar{v} \end{bmatrix} - \begin{vmatrix} \bar{\omega}_2 & \bar{\omega}_3 \\ 1 & Z \end{vmatrix} \begin{bmatrix} \bar{\omega}_2 \\ \bar{\omega}_1 \end{bmatrix} \tag{5.115}$$

We have

$$\bar{a} = \bar{a} - a + a$$

$$= a + \begin{vmatrix} \bar{\omega}_1-\omega_1 & \bar{\omega}_3-\omega_3 \\ X & Z \end{vmatrix} \begin{bmatrix} X \\ Z \end{bmatrix} + \begin{bmatrix} \bar{u}-u \\ \bar{v}-v \end{bmatrix} - \begin{bmatrix} \begin{vmatrix} \bar{\omega}_2-\omega_2 & \bar{\omega}_3-\omega_3 \\ 1 & Z \end{vmatrix} \\ \begin{vmatrix} \bar{\omega}_1-\omega_1 & \bar{\omega}_2-\omega_2 \\ X & 1 \end{vmatrix} \end{bmatrix}$$

Thus, when a=0 we obtain

$$\begin{aligned} \|\bar{a}\| &= \|\bar{a}-a\| \\ &\leq (|\bar{\omega}_1-\omega_1|+|\bar{\omega}_3-\omega_3|)(|X|+|Z|)^2 + (|\bar{u}-u|+|\bar{v}-v|) \\ &+(|\bar{\omega}_2-\omega_2|+|\bar{\omega}_3-\omega_3|)(|Z|+1)+(|\bar{\omega}_1-\omega_1|+|\bar{\omega}_2-\omega_2|)(|X|+1) \\ &\leq \delta + \|\bar{\Omega}-\Omega\|\{(|X|+|Z|)^2+|X|+|Z|+2\} \end{aligned} \tag{5.116}$$

Lemma 5.8. Assume that the translational velocity k=0 and the perturbation is small enough. Then for any pair $[(X,Z),(\bar{u},\bar{v})]$ there holds

$$\|\bar{a}\| \leq \delta + \varepsilon_0\{(|X|+|Z|)^2+|X|+|Z|+2\} \tag{5.117}$$

Corollary 1. If for some pair $[(X,Z),(\bar{u},\bar{v})]$

$$\|\bar{a}\| > \delta + \varepsilon_0\{(|X|+|Z|)^2+|X|+|Z|+2\} \tag{5.118}$$

then $k\neq 0$.

Corollary 2. If there holds

$$\frac{1}{N}\sum^{1}\|\bar{a}\| > \delta + \frac{1}{N}\sum^{1}\varepsilon_0\{(|X|+|Z|)^2+|X|+|Z|+2\}, \tag{5.119}$$

then $k \neq 0$ where N is the number of optic flow image points.

Let

$$\bar{b} = \begin{bmatrix} \bar{k}_1^* \\ \bar{k}_3^* \end{bmatrix} - \bar{k}_2^* \begin{bmatrix} X \\ Z \end{bmatrix} \tag{5.120}$$

Assume $k \neq 0$. Then, $k/||k|| = \pm k^*/||k^*||$. Assume the perturbation is so small that $k/||k|| = k^*/||k^*||$ if and only if

$$\frac{1}{N}||\bar{a}\cdot||\bar{b}|| + \bar{b}\cdot||\bar{a}||\,|| > \frac{1}{N}\sum||\bar{a}\cdot||\bar{b}|| - \bar{b}\cdot||\bar{a}||| \tag{5.121}$$

and $k/||k|| = -k^*/||k^*||$ if and only if

$$\frac{1}{N}||\bar{a}\cdot||\bar{b}|| - \bar{b}\cdot||\bar{a}|||| > \frac{1}{N}\sum||\bar{a}\cdot||\bar{b}|| + \bar{b}\cdot||\bar{a}|||| \tag{5.122}$$

Then, when (5.121) holds we have an estimation $\bar{k}^*/||\bar{k}^*||$ for $k/||k||$ and

$$\left|\left| \frac{k}{||k||} - \frac{\bar{k}^*}{||\bar{k}^*||} \right|\right| = \left|\left| \frac{k^*}{||k^*||} - \frac{\bar{k}^*}{||\bar{k}^*||} \right|\right|$$

$$= \frac{||\,||k^*||(k^*-\bar{k}^*)-(||k^*||-||\bar{k}^*||)\,k^*||}{||k^*||\cdot||\bar{k}^*||}$$

$$\leq \frac{2||k^*||\cdot||k^*-\bar{k}^*||}{||k^*||\cdot||\bar{k}^*||} \leq 2\xi_i \quad (i = 1, 2, \text{ or } 3) \tag{5.123}$$

Similarly, when (5.122) holds we have

$$\left\| \frac{k}{\|k\|} + \frac{\bar{k}^*}{\|\bar{k}^*\|} \right\| < 2\xi_i \quad (i = 1, 2, \text{ or } 3) \qquad (5.124)$$

Therefore, we have

Theorem 5.8. Under the small perturbations, (5.118) and (5.121) imply (5.123) and (5.118) and (5.122) imply (5.124).

Noticing (5.114), we have

Theorem 5.9. When (5.118) holds, the estimation of relative depth $y/\|k\|$ is given by $-\|\bar{b}\|/(\|\bar{k}^*\|\cdot\|\bar{a}\|)$ and the approximation is characterized by

$$\left| \frac{y}{\|k\|} - \frac{\|\bar{b}\|}{\|\bar{k}^*\|\cdot\|\bar{a}\|} \right| \leq \eta_i \qquad (5.125)$$

where η_i is defined by (5.126).

Proof. (118) implies $k \neq 0$ and hence the relative depth

$$\frac{z}{\|k\|} = -\frac{1}{\|k^*\|} \cdot \frac{\|b\|}{\|a\|}$$

When the perturbation is small, $\|\bar{b}\|/(\|\bar{k}^*\|\cdot\|\bar{a}\|)$ is a good approximation of the relative depth and

$$\left| \frac{y}{\|k\|} - \frac{\|\bar{b}\|}{\|\bar{k}^*\|\cdot\|\bar{a}\|} \right| = \left| \frac{\|b\|}{\|k^*\|\cdot\|a\|} - \frac{\|\bar{b}\|}{\|\bar{k}^*\|\cdot\|\bar{a}\|} \right|$$

$$\leq \frac{\|k^*\|\cdot\|a\|\cdot\|\bar{b}-b\|+\|b\|(\|\bar{k}^*-k^*\|\cdot\|a\|+\|\bar{k}^*\|\cdot\|\bar{a}-a\|)}{\|\bar{k}^*\|\cdot\|k^*\|\cdot\|\bar{a}\|\cdot\|a\|}$$

Noticing

$$\|\bar{a}-a\| \leq \delta + \varepsilon_i\{(|X|+|Z|)^2+|X|+|Z|+2\}$$

$$\|\bar{b}-b\| \leq \|\bar{k}^*-k^*\|(|X|+|Z|+1)$$

$$\|\bar{k}^*-k^*\| \leq \xi_i\|\bar{k}^*\|$$

we obtain

$$\left|\frac{y}{\|k\|}-\frac{\|\bar{b}\|}{\|\bar{k}^*\|\cdot\|\bar{a}\|}\right| \leq \frac{\|\bar{b}-b\|}{\|\bar{k}^*\|\cdot\|\bar{a}\|}$$

$$+\frac{(\|\bar{b}\|+\|\bar{b}-b\|)\cdot\|\bar{k}^*-k^*\|}{\|\bar{k}^*\|\cdot(\|\bar{k}^*\|-\|\bar{k}^*-k^*\|)\cdot\|\bar{a}\|}$$

$$+\frac{(\|\bar{b}\|+\|\bar{b}-b\|)\cdot\|\bar{a}-a\|}{(\|\bar{k}^*\|-\|\bar{k}^*-k\|)\cdot\|\bar{a}\|\cdot(\|\bar{a}\|-\|\bar{a}-a\|)}$$

$$\leq \frac{\|\bar{k}^*-k\|\cdot(|X|+|Z|+1)}{\|\bar{k}^*\|\cdot\|\bar{a}\|}$$

$$+\frac{[\|\bar{b}\|+\|\bar{k}^*-k\|\cdot(|X|+|Z|+1)]\cdot\xi_i\|\bar{k}^*\|}{\|\bar{k}^*\|(\|\bar{k}^*\|-\xi_i\|\bar{k}^*\|)\|\bar{a}\|}$$

$$+\frac{[\|\bar{b}\|+\|\bar{k}^*-k\|\cdot(|X|+|Z|+1)](\delta+\varepsilon_i\{(|X|+|Z|)^2+|X|+|Z|+1\})}{(\|\bar{k}^*\|-\|\bar{k}^*-k\|)\cdot\|\bar{a}\|(\|\bar{a}\|-\delta-\varepsilon_i\{(|X|+|Z|)^2+|X|+|Z|+2\})}$$

$$\leq \frac{\xi_i(|X|+|Z|+1)}{||\bar{a}||} + \frac{[||\bar{b}||+\xi_i||\bar{k}^*||(|X|+|Z|+1)]\xi_i}{||\bar{k}^*||(1-\xi_i)||\bar{a}||}$$

$$+ \frac{[||\bar{b}||+\xi_i||\bar{k}^*||(|X|+|Z|+1)](\delta+\varepsilon_i\{(|X|+|Z|)^2+|X|+|Z|+2\})}{||\bar{k}^*||(1-\xi_i)\cdot||\bar{a}||(||\bar{a}||-\delta-\varepsilon_i\{(|X|+|Z|)^2+|X|+|Z|+2\})}$$

$$= \eta_i \qquad (5.126)$$

Q.E.D.

5.5 Recapitulation and Experimental Result

In this section, we, first, recaptulate the motion and relative estimation from optic flow image described in the previous sections and then show some experimental results.

Let a rigid body motion (k,Ω), $k=(k_1,k_2,k_3)^t$ and $\Omega=(\omega_1,\omega_2,\omega_3)$, generate an optic flow image $\{[(X,Z),(u,v)]\}$. Suppose the optic flow image experiences a small noise perturbation and becomes $\{[(X,Z),(\bar{u},\bar{v})]\}$ where $|\bar{u}-u|+|\bar{v}-v|\leq\delta$. From the perturbed optic flow image, we estimate the rigid body motion $(\bar{k},\bar{\Omega})$, $\bar{k}=(\bar{k}_1,\bar{k}_2,\bar{k}_3)^t$ and $\bar{\Omega}=(\bar{\omega}_1,\bar{\omega}_2,\bar{\omega}_3)^t$, and relative depth of the rigid body surface points. Let

$$\bar{W} = \sum_{[(X,Z),(\bar{u},\bar{v})]} \bar{B}^t\bar{B}$$

where

$$\bar{B} = [X^2,1,Z^2,X,XZ,Z,-\bar{v},\bar{v}X-\bar{u}Z,\bar{u}]$$

and let

$$\bar{h} = [\bar{h}_1,\bar{h}_2,\bar{h}_3,\bar{h}_4,\bar{h}_5,\bar{h}_6,\bar{h}_7,\bar{h}_8,\bar{h}_9]^t$$

$$\bar{k}^* = [\bar{k}_1^*,\bar{k}_2^*,\bar{k}_3^*]^t = [\bar{h}_7,\bar{h}_8,\bar{h}_9]^t$$

And let $||\cdot||$ be the l_1-vector norm defined by

$$||x_i|| = \sum|x_i| \text{ where } x \text{ is a column vector.}$$

Then the estimation of the rigid body motion and relative depth can be described by the following algorithm

Algorithm: Linear Motion and Depth Estimation

Step 1. Compute λ and $\bar{h}$: $\lambda=\bar{h}^t\bar{W}\bar{h} = \min_{||h||_2=1} h^t\bar{W}h$

Step 2. Set $\bar{k}^* = [\bar{h}_7, \bar{h}_8 \bar{h}_9]^t$

Step 3. If $|\bar{k}_1^*| \geq |\bar{k}_2^*|, |\bar{k}_3^*|$, then

set i = 1 and compute

$$\bar{\omega}_1=\frac{\bar{h}_2+\bar{h}_3-\bar{h}_1}{2\bar{k}_1^*}, \quad \bar{\omega}_2=\frac{-\bar{k}_2^*\bar{\omega}_1-\bar{h}_4}{\bar{k}_1^*}, \text{ and } \bar{\omega}_3=\frac{-\bar{k}_3^*\bar{\omega}_1-\bar{h}_5}{\bar{k}_1^*}$$

If $|\bar{k}_2^*| > |\bar{k}_1^*|, |\bar{k}_3^*|$, then

set i = 2 and compute

$$\bar{\omega}_2=\frac{\bar{h}_1+\bar{h}_3-\bar{h}_2}{2\bar{k}_2^*}, \quad \bar{\omega}_1=\frac{-\bar{k}_1^*\bar{\omega}_2-\bar{h}_4}{\bar{k}_2^*}, \text{ and } \bar{\omega}_3=\frac{-\bar{k}_3^*\bar{\omega}_2-\bar{h}_6}{\bar{k}_2^*}$$

If $|\bar{k}_3^*| > |\bar{k}_1^*|, |\bar{k}_2^*|$, then

set i = 3 and compute

$$\bar{\omega}_3=\frac{\bar{h}_1+\bar{h}_2-\bar{h}_3}{2\bar{k}_3^*}, \quad \bar{\omega}_1=\frac{-\bar{k}_1^*\bar{\omega}_3-\bar{h}_5}{\bar{k}_3^*}, \text{ and } \bar{\omega}_2=\frac{-\bar{k}_2^*\bar{\omega}_3-\bar{h}_6}{\bar{k}_3^*}$$

Estimate the rotational motion components by

$$\bar{\Omega} = [\bar{\omega}_1, \bar{\omega}_2, \bar{\omega}_3]^t$$

Step 4 Let ε_0 be given by (5.100).

If $||\bar{a}|| \leq \delta + \varepsilon_0\{(|X|+|Z|)^2+|X|+|Z|+2\}$

for all image point pair $\{[(X,Z),(\bar{u},\bar{v})]\}$,

then the motion is a (pseudo) pure rotational motion.

Thus, estimate the rotational motion error bound by

$$||\bar{\Omega}-\Omega|| < \varepsilon_0$$

and stop.

Step 5. Estimation of translational motion

If $\frac{1}{N}\sum||\bar{a}\cdot||\bar{b}||+\bar{b}\cdot||\bar{a}||| < \frac{1}{N}\sum||\bar{a}\cdot||\bar{b}||-\bar{b}\cdot||\bar{a}||||$,

then estimate the scaled translational motion by

$$\bar{k} = \bar{k}^*$$

otherwise $\bar{k} = -\bar{k}^*$.

Step 6. Motion estimation error bound

Let i be the index determined at the step 3.

Let ξ_1, ξ_2, and ξ_3 be given by (5.88), (5.94), and (5.79), respectively.

Let ε_1, ε_2, and ε_3 be given by (5.104), (5.105), and (5.101), respectively.

then the translational motion direction estimation

error is given by

$$\left\| \frac{\mathbf{k}}{\|\mathbf{k}\|} - \frac{\bar{\mathbf{k}}^*}{\|\bar{\mathbf{k}}^*\|} \right\| \leq 2\xi_i$$

and the rotational motion estimation error is given by

$$\|\bar{\Omega}-\Omega\| \leq \varepsilon_i$$

Step 7. Estimation of relative depth and its error bound.

Let i be the index determined at the step 3 and let η_1, η_2, and η_3 be given by (5.126), then the relative depth is given by

$$\frac{y}{\|\mathbf{k}\|} = \frac{\|\bar{\mathbf{b}}\|}{\|\bar{\mathbf{k}}^*\| \cdot \|\bar{\mathbf{a}}\|}$$

and its error bound is given by

$$\left| \frac{y}{\|\mathbf{k}\|} - \frac{\|\bar{\mathbf{b}}\|}{\|\bar{\mathbf{k}}^*\| \cdot \|\bar{\mathbf{a}}\|} \right| \leq \eta_i$$

Step 8. Stop

To verify the theory developed in this chapter, we generate optic flow images of an ellipsoid in motion, perturb the optic flow images by adding noises, and apply the above algorithm to estimate the motion parameters and relative depth of the ellipsoid. In the following

experiment, we use $\gamma_0 = \gamma_1 = \gamma_2 = \gamma_3 = 1$ for the estimation of maximum error norm. The ideal depth of the ellipsoid we use is shown in Fig 5.1.

First, we assume that the ellipsoid moves with the instantaneous translation k=0 and the instantaneous rotation $\Omega=(.1,-.5,.2)^t$. From the motion parameters we can compute the instantaneous 3D velocity at each surface point of the ellipsoid and determine the optic flow image shown in Fig 5.2 by projecting the velocity on the image plane. We apply the above algorithm to the ideal optic flow image and its noisy perturbations.

For the optic flow image in Fig 5.2, we recovered the exact rotational velocity and normalized translational velocity as we see from the first column in Table 5.1. In Table 5.1, δ means the magnitude of the maximum absolute random noise vector added to each flow vector in Fig 5.2 and $\bar{\omega}_1$, $\bar{\omega}_2$, and $\bar{\omega}_3$ are the estimated rotational velocity comopnents. The error between the true rotational velocity and the estimated one is the l_1 vector norm $||\bar{\Omega}-\Omega||$ and the theoretical error bound computed by the algorithm is ε in the table.

To see the behavior of the algorithm with noise, we perturb the optic flow image in Fig 5.2 with δ = .01, .05, and .1. For each case of δ, we estimate the rotational velocity successfully within its expected error estimation

as Table 5.1 indicates.

Next, we assume that the ellipsoid moves with $k=(1,-5,2)'$ and $\Omega=0$. From these motion parameters, we compute the ideal optic flow image in Fig 5.3. Applying the algorithm to this ideal optic flow image and its noisy perturbations by various δ (δ = .01, .05, .1), we obtain Table 5.2. The table indicates that the algorithm estimates the translational velocity succesfully with comparable error estimation. Because the ellipsoid moves with nonzero translational velocity, we can estimate relative depth from the optic flow image. From the ideal optic flow image in Fig 5.3 we recover the ideal depth image in Fig 5.1. However, when this optic flow image is perturbed by δ =.01, .5, and .1, we estimate the perturbed depth images in Fig 5.4, Fig 5.5, and Fig 5.6, respectively.

For a general motion, $k=(1,5,1)$ and $\Omega=(.1,.2,.1)$, of the ellipsoid, we obtain the ideal optic flow image in Fig 5.7. In the same way, we perturb this optic flow image and apply the algorithm to them. Table 5.3 shows the result obtained from the algorithm. Recovered relative depth images are shown in Fig 5.8, Fig 5.9, and Fig 5.10.

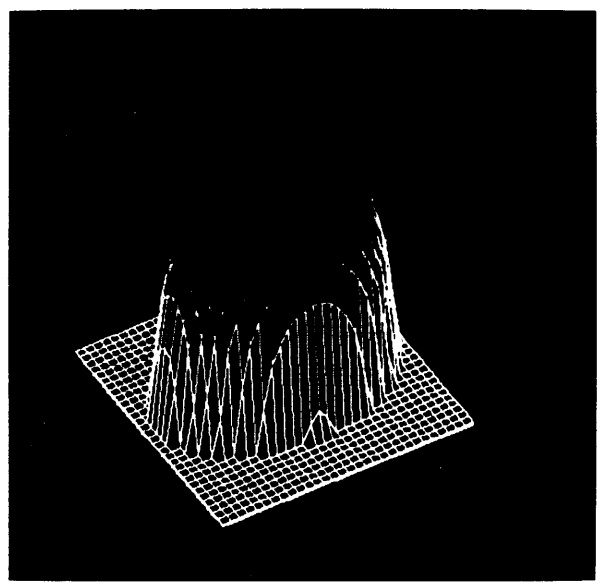

Fig 5.1. Ideal (Synthesized) Depth Image of an Ellipsoid

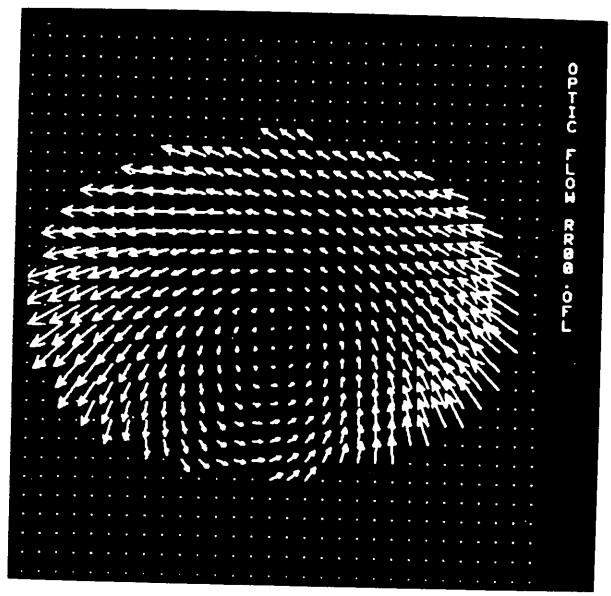

Fig 5.2. Ideal Optic Flow Image from the Motion, k=0 and Ω=(.1,-.5,.2), of the Ellipsoid

δ	$\bar{\omega}_1$	$\bar{\omega}_2$	$\bar{\omega}_3$	$\|\|\bar{\Omega}-\Omega\|\|$	ε_i
0.0	.1	-.5	.2		
.01	.09982	-.50003	.19986	.00036	.01521
.05	.09909	-.50017	.19927	.00181	.01520
0.1	.09817	-.50035	.19852	.00366	.01519

Table 5.1 Estimated Rotational Motion and Errors from Various Noise Perturbations of Optic Flow Image in Fig 5.2

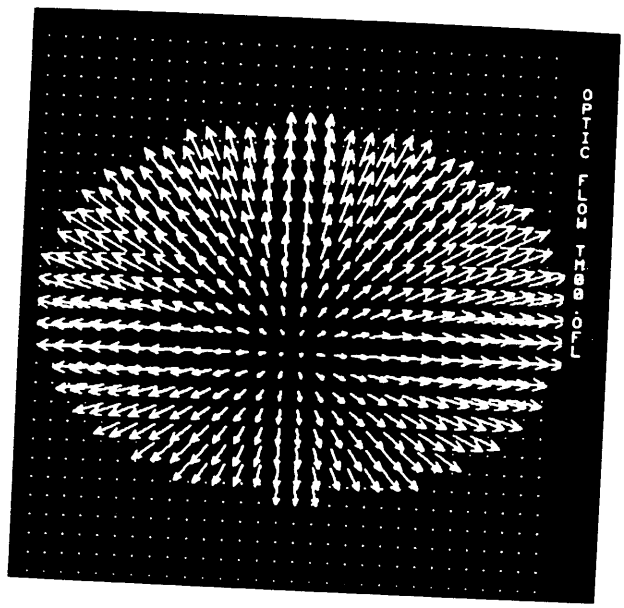

Fig 5.3 Ideal Optic Flow Image from the Motion, $k=(1,-5,2)$ and $\Omega=0$, of the Ellipsoid.

δ	$\bar{k}_x$	$\bar{k}_y$	$\bar{k}_z$	$\|\|\bar{k}-k\|\|$	ε_i
0.0	.11111	-.55556	.33333		
.01	.11122	-.55572	.33305	.00056	.00030
.05	.11209	-.55566	.33225	.00316	.00753
0.1	.11423	-.55384	.33193	.00623	.03159

Table 5.2 Estimated Translational Motion and Errors from Various Noise Perturbations of Optic Flow Image in Fig 5.3

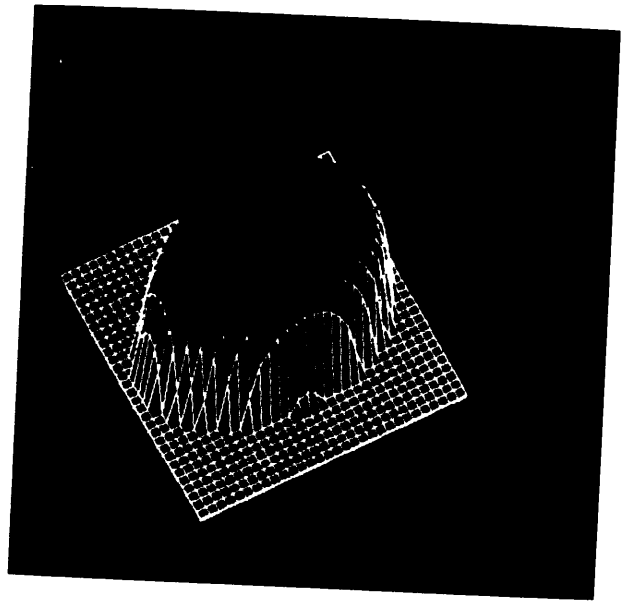

Fig 5.4. Recovered Depth Image from the Perturbed Optic Flow Image of Fig 5.3 with $\delta = .01$

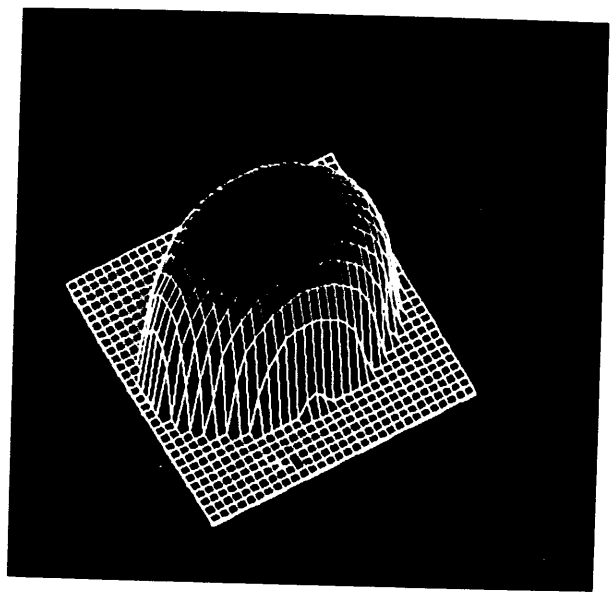

Fig 5.5. Recovered Depth Image from the Perturbed Optic Flow Image of Fig 5.3 with $\delta = .05$

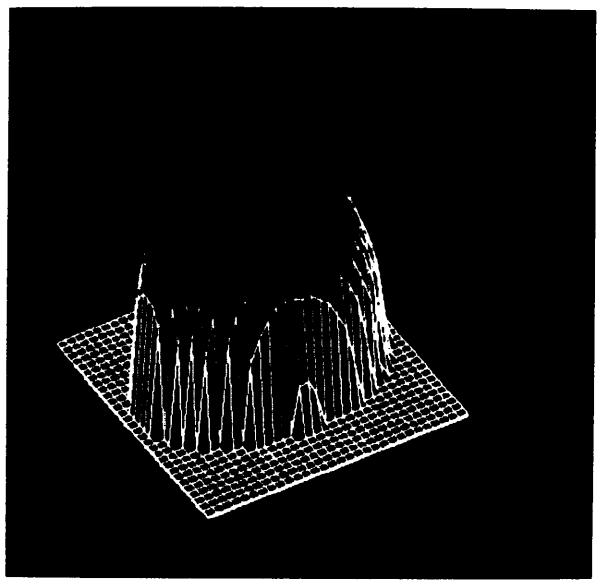

Fig 5.6. Recovered Depth Image from the Perturbed Optic Flow Image of Fig 5.3 with $\delta = .1$

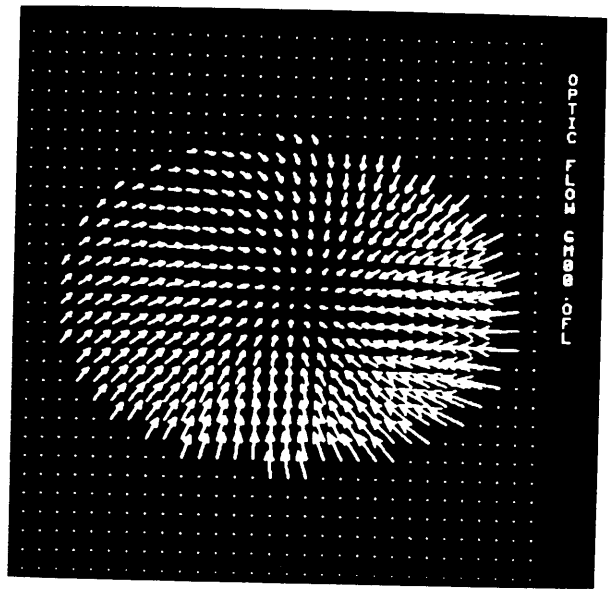

Fig 5.7. Ideal Optic Flow Image from the Motion, k=(1,5,1) and Ω=(.1,.2,.1), of the Ellipsoid

δ	t	$\bar{\Omega}$	$\|\|t-t^*\|\|$	$2\xi_i$	$\|\|\bar{\Omega}-\Omega\|\|$	ε_i
0.0	.14286 .71429 .14286	.1 .2 .1				
.01	.14328 .71431 .14241	.10024 .19998 .10073	.0009	.0007	.0009	.0005
.05	.14631 .71313 .14056	.10103 .19970 .10552	.00691	.01784	.00685	.01340
.1	.15340 .70847 .13813	.10159 .19883 .11612	.02108	.07267	.01887	.05516

where $t = \dfrac{k}{\|k\|}$, $t^* = \dfrac{\pm\bar{k}^*}{\|\bar{k}^*\|}$

('+' or '-' is determined by the algorithm)

Table 5.3 Estimated General Motion Parameters and Errors from Various Noise Perturbations of Optic Flow Images in Fig 5.7

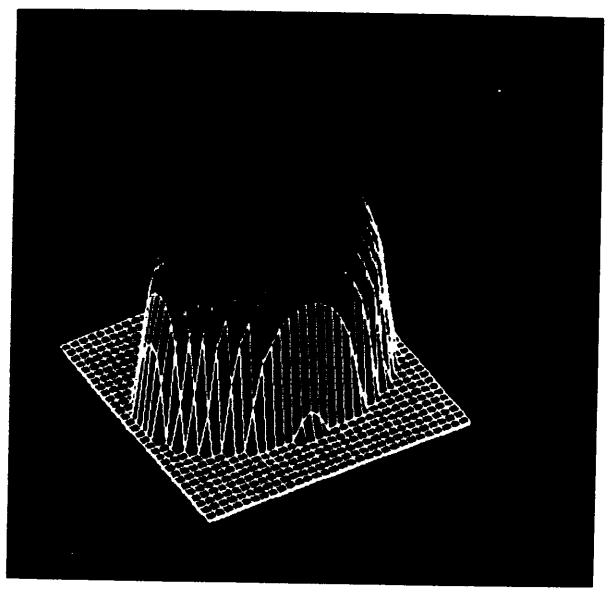

Fig 5.8. Recovered Depth Image from the Perturbed Optic Flow Image of Fig 5.7 with δ =.01

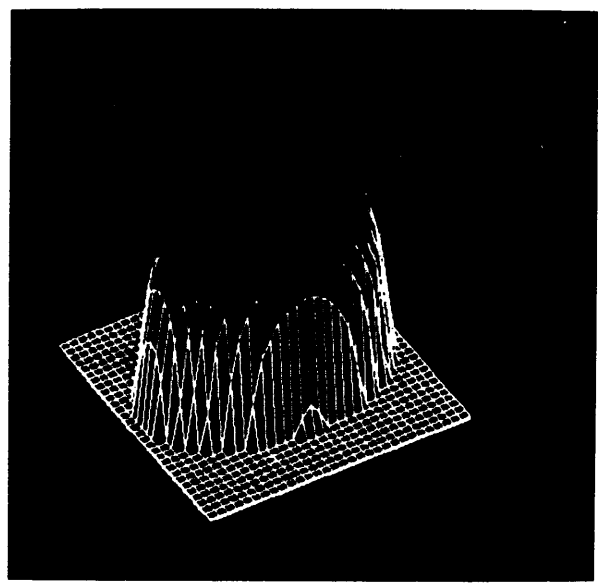

Fig 5.9. Recovered Depth Image from the Perturbed Optic Flow Image of Fig 5.7 with $\delta = .05$

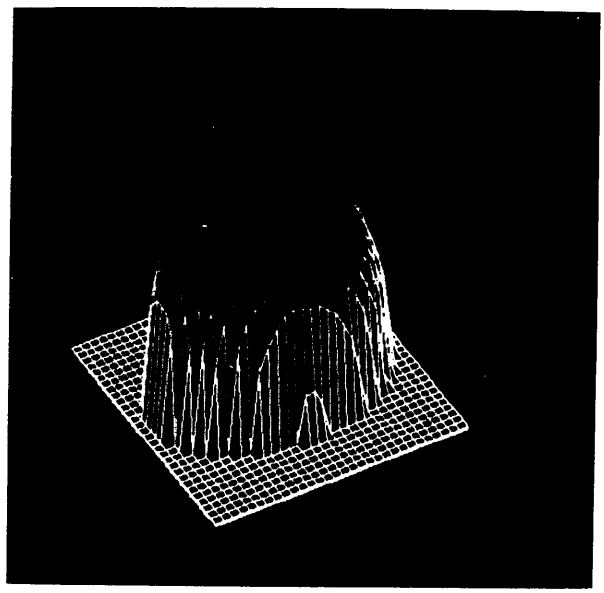

Fig 5.10. Recovered Depth Image from the Perturbed Optic Flow Image of Fig 5.7 with δ=.1

CHAPTER VI

USING OPTIC FLOW AND ITS TIME DERIVATIVE

In the previous two chapters, we discuss the techniques for recovering motion parameters from optic flow field only. The optic flow field is instantaneous in a time varying scene and, thus, the temporal change of the field can be observed.

In this chapter, we describe a technique for recovering motion and depth information from an optic flow field and its temporal change and extend the technique for the optic flow image segmentation. The technique requires a single optic flow vector and its time derivative to determine pure translational or rotational motion components determination. For the general motion, the technique requires three optic flows and their time derivatives to determine the motion parameters.

For the multiple object motion, we use the Hough transform technique to segment the optic flow field based on the rotational motion constraint derived at each optic flow and its time derivative. This technique requires a three dimensional Hough parameter space for the three rotational motion components. The optic flows with the same rotational motion are further classified by the motion parameters

corresponding to the translational motion.

In section 6.1, we derive a general motion equation from the optic flow and its time derivative; in sections 6.2 and 6.3, we consider pure translational motion and rotational motion with k=0. In section 6.4, we use the derived motion equation for motion based image segmentation.

6.1 General Motion Equations

Recall that the first fundamental optic flow equation is given by

$$\frac{P_y}{f}\begin{bmatrix} u \\ 0 \\ v \end{bmatrix} = \frac{P_y}{f}\,\Omega \times \begin{bmatrix} x \\ f \\ z \end{bmatrix} - \frac{P_y}{f}\begin{bmatrix} \dot{x} \\ \dot{f} \\ \dot{z} \end{bmatrix} + k \qquad (6.1)$$

Suppose that the motion parameters and k are uniform over the time. Differentiating the above equation with respect to the time, we have

$$\frac{P_y}{f}\begin{bmatrix} \dot{u} \\ 0 \\ \dot{v} \end{bmatrix} = \frac{P_y}{f}\dot{\Omega} \times \begin{bmatrix} x \\ f \\ z \end{bmatrix} + \frac{P_y}{f}\Omega \times \begin{bmatrix} u \\ 0 \\ v \end{bmatrix} - \frac{2P_y}{f}\begin{bmatrix} \dot{u} \\ 0 \\ \dot{v} \end{bmatrix} - \frac{P_y}{f}\begin{bmatrix} \ddot{x} \\ \ddot{f} \\ \ddot{z} \end{bmatrix} \qquad (6.2)$$

The cross product of both sides of the vector equation (6.2) with $[x,f,z]^T$ eliminates the second order partial derivative

of P_y. Rearranging the result and dividing it by unknown depth P_y, we have

$$\begin{bmatrix} x \\ f \\ z \end{bmatrix} \times \left\{ \begin{bmatrix} \dot{u} \\ 0 \\ \dot{v} \end{bmatrix} - \Omega x \begin{bmatrix} u \\ 0 \\ v \end{bmatrix} \right\} = \frac{\dot{P}_y}{P_y} \begin{bmatrix} x \\ f \\ z \end{bmatrix} \times \left\{ \Omega x \begin{bmatrix} x \\ f \\ z \end{bmatrix} - 2 \begin{bmatrix} u \\ 0 \\ v \end{bmatrix} \right\} \qquad (6.3)$$

or

$$\begin{bmatrix} \dot{v}f \\ \dot{u}z - \dot{v}x \\ -\dot{u}f \end{bmatrix} - \begin{bmatrix} -uf\omega_y - uz\omega_z + vz\omega_x \\ vz\omega_y + xu\omega_y \\ xu\omega_z - vx\omega_x - vf\omega_y \end{bmatrix}$$

$$= \frac{\dot{P}_y}{P_y} \left\{ \begin{bmatrix} (f^2+z^2)\omega_x - xf\omega_y - xz\omega_z \\ -xf\omega_x + (x^2+z^2)\omega_y - fz\omega_z \\ -xz\omega_x - fz\omega_y + (x^2+f^2)\omega_z \end{bmatrix} - 2 \begin{bmatrix} fv \\ uz - vx \\ -uf \end{bmatrix} \right\} \qquad (6.4)$$

With the vector and matrix notation, we have

$$\begin{bmatrix} vz & -uf & -uz \\ 0 & ux+vz & 0 \\ -vx & -vf & ux \end{bmatrix} \begin{bmatrix} \omega_x \\ \omega_y \\ \omega_z \end{bmatrix} + \frac{\dot{P}_y}{P_y} \begin{bmatrix} f^2+z^2 & -xf & -xz \\ -xf & x^2+z^2 & -fz \\ -xz & -fz & x^2+f^2 \end{bmatrix} \begin{bmatrix} \omega_x \\ \omega_y \\ \omega_z \end{bmatrix}$$

$$- \frac{2\dot{P}_y}{P_y} \begin{bmatrix} vf \\ uz - vx \\ -uf \end{bmatrix} - \begin{bmatrix} \dot{v}f \\ \dot{u}z - \dot{v}x \\ -\dot{u}f \end{bmatrix} = 0 \qquad (6.5)$$

The three equations in (6.4) or (6.5) are not independent because the vector product operation for the elimination of the term $\dot{P}_y/P_y$ makes one redundant. The middle equation can

be derived from the other two. Thus we have two independent equations for three unknown rotational components and one unknown positional dependent $\dot{P}_y/P_y$ from each optic flow and its time derivative as

$$\begin{aligned}
\dot{v}f-vz\omega_x+uf\omega_y+uz\omega_z &= \frac{\dot{P}_y}{P_y}\{(f^2+z^2)\omega_x-xf\omega_y-xz\omega_z-2fv\} \\
-\dot{u}f+vx\omega_x+vf\omega_y-xu\omega_z &= \frac{\dot{P}_y}{P_y}\{-xz\omega_x-fz\omega_y+(x^2+f^2)\omega_z+2uf\}
\end{aligned} \tag{6.6}$$

From (6.6), we can set up a nonlinear system of six second order polynomial equations for the rotational components and the position dependent variable $\dot{P}_{yn}/P_{yn}$ for n=1, 2, and 3 when three optic flows and their time derivatives are given. However, the position dependent term can be eliminated from the two equations in (6.6) as

$$\begin{aligned}
&vfx\omega_x^2 + \{x(uz-vx)+vf^2\}\omega_x\omega_y + f(uz-vx)\omega_y^2 \\
&+ \{z(uz-vx)-uf^2\}\omega_y\omega_z - ufz\omega_z^2 + f(vz-ux)\omega_x\omega_z \\
&+ \{2v(uz-vx)+\dot{u}x^2+\dot{v}xz-(x^2+f^2+z^2)\dot{u}\}\omega_x \\
&+ \{-2f(u^2+v^2)+f(\dot{u}x+\dot{v}z)\}\omega_y \\
&+ \{2u(vx-uz)+\dot{u}xz+\dot{v}z^2-(x^2+f^2+z^2)\dot{v}\}\omega_z \\
&- 2f(\dot{u}v-u\dot{v}) = 0
\end{aligned} \tag{6.7}$$

The same equation can also be derived from the dot product of (6.3) with

$$\Omega \times \begin{bmatrix} x \\ f \\ z \end{bmatrix} - 2 \begin{bmatrix} u \\ 0 \\ v \end{bmatrix},$$

i.e., from the expansion of

$$\begin{bmatrix} x \\ f \\ z \end{bmatrix} \times \left\{ \begin{bmatrix} \dot{u} \\ 0 \\ \dot{v} \end{bmatrix} - \Omega \times \begin{bmatrix} u \\ 0 \\ v \end{bmatrix} \right\} \quad \left\{ \Omega \times \begin{bmatrix} x \\ f \\ z \end{bmatrix} - 2 \begin{bmatrix} u \\ 0 \\ v \end{bmatrix} \right\} = 0 \qquad (6.8)$$

The above second order polynomial equation (6.7) imposes a constraint on the rotational components regardless of k. Thus, the rotational components of an object in general motion are determined when three optic flows and their time derivatives are observed from the object.

When the rotational components ω_x, ω_y, and ω_z are determined at an optic flow, the scaled motion parameter k is easily determined from (6.1) by

$$\frac{f}{P_y} k = \begin{bmatrix} u \\ 0 \\ v \end{bmatrix} + \frac{\dot{P}_y}{P_y} \begin{bmatrix} x \\ f \\ z \end{bmatrix} - \Omega \times \begin{bmatrix} x \\ f \\ z \end{bmatrix} \qquad (6.9)$$

where, from (6.4),

$$\frac{\dot{P}_y}{P_y} = \frac{\dot{v}f + uf\omega_y + uz\omega_z - vz\omega_x}{(f^2+z^2)\omega_x - xf\omega_y - xz\omega_z - 2fv}$$

$$= \frac{-\dot{u}f - xu\omega_z + vx\omega_x + vf\omega_y}{-xz\omega_x - fz\omega_y + (x^2+f^2)\omega_z + 2uf}$$

When the scaled parameter $k = (k_x, k_y, k_z)^T$ is determined at two object points, the relative depth of the two points can be easily determined from (6.8). Suppose that two scaled parameters $k_1 = (k_{1x}, k_{1y}, k_{1z})^T$ and $k_2 = (k_{2x}, k_{2y}, k_{2z})^T$ are computed at the two object image points whose depth are P_{y1} and P_{y2}, respectively. Then

$$k_x = \frac{P_{y1}}{f}k_{1x} = \frac{P_{y2}}{f}k_{2x}, \quad \text{i.e.} \quad \frac{P_{y1}}{P_{y2}} = \frac{k_{2x}}{k_{1x}}$$

or

$$\frac{P_{y1}}{P_{y2}} = \frac{k_{2y}}{k_{1y}}, \quad \frac{P_{y1}}{P_{y2}} = \frac{k_{2z}}{k_{1z}}$$

from the second and third equation of (6.9).

Example 6.1 General Motion Determination

For three object points (10,10,30), (12.5,6.25,31.25), and (25,8.33,16.67) moving at the moment with $\Omega=(.1,-.2,.5)^T$ and $k=(1,3,2)^T$, we observe the optic flow (-1.5,-1), (-3.3,-4.08), and (-5.76,-2.38) and their time derivatives (1.7,2.5), (7.32,11.59), and (19.56,8.88) on the image coordinates (1,3), (2,5), and (3,2), respectively on the

image plane at y=1. Deriving the nonlinear system from (6.7) from each optic flow and its time derivative, we have

$$-\omega_x^2 - 4.5\omega_x\omega_y - 3.5\omega_y^2 - 9\omega_y\omega_z + 4.5\omega_z^2 - 1.5\omega_x\omega_z$$
$$- 20.05\omega_x + 2.7\omega_y - 10.4\omega_z + 4.1 = 0$$

$$-8.16\omega_x^2 - 20.76\omega_x\omega_y - 8.34\omega_y^2 - 38.4\omega_y\omega_z + 16.5\omega_z$$
$$-13.8\omega_x\omega_z - 6.35\omega_x + 17.5\omega_y - 39.8\omega_z + 16.76 = 0$$

$$-7.14\omega_x^2 - 15.52\omega_x\omega_y - 4.38\omega_y^2 - 3\omega_y\omega_z + 11.52\omega_z$$
$$+ 12.52\omega_x\omega_z - 23.66\omega_x - 1.25\omega_y - 21.91\omega_z + 9.2 = 0$$

Solving the above nonlinear system using the iterative modified Levenberg-Marquardt method implemented in the Minpack, we have $\Omega=(.1,-.2,.5)$ after 17 iterations with $\Omega=0$ initially. Determining the scaled k from (6.9), we have

for the image coordinate (1,3)

$$\frac{f}{P_y}k = (.1,.3,.2)^T \text{ and } \frac{\dot{P}_y}{P_y} = .5$$

for the image coordinate (2,5)

$$\frac{f}{P_y}k = (.16,.48,.32)^T \text{ and } \frac{\dot{P}_y}{P_y} = .98$$

and for the image coordinate (3,2)

$$\frac{f}{P_y}k = (.12,.36,.24)^T \text{ and } \frac{\dot{P}_y}{P_y} = 1.66$$

And the relative depths are easily determined from the scaled k.

Combining (6.6) with (6.1), we can set up a nonlinear system for the motion parameters and the relative depth from two optic flows and their time derivatives. Specifically, we have from (6.1)

$$\begin{bmatrix} u \\ 0 \\ v \end{bmatrix} = \Omega \times \begin{bmatrix} x \\ f \\ z \end{bmatrix} - \frac{\dot{P}_y}{P_y} \begin{bmatrix} x \\ f \\ z \end{bmatrix} + \frac{f}{P_y} k \tag{6.10}$$

Substituting either one of (6.6) in (6.10) for $\dot{P}_y/P_y$, we derive three equations. Together with (6.7), we have four nonlinear equations from one optic flow and its time derivative. Suppose we observe two optic flows (u_1, v_1) and (u_2, v_2) and their time derivatives $(\dot{u}_1, \dot{v}_1)$ and $(\dot{u}_2, \dot{v}_2)$ at two image points (x_1, z_1) and (x_2, z_2) on the image plane at $y=f$ from a moving object. Suppose that the depths of the two image points are P_{y1} and P_{y2} and their relative depth P_{y2}/P_{y1} be α. Then, we have

$$\begin{bmatrix} u_1 \\ 0 \\ v_1 \end{bmatrix} = \Omega \times \begin{bmatrix} x_1 \\ f \\ z_1 \end{bmatrix} - \frac{\dot{P}_{y1}}{P_{y1}} \begin{bmatrix} x_1 \\ f \\ z_1 \end{bmatrix} + \frac{f}{P_{y1}} k \tag{6.11}$$

$$\text{where } \frac{\dot{P}_{y1}}{P_{y1}} = \frac{\dot{v}_1 f + u_1 f\omega_y + u_1 z_1 \omega_z - v_1 z_1 \omega_x}{(f^2+z_1^2)\omega_x - x_1 f\omega_y - x_1 z_1 \omega_z - 2fv_1}$$

and

$$\begin{bmatrix} \dot{u}_2 \\ 0 \\ \dot{v}_2 \end{bmatrix} = \Omega \times \begin{bmatrix} x_2 \\ f \\ z_2 \end{bmatrix} - \frac{\dot{P}_{y2}}{P_{y2}} \begin{bmatrix} x_2 \\ f \\ z_2 \end{bmatrix} - \frac{f}{\alpha P_{y1}} k \qquad (6.12)$$

$$\text{where } \frac{\dot{P}_{y2}}{P_{y2}} = \frac{\dot{v}_2 f + u_2 f\omega_y + u_2 z_2 \omega_z - v_2 z_2 \omega_x}{(f^2+z_2^2)\omega_x - x_2 f\omega_y - x_2 z_2 \omega_z - 2fv_2}$$

And from (6.7), we have

$$\begin{aligned} & v_1 f x_1 \omega_x^2 + \{x_1(u_1 z_1 - v_1 x_1) + v_1 f^2\}\omega_x\omega_y + f(u_1 z_1 - v_1 x_1)\omega_y^2 \\ & + \{z_1(u_1 z_1 - v_1 x_1) - u_1 f^2\}\omega_y\omega_z - u_1 f z_1 \omega_z^2 + f(v_1 z_1 - u_1 x_1)\omega_x\omega_z \\ & + \{2v_1(u_1 z_1 - v_1 x_1) + \dot{u}_1 x_1^2 + v_1 x_1 z_1 - (x_1^2+f^2+z_1^2)\dot{u}_1\}\omega_x \\ & + \{-2f(u_1^2+v_1^2) + f(\dot{u}_1 x_1 + \dot{v}_1 z_1)\}\omega_y \\ & + \{2u_1(v_1 x_1 - u_1 z_1) + \dot{u}_1 x_1 z_1 + \dot{v}_1 z_1^2 - (x_1^2+f^2+z_1^2)\dot{v}_1\}\omega_z \\ & - 2f(\dot{u}_1 v_1 - \dot{u}_1 v_1) = 0 \end{aligned} \qquad (6.13)$$

$$\begin{aligned} & v_2 f x_2 \omega_x^2 + \{x_2(u_2 z_2 - v_2 x_2) + v_2 f^2\}\omega_x\omega_y + f(u_2 z_2 - v_2 x_2)\omega_y^2 \\ & + \{z_2(u_2 z_2 - v_2 x_2) - u_2 f^2\}\omega_y\omega_z - u_2 f z_2 \omega_z^2 + f(v_2 z_2 - u_2 x_2)\omega_x\omega_z \\ & + \{2v_2(u_2 z_2 - v_2 x_2) + \dot{u}_2 x_2^2 + v_2 x_2 z_2 - (x_2^2+f^2+z_2^2)\dot{u}_2\}\omega_x \\ & + \{-2f(u_2^2+v_2^2) + f(\dot{u}_2 x_2 + \dot{v}_2 z_2)\}\omega_y \\ & + \{2u_2(v_2 x_2 - u_2 z_2) + \dot{u}_2 x_2 z_2 + \dot{v}_2 z_2^2 - (x_2^2+f^2+z_2^2)\dot{v}_2\}\omega_z \\ & - 2f(\dot{u}_2 v_2 - \dot{u}_2 v_2) = 0 \end{aligned} \qquad (6.14)$$

Thus, we have 8 nonlinear equations from (three from (6.11), three from (6.12), (6.13), and (6.14)) for 7 unknowns (3 from Ω, 3 from fk/P_{y1}, and one relative depth

α).

Example 6.2 General Motion from Two Optic Flows and Their Time Derivatives.

For the same optic flows and their time derivatives at the image points (1,3) and (2,5), we applied the above method. With the unknowns set zero initially, we could not get the desirable answer using the Minpack. But, setting $\Omega=0$, $k=(.2,.2,.1)^T$, and $\alpha=1$, we obtain the desirable answer as

$$\omega_x=.1,\ \omega_y=-.2,\ \omega_z=.5$$

$$\frac{f}{P_{y1}}k_x=.1,\quad \frac{f}{P_{y1}}k_y=.3,\quad \frac{f}{P_{y1}}k_z=.2,\ \text{and}$$

$$\alpha=.625$$

In the following sections, we consider special cases ($\Omega=0$ or $k=0$) of the motion and use the rotational motion constraint (6.7) for image sequence segmentation.

6.2 Pure Translational Motion

For the pure translational motion case, Eq.(6.1) becomes

$$\frac{P_y}{f}\begin{bmatrix} u \\ 0 \\ v \end{bmatrix} = -\frac{\dot{P}_y}{f}\begin{bmatrix} x \\ f \\ z \end{bmatrix} + k \qquad (6.15)$$

Differentiating both sides of the above equations with respect to time, we have

$$\frac{P_y}{f}\begin{bmatrix} \dot{u} \\ 0 \\ \dot{v} \end{bmatrix} + \frac{2\dot{P}_y}{f}\begin{bmatrix} u \\ 0 \\ v \end{bmatrix} + \frac{\ddot{P}_y}{f}\begin{bmatrix} x \\ f \\ z \end{bmatrix} = 0 \qquad (6.16)$$

Because f is a positive value, $\dot{P}_y=0$ from (6.16). Thus, we have

$$\frac{2\dot{P}_y}{P_y}\begin{bmatrix} u \\ 0 \\ v \end{bmatrix} = -\begin{bmatrix} \dot{u} \\ 0 \\ \dot{v} \end{bmatrix} \qquad (6.17)$$

Suppose that $u \neq 0$, then

$$\frac{\dot{P}_y}{P_y} = -\frac{\dot{u}}{2u} \qquad (6.18)$$

which implies that

$$P_y(t) = \exp \int_0^t \left(-\frac{\dot{u}(s)}{2u(s)}\right) ds.$$

Substituting $-\dot{u}/2u$ for $\dot{P}_y/P_y$ in (6.15), we can derive equations for the scaled k as

$$\frac{f}{P_y} k = -\frac{\dot{u}}{2u}\begin{bmatrix} x \\ f \\ z \end{bmatrix} + \begin{bmatrix} u \\ 0 \\ v \end{bmatrix} \tag{6.19}$$

or

$$\begin{aligned} \frac{f}{P_y} k_x &= -\frac{\dot{u}}{2u}x + u \\ \frac{f}{P_y} k_y &= -\frac{\dot{u}}{2u}f \\ \frac{f}{P_y} k_z &= -\frac{\dot{u}}{2u}z + v \end{aligned} \tag{6.20}$$

The relative depth of two object points can be determined easily from (6.20). Let (u_1, v_1) and $(\dot{u}_1, \dot{v}_1)$ be an optic flow and its time derivative observed at an object image point (x_1, z_1) whose depth is P_{y1} and let (u_2, v_2) and $(\dot{u}_2, \dot{v}_2)$ be the optic flow and its time derivative observed at another image point (x_2, z_2) of the same object whose depth is P_{y2}. Because they have the same motion parameter k, we have from the first equation of (6.20)

$$k_x = \left(-\frac{\dot{u}_1 x_1}{2u_1 f} + \frac{u_1}{f} \right) P_{y1} = \left(-\frac{\dot{u}_2 x_2}{2u_2 f} + \frac{u_2}{f} \right) P_{y2}$$

Thus,

$$\frac{P_{y1}}{P_{y2}} = \frac{(-\dot{u}_2 x_2 + 2u_2^2)u_1}{(-\dot{u}_1 x_1 + 2u_1^2)u_2} \tag{6.21a}$$

In the same way, we have, from the equations of (6.20),

$$\frac{P_{y1}}{P_{y2}} = \frac{u_1 u_2}{u_1 u_2} \tag{6.21b}$$

$$\frac{P_{y1}}{P_{y2}} = \frac{(-\dot{u}_2 z_2 + 2u_2 v_2)u_1}{(-\dot{u}_1 z_1 + 2u_1 v_1)u_2} \tag{6.21c}$$

Thus, the relative depth can be determined by any of (6.21) or their average.

In the same way, when $v \neq 0$ we can determine the scaled parameter k and the relative depth from

$$\frac{\dot{P}_y}{P_y} = -\frac{\dot{v}}{2v} \tag{6.22}$$

$$P_y(t) = \exp \int_0^t \left(-\frac{\dot{v}(s)}{2v(s)}\right) ds \tag{6.23}$$

$$\begin{aligned} \frac{f}{P_y} k_x &= -\frac{\dot{v}}{2v} x + u \\ \frac{f}{P_y} k_y &= -\frac{\dot{v}}{2v} f \\ \frac{f}{P_y} k_z &= -\frac{\dot{v}}{2v} z + v \end{aligned} \tag{6.24}$$

$$\frac{P_{y1}}{P_{y2}} = \frac{(-\dot{v}_2 x_2 + 2u_2 v_2) v_1}{(-\dot{v}_1 x_1 + 2u_1 v_1) v_2}$$

$$\frac{P_{y1}}{P_{y2}} = \frac{\dot{v}_1 v_2}{v_1 \dot{v}_2} \qquad (6.25)$$

$$\frac{P_{y1}}{P_{y2}} = \frac{(\dot{v}_2 z_2 + 2v_2^2) v_1}{(v_1 z_1 + 2v_1^2) v_2}$$

Example 6.2 Experiment with ideal observables

For two object points $P_1=(10,10,30)'$ and $P_2=(12.5,6.25,31.25)'$ moving at the moment with $k=(1,3,2)'$ we observe two optic flows $(-.2,-.1)$ and $(-.8,-2.08)$ and their time derivatives $(.12,.42)$ and $(.768,1.9968)$ at their image coordinates $(1,3)$ and $(2,5)$, respectively, on the image plane at $f=1$. Computing two scaled k's, we have $(.1,.3,.2)'$ for the point P_1 and $(.6,.48,.32)'$. for the point P_2. We compute the relative depth of the two points to be 1.6 from all equations of (6.21) and (6.25).

Equations (6.18) and (6.22) with $P_y=0$ are the necessary conditions for the pure translational motion. In the following theorem, we prove that they are also sufficient.

Theorem 6.1 The necessary and sufficient conditions for an object point to be in the pure translational motion are

$$\frac{\dot{P}_y}{P_y} = -\frac{\dot{u}}{2u} = -\frac{\dot{v}}{2v} \quad \text{and} \quad \ddot{P}_y = 0.$$

Proof The necessity of the conditions has already been proven because they are derived from the pure translational motion assumption. For the proof of the sufficiency, plug the conditions in (6.2), then we have

$$\Omega \times \left\{ \frac{\dot{u}}{2u} \begin{bmatrix} x \\ f \\ z \end{bmatrix} - \begin{bmatrix} u \\ 0 \\ v \end{bmatrix} \right\} = 0$$

Thus, $\Omega=0$ since $f \neq 0$, and thus right side is not zero when the derivative of u is not zero.

Q.E.D.

6.3 Pure Rotational Motion

When k is zero, (6.1) becomes

$$\frac{P_y}{f} \begin{bmatrix} u \\ 0 \\ v \end{bmatrix} = \frac{P_y}{f} \Omega \times \begin{bmatrix} x \\ f \\ z \end{bmatrix} - \frac{\dot{P}_y}{f} \begin{bmatrix} x \\ f \\ z \end{bmatrix} \tag{6.26}$$

Differentiating both sides of (6.26) and dividing the result by P_y/f, we have

$$\begin{bmatrix}\dot{u}\\0\\\dot{v}\end{bmatrix} - \Omega \times \begin{bmatrix}u\\0\\v\end{bmatrix} = \frac{\dot{P}_y}{P_y}\left\{\Omega \times \begin{bmatrix}x\\f\\z\end{bmatrix} - 2\begin{bmatrix}u\\0\\v\end{bmatrix}\right\} - \frac{\ddot{P}_y}{P_y}\begin{bmatrix}x\\f\\z\end{bmatrix} \tag{6.27}$$

The vector product of (6.27) with $[x,f,z]^T$ eliminates the last term on the right side of (6.27). Rearranging the result, we have

$$\begin{bmatrix}x\\f\\z\end{bmatrix} \times \left\{\begin{bmatrix}\dot{u}\\0\\\dot{v}\end{bmatrix} - \Omega \times \begin{bmatrix}u\\0\\v\end{bmatrix}\right\} = \frac{\dot{P}_y}{P_y}\begin{bmatrix}x\\f\\z\end{bmatrix} \times \left\{\Omega \times \begin{bmatrix}x\\f\\z\end{bmatrix} - 2\begin{bmatrix}u\\0\\v\end{bmatrix}\right\} \tag{6.28}$$

From (6.26), we observe that

$$\dot{P}_y/P_y = (\omega_z x - \omega_x z)/f \tag{6.29}$$

and

$$u + (\dot{P}_y/P_y)x = \omega_y z - \omega_z f \tag{6.30}$$

$$v + (\dot{P}_y/P_y)z = \omega_x f - \omega_y x \tag{6.31}$$

Substituting (6.29) in (6.30) and (6.31), we have

$$xz\omega_x + fz\omega_y - (x^2+f^2)\omega_z - uf = 0 \tag{6.32}$$

$$(z^2+f^2)\omega_x - xf\omega_y - xz\omega_z - vf = 0 \tag{6.33}$$

Eliminating ω_z from (6.32) and (6.33), we have

$$\omega_x = -\frac{x}{f}\omega_y + \frac{v(x^2+f^2)-xzu}{f(x^2+f^2+z^2)} \tag{6.34}$$

Substituting (6.34) in (6.32), we have

$$\omega_x = -\frac{z}{f}\omega_y + \frac{vxz-u(f^2+z^2)}{f(x^2+f^2+z^2)} \tag{6.35}$$

Substituting (6.29), (6.34), and (6.35) in the first equation of (6.26), we can derive an equation of one variable ω_y. The equation seems to be a second order polynomial of ω_y, but the second order term vanishes when substituted. The result is as follows

$$(f^2u+z^2u-xzv)\omega_y + \frac{f^2\dot{v}(x^2+f^2+z^2)-(x^2+2f^2)zv^2+x(2z^2-f^2)uv-(f^2+z^2)zu^2}{x^2+f^2+z^2} = 0$$

Thus, if $u(f^2+z^2)\neq xzv$, we can determine ω_y directly from

$$\omega_y = \frac{-f^2\dot{v}}{u(f^2+z^2)-xzv} + \frac{(x^2+2f^2)zv^2-x(2z^2-f^2)uv+(f^2+z^2)zu^2}{\{u(f^2+z^2)-xzv\}(x^2+f^2+z^2)} \tag{6.36}$$

Substituting (6.36) back in (6.34) and (6.35), we determine ω_x, ω_y, and ω_z.

$$\omega_x = \frac{-xf\dot{v}}{u(f^2+z^2)-xzv} + \frac{xfzv^2+f(2x^2+f^2+z^2)uv}{\{u(f^2+z^2)-xzv\}(x^2+f^2+z^2)} \tag{6.37}$$

$$\omega_z = \frac{-fz\dot{v}}{u(f^2+z^2)-xzv} + \frac{2fz^2v^2+3xfzuv-f(f^2+z^2)u^2}{\{u(f^2+z^2)-xzv\}(x^2+f^2+z^2)} \qquad (6.38)$$

The rotational components ω_x, ω_y, and ω_z can also be determined from the third equation of (6.26) with the same substitutions. They are

$$\omega_y = \frac{-f^2\dot{u}}{xzu-(x^2+f^2)v} + \frac{x(x^2+f^2)v^2+x(2f^2+z^2)uv-(2x^2-f^2)zuv}{\{xzu-(x^2+f^2)v\}(x^2+f^2+z^2)} \qquad (6.39)$$

Substituting (6.39) in (6.34) and (6.35), we have

$$\omega_x = \frac{-xf\dot{u}}{xzu-(x^2+f^2)v} + \frac{-f(x^2+f^2)v^2+2x^2fu^2+3xfzuv}{\{xzu-(x^2+f^2)v\}(x^2+f^2+z^2)} \qquad (6.40)$$

$$\omega_z = \frac{-zf\dot{u}+fuv}{xzu-(x^2+f^2)u} + \frac{xfzu^2+fz^2uv}{\{xzu-(x^2+f^2)v\}(x^2+f^2+z^2)} \qquad (6.35)$$

Thus, the rotational components can be determined from either of two equations or the average of two different calculations.

Example 6.3 Motion with k=0

For an object point (10,10,30) moving at the moment with $\Omega=(.1,-.2,.5)^T$ and k=0, we observe the optic flow (-1.3,-.3)

and its time derivative (.94,1.66) at the image coordinate (1,3) on the image plane at y=1. From either (6.36)-(6.38) or (6.39)-(6.41), we recover the exact rotational component values.

6.4 Motion Based Image Segmentation

In this section, we will present a scheme to segment an optic flow field with its time derivatives using the motions equations derived in the previous sections.

For a scene containing objects in pure translation or rotation with k=0, its optic flow field can be easily segmented because at each optic flow with its time derivative given, the motion parameters can be determined in closed form. However, for objects in general motion their motion can not be determined from a single optic flow and its time derivative but from a nonlinear system of second order polynomial equations derived from three optic flows and their time derivatives. Computing motion parameters from the nonlinear system for every possible combination of three optic flows to find sets of dominant motion parameters is formidable when the number of optic flows is great. Instead, we can use the Hough transform technique, using the second order polynomial equation (6.7) constraining the

rotational components for the optic flow image segmentation.

Specifically, let (u,v) and $(\dot{u},\dot{v})$ be the optic flow and its time derivative observed at an image coordinate (x,z) on the image plane at $y=f$ and let

$$a_1 = vfx$$

$$a_2 = x(uz-vx) + vf^2$$

$$a_3 = f(uz-vx)$$

$$a_4 = z(uz-vx) - uf^2$$

$$a_5 = -ufz$$

$$a_6 = f(vz-ux)$$

$$a_7 = 2v(uz-vx) - \dot{u}x^2 + \dot{v}xz - (x^2+f^2+z^2)\dot{u}$$

$$a_8 = -2f(u^2+v^2) + f(\dot{u}x+\dot{v}z)$$

$$a_9 = 2u(vx-uz) + \dot{u}xz + \dot{v}z^2 - (x^2+f^2+z^2)\dot{v}$$

$$a_{10} = -2f(\dot{u}v-u\dot{v})$$

Then (6.7) becomes

$$a_1\omega_x^2 + (a_2\omega_y+a_6\omega_z+a_7)\omega_x + a_3\omega_y^2 + a_5\omega_z^2+a_8\omega_y+a_9\omega_z+a_{10} = 0$$

Let

$$D=(a_2\omega_y+a_6\omega_z+a_7)^2-4a_1(a_3\omega_y^2+a_4\omega_y\omega_z+a_5\omega_z^2+a_8\omega_y+a_9\omega_z+a_{10})\}$$

Thus, for given ω_y and ω_z, two ω_x's are obtained from

$$\omega_x = \frac{1}{2a_1}\{-(a_2\omega_y+a_6\omega_z+a_7) \pm \mathrm{SQRT}\{ D \} \qquad (6.42)$$

when $D \geq 0$.

The rotational component values range from $-\pi$ to π radians/sec theoretically. However, from the practical reason or human perception of limited range of velocity, we restrict the rotational velocity range from $-c$ to c radians/sec where $c<\pi$ for the Hough parameter space.

Suppose we have a Hough parameter space for the rotational components ω_x, ω_y, and ω_z quantized evenly into n x n x n cells within the above range. We assign, to each cell, an accumulator initialized with zero. Then the Hough technique computes, for each optic flow and its time derivative, two ω_x's from (6.42) using each quantized ω_y and ω_z and increases the accumulator corresponding to the computed ω_x's. After we go through all the optic flows, we search the accumulators having the highest value and consider the corresponding quantized rotational component values. When this rotational component value satisfies (6.42) at an image point the image point must be from the object in motion with this rotation. Thus, each image point

satisfying (6.42) with this rotation is labeled uniquely.

Next, we remove the image point labeled from the optic flow image and its time derivative image and for the remaining optic flow vectors and its time derivatives we repeat the same process to find next moving object with a different rotation. When every image point is labeled, we have the image segmented based on the rotational motion. For each region of this segmented image, we can compute the translation k at each image point from (6.9) and the rotational component values determined. Further image segmentation can be carried out based on the the computed translation at each pixel.

Experimental Result Let two ellipsoids have the relative depth image as shown in Fig 6.1. Suppose that the left ellipsoid move with $k=(1,3,2)^T$ and $\Omega=(-.1,.22,-.14)^T$ and the right one move with $k=(1,2,3)^T$ and $\Omega=(.1,-.22,.14)^T$. Using the motion parameters and the depth at each image point, we compute the optic flow image in Fig 6.2a and its time derivative in Fig 6.2b. We apply the above method to this optc flow image and its time derivative image with 50x50x50 cells dividing the rotation angle between -1 and 1 radian and have the segmented image in Fig 6.3.

Next, we position the two ellipsoids such that one occludes the other partly as shown in Fig 6.4. Computing the optic flow image and its time derivative image for the same

motion parameter values, we have Fig 6.5. Applying the above method in the same way, we have the segmented image in Fig 6.6.

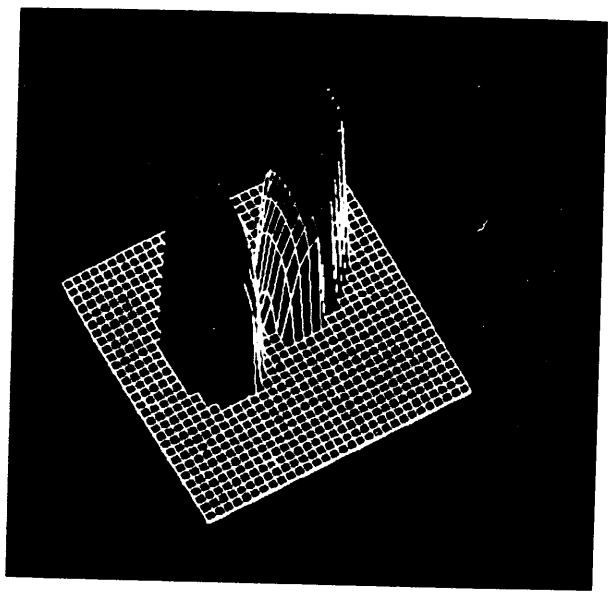

Fig 6.1 Relative Depth Image of Two Ellipsoids.

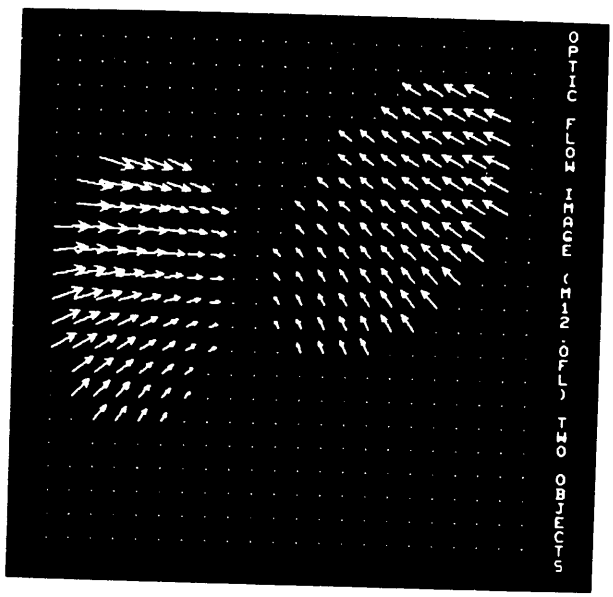

Fig 6.2a Optic Flow Image of Two Ellipsoids in Fig 6.1. The left ellipsoid moves with $k=(1,3,2)^T$ and $\Omega=(-.1,.22,-.14)^T$ and the right one moves with $k=(1,2,3)^T$ and $\Omega=(.1,-.22,.14)^T$.

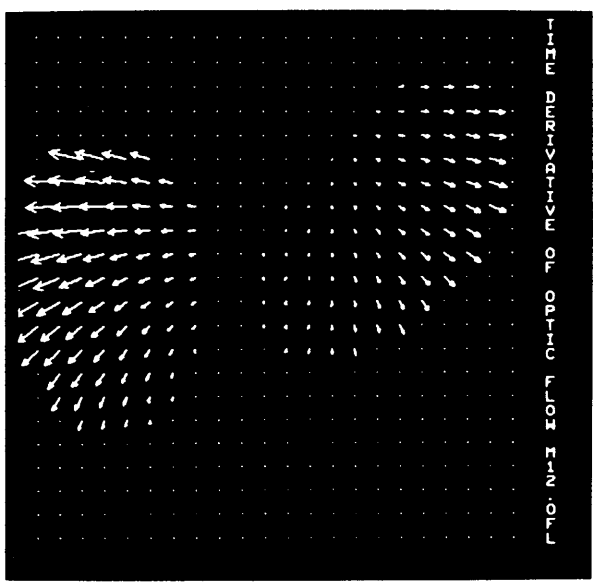

Fig 62b Time Derivative Image of Two Ellipsoids in Fig 6.1. The left ellipsoid moves with $k=(1,3,2)^T$ and $\Omega=(-.1,.22,-.14)^T$ and the right one moves with $k=(1,2,3)^T$ and $\Omega=(.1,-.22,.14)^T$.

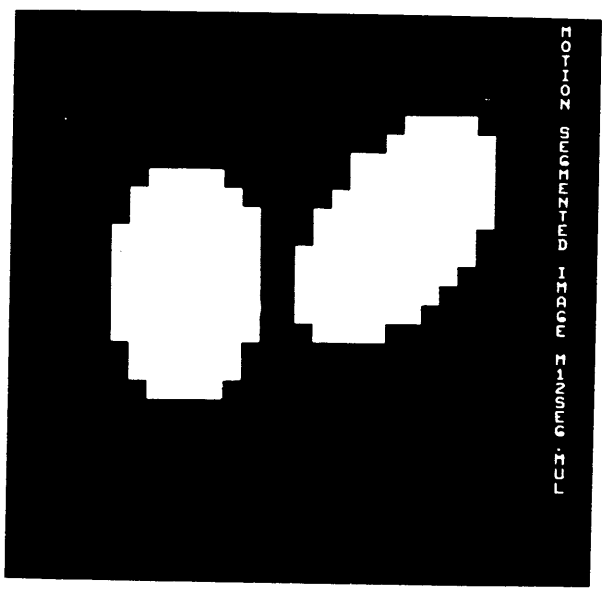

Fig 6.3 Segmented Image from the Optic Flow Image and Its Time Derivative Image in Fig 6.2.

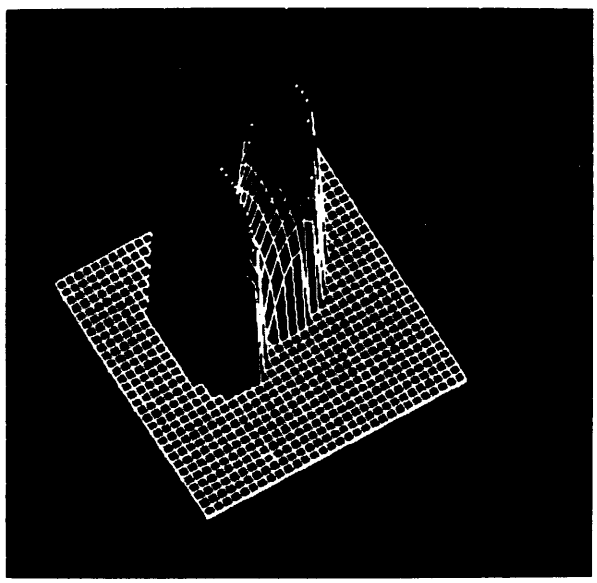

Fig 6.4 Relative Depth Image of Two Elipsoids Occluding Each Other Partly

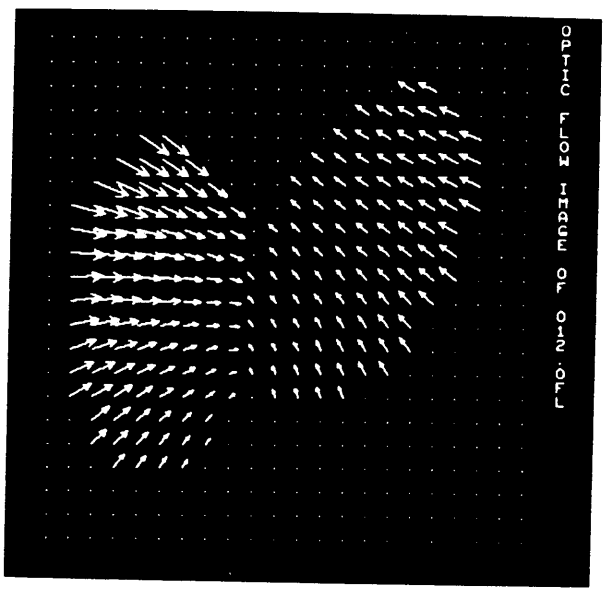

Fig 6.5a Optic Flow Image of Two Ellipsoids in Fig 6.4. The left ellipsoid moves with $k=(1,3,2)^T$ and $\Omega=(-.1,.22,-.14)^T$ and the right one moves with $k=(1,2,3)^T$ and $\Omega=(.1,-.22,.14)^T$.

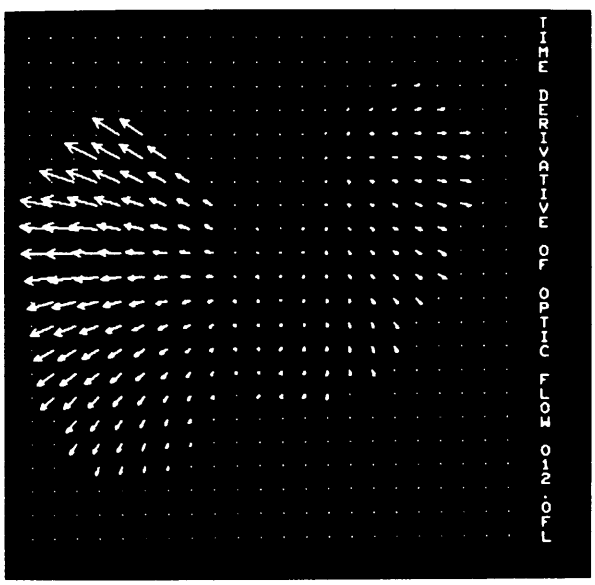

Fig 6.5b Time Derivative Image of Two Ellipsoids in Fig 6.4. The left ellipsoid moves with $k=(1,3,2)^T$ and $\Omega=(-.1,.22,-.14)^T$ and the right one moves with $k=(1,2,3)^T$ and $\Omega=(.1,-.22,.14)^T$.

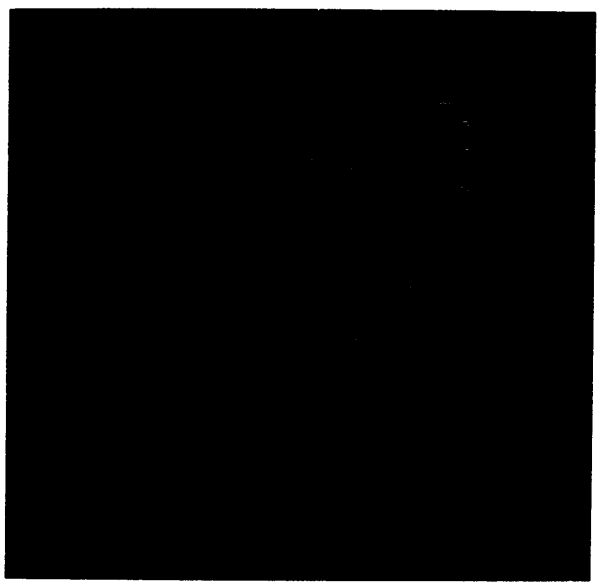

Fig 6.6 Segmented Image from the Optic Flow Image and Its Time Derivative Image in Fig 6.5.

CHAPTER VII

CONCLUSION

In this dissertation, we describe a technique for computing optic flow, two techniques for estimating 3D motion and surface structure from the computed optic flow image, and a technique for the motion based image segmentation using both the computed optic flow image and the optic flow time derivative image. Determining the optic flow with the facet technique is not complete enough because it cannot determine the optic flow vector for pixels when the estimated underlying surface has large fitting error or small curvature.

To recover 3D motion parameters from the optic flow, we developed two techniques, one based on the least square problem and the other based on the linear scheme. The first one iteratively determines motion parameters and relative depth, simultaneously, of an object in general motion. If the object translates or rotates, then the technique does not need the iteration. The other one first determines motion parameters and then computes relative depths. The technique also estimates the error of computed motion parameters and relative depth when optic flows are perturbed

with small random noise. To segment an image based on different motions of separated objects, we use the Hough technique for the equation derived from the optic flow and its time derivative. The equation is a second order polynomial equation in the three rotational components. The solution of this equation may be erroneous when the quantization error is significant in the Hough space.

In the limited experimental studies of the techniques discussed, we observe that the techniques can be used in a vision system understanding images. Further experimental studies should be carried out for the real application of the techniques.

References

ADIV(1983)
Recovering 2D Motion Parameters in Scenes Containing Multiple Moving Objects
G. Adiv
DARPA Image Understanding Workshop, Arlington VA, June 1983

AGGARWAL and DUDA(1975)
Computer Analysis of Moving Polygonal Images
J.K. Aggarwal and R.O. Duda
IEEE Trans. Computers, Vol.C-24, Oct. 1975, pp.966-976

AGGARWAL et al.(1981)
Correspondence Processes in Dynamic Scene Analysis,
J.K. Aggarwal, L.S. Davis, and W.N. Martin
Proceedings of the IEEE, Vol. 69, No.5, May 1981, pp. 562-572.

AGGARWAL(1983)
Three Dimensional Description of Objects and Dynamic Scene Analysis,
J.K. Aggarwal
TR-83-1-20, The University of Texas at Austin, Laboratory for Image and Signal Analysis, January 1983

ALTMANN and REITBOCK(1984)
A Fast Correlation Method for Scale-and Translation-Invariant Pattern Recognition,
D.J. Altmann and H.J.P. Reitbock
IEEE on PAMI, Vol. PAMI-6 No.1, January 1984, pp.46-57

AYALA et al.(1982)
Moving Target Tracking Using Symbolic Registration
I.L. Ayala, D.A. Orton, J.B. Larson, and D.F. Elliott
IEEE Trans. on PAMI, Vol. PAMI4, No.5, September 1982, pp. 515-520.

BALLARD(1981a)
Generalizing the Hough Transform to detect Arbitrary Shape
D.H. Ballard
Pattern Recognition, Vol.13 No.2, 1981, pp.111-122

BALLARD(1981b)
On Shapes
D.H. Ballard
Proc., 7th IJCAI, Vancouver, B. C., August 1981

BALLARD and BROWN(1982)
Computer Vision
D.H. Ballard and C.M. Brown
Englewood Cliffs, N.J., Prentice Hall, 1982

BALLARD and KIMBALL(1983)
Rigid Body Motion from Depth and Optic Flow
D.H. Ballard and O.A. Kimball
Computer Vision, Graphics, and Image Processing, Vol.22, 1983, pp.95-115

BARNARD and THOMPSON(1980)
Disparity Analysis of Images,
S.T. Barnard and W.B. Thompson
IEEE Trans. on PAMI, Vol. PAMI-2, No.4, July 1980, pp. 333-340.

BARNEA and SILVERMAN(1972) A Class of Algorithm For Fast Image Registration
D.I. Barnea and H.H. Silverman
IEEE Transactions On Computers, Vol. C-21, No.2, 1972, pp. 179-186.

BROWN and DENNIS(1972)
Derivative Free Analogues of the Lavenberg-Marquardt and Gauss Algorithms for Nonlinear Least Squares,
K.M. Brown and J.E. Dennis
Numer. Math., Vol.18, 1972, pp.289-297

BRUSS and HORN(1983)
Passive Navigation
A.R. Bruss and B.K.P. Horn
Computer Vision, Graphics, and Image Processing, Vol.21, 1983, pp.3-20

CAFFORIO and ROCCA(1976)
Methods for Measuring Small Displacements of Television Images
C. Cafforio and F. Rocca
IEEE Trans. Information Theory, Vol.22, No.5, Sept. 1976, pp.573-579

CAFFORIO and ROCCA(1979)
Tracking Moving Objects in TV Images
C. Cafforio and F. Rocca
Signal Process. 1, 1979, pp.133-140

CHOW and AGGARWAL(1977)
Computer Analysis of Planar Curvilinear Moving Images
W.K. Chow and J.K. Aggarwal
IEEE Trans. Computers, Vol.C-26, Feb. 1977, pp.179-185

CLOCKSIN(1980)
Perception of Surface Slant and Edge Labels from Optic Flow
W.F. Clocksin
Perception Vol.9, 1980, pp.253-269

CORNSWEET(1970)
Visual Perception
T. Cornsweet
Academic Press, New Yofk, 1970

DAVIS et al.(1983)
Contour-Based Motion Estimation
L.S. Davis, Z. Wu, and H. Sun
Computer Vision, Graphics, and Image Processing, vol 23, pp.313-326

DONGARRA et al.(1979)
Linpack Users' Guide
J.J. Dongarra, C.B. Moler, J.R. Bunch, and G.W. Stewart
Siam, Philadelphia, 1979

DRESCHLER and NAGEL(1982)
Volumetric Model and 3D-Trajectory of a Moving Car Derived from Monocular TV-Frame Sequences of a Street Scene
L. Dreschler and H.-H. Nagel
Computer Graphics and Image Processing, Vol.20(3) 1982, pp.199-228

DUBOIS et al.(1981)
Image Sequence Coding
E. Dubois, B. Prasada, and M.S. Sabri
Image Sequence Analysis, T.S. Huang edt., pp.229-287, Springer-Verlag, Berlin/Heidelberg/Newyork, 1981

DUDA and HART(1972)
Use of the Hough Transformation to Detect Lines and Curves in Pictures
R.O. Duda and P.E. Hart
Commum. Ass. Compu. Mach., Vol 15, pp. 11-15, Jan 1972

ENDLICH et al.(1971)
Use of a Pattern Recognition Technique for determining Cloud Motions from Sequences of Satellite Photographs,
R.M. Endlich, D.E. Wolf, D.J. Hall, and A.E. Brain
J. Appl. Meteorol., Vol.10, Feb. 1971, pp.105-117

ESKENAZI and CUNNINGHAM(1978)
Real Time-Tracking of Moving Objects in TV Images
R. Eskenazi and R.T. Cunningham
IEEE Workshop Pattern Recognition and Artificial Intelligence, Princeton, N.J., April 1978, pp.4-6

FENNEMA and THOMPSON(1979)
Velocity Determination in Scenes Containing Several Moving Objects
C.L. Fennema and W.B. Thompson
Computer Graphics and Image Processing, Vol.9, Apr. 1979, pp.301-315

FORSYTHE(1957)
Generation and Use of Orthogonal Polynomials for Data-Fitting with a Digital Computer
G.E. Forsythe
J. Soc. Indust. Appl. Math., Vol. 5, No. 2, June, 1957

FRANKLIN(1968)
Matrix Theory
J.N. Franklin
Englewood Cliffs, N.J., Prentice Hall 1968.

GIBSON(1950a)
The Perception of the Visual World
J.J. Gibson
Houghton Mifflin, Boston, 1950

GIBSON(1950b)
The Senses Considered as Perceptual System
J.J. Gibson
Houghton Mifflin, Boston, 1950

GIBSON(1950c)
The Ecological Approach to Visual Perception
J.J. Gibson
Houghton Mifflin, Boston, 1950

GORDON(1965)
Static and Dynamic Visual Fields in Human Space Perception
D.A. Gordon
Journal of the Optic Society of America Vol.55 No.10, October 1965, pp1296-1303

GOSHTASBY et al.(1984)
A Two-Stage Cross Correlation Approach to Template Matching
A. Goshtasby, S.H. Gage, and J.F. Bartholic
IEEE Trans. on PAMI, Vol. PAMI-6 No.3, May 1984

GRIMSON and MARR(1979)
A Computer Implementation of a Theory of Human Stereo Vision
W.E.L Grimson and D. Marr
Proc. Image Understanding Workshop, (Baumann, L.S. edt.), Palo Alto, Calif, April 1979, pp.41-47

HALL et al.(1980)
The Selection of Critical Subsets for Signal, Image, and Scene Matching
E.L. Hall D.L. Davies, and M.E. Casey
IEEE Trans. on PAMI, Vol. PAMI-2 No.4, July 1980, pp.313-322

HARALICK and WATSON(1981)
A Facet Model for Image Data
R.M. Haralick and L. Watson
Computer Graphics and Image Processing, Vol. 15, pp. 113-129, 1981

HARALICK and LEE(1983)
Facet Approach to Optic Flow
R.M. Haralicj and J.S. Lee
DARPA Image Understanding Workshop, ARlington VA, June 1983

HARALICK(1984)
Digital Step Edges from Zero Crossing of Second Directional Derivative
R.M. Haralick
IEEE Transaction on PAMI, Vol. PAMI-6 No.1, pp. 58-68, Jan 1984

HARALICK and ZHUANG(1984) A Note on 'Rigid Body Motion from Depth and Optical Flow'
R.M. Haralick and X. Zhuang
submitted for CGIP publication.

HAYNES and JAIN(1983)
Detection of Moving Edges
S.M. Haynes and R. Jain
Computer Vision, Graphics, and Image Processing, Vol.21, 1983, pp.345-367

HELMHOLTZ(1925)
The Treatise on Physiological Optics
H. von Helmholtz
J.P.C. Southhall edt., New York Dover, 1925

HORN and SCHUNK(1981)
Determining Optic Flow

B.K.P. Horn and B.G. Schunk
Artificial Intelligence, No. 17, 1981, pp. 185-203

HOUGH(1962)
Method and Means for Recognizing Complex Pattern
P.V.C. Hough
U.S. Patent 3069654, Dec 18, 1962

JACOUBS et al.(1980)
Motion Detection and Analysis of Matching Graphs of Intermediate-Level Primitives,
C.J. Jacoubs, R.T. Chien, and J.M. Selander
IEEE Trans. on PAMI, Vol. PAMI-2, No.6, November 1980, pp. 495-510.

JAIN et al.(1977)
Separating Nonstationary from Stationary Scene Components in a Sequence of Real World TV Images
R. Jain, D. Militzer, and H.-H. Nagel
Proc. IJCAI 5, Cambridge, MA., 1977, pp.612-618

JAIN et al.(1979a)
Segmentation through the Detection of Changes due to Motion
R. Jain W.N. Martin, and J.K. Aggarwal
Computer Graphics and Image Processing, Vol.11, 1979, pp.13-34

JAIN and NAGEL(1979b)
On a Motion Analysis Process for Image Sequences from Real World Scenes
R. Jain and H.-H. Nagel
IEEE Trans. PAMI, Vol.PAMI-1 No.2, April 1979, pp.206-214

JAIN and NAGEL(1979c)
On the Analysis of Accumulative Difference Pictures from Image Sequences of Real World Scene,
R. Jain and H.-H. Nagel
IEEE Trans. on PAMI, Vol.PAMI-1 No.2, April 1979

JAIN(1981)
Extraction of Motion Information from Peripheral Processes
R. Jain
IEEE Trans. on PAMI, Vol.PAMI-3 No.5, September 1981, pp.489-503

KIMME et al.(1978)
Finding Circles by Array of Accumulator
C. Kimme, D.H. Ballard, and J. Sklansky
ACM commun, Vol 18 No.2 Feb 1978

KITCHEN and ROSENFELD(1980)
Grey-Level Corner Detection
L. Kitchen and A. Rosenfeld
TR-887, Computer Science Center, University of Maryland, College Park, 1980

KOENDERINK and van DOORN(1976)
Local Structure of Movement Parallax of the plane
J.J. Koenderink and A.J. van Doorn
Journal of the Optical Society of America, Vol.66, 1976, pp.717-723

KOLERS(1972)
Aspects of Motion Perception
P.A. Kolers
Pergamon, Oxford, 1972

LAVENBERG(1944)
A Method for the Solution of Certain Non-linear Problems in Least Squares
K. Lavenberg
Quart. Appl. Math., Vol.2, 1944, pp.164-168

LEE(1980)
The Optic Flow Field: The Foundation of Vision
D.N. Lee
Phil. Trans. Soc. Lond. B290, pp.169-179, 1980

LEE(1981)
River Temperature Processing
J.S. Lee
Master Thesis, VPIβSU, August, 1981.

LEE(1984)
Recovering 3D Motions of Multiple Objects from Facet Model Optic Flow
J.S. Lee
Ph.D. Dissertation Proposal Va. Tech, April, 1984

LEESE et al.(1970) The determination of Cloud Pattern Motions from Geosynchronous Satellite Image Data
J.A. Leese, C.S. Novak, and V.R. Taylor
Pattern Recognition, Vol.2 No.4, December 1970, pp.279-292

LILLESTRAND(1972)
Techniques for Change Detection
R.L. Lillestrand
IEEE Trans. Computers, Vol.C-21, 1972, pp.654-659

LIMB and MURPHY(1975)
Estimating the Velocity of Moving Images in Television Signals
J.O. Limb and J.A. Murphy
Computer Graphics and Image Processing vol 4, pp.311-327, 1975

LONGUET-HIGGINS and PRAZDNY(1980)
The Interpretation of a Moving Retinal Image
H.C. Longuet-Higgins and K. Prazdny
Proc. R. Soc. Lond.B Vol.208, 1980, pp.385-397

MANGASARIAN(1969)
Nonlinear Programming
O.L. Mangasarian
New York, McGraw-Hill 1969

MARR and POGGIO(1979)
A Computational Theory of Human Stereo Vision
D. Marr and T. Poggio
Proc. Soc. London Ser. B Vol.204, 1979, pp.301-308

MARR and HILDRETH(1980)
Theory of Edge Detection
D. Marr and E. Hildreth
Proc. Roy. Soc. London Ser. B Vol.207, 1980, pp.187-217.

MARTIN and AGGARWAL(1978)
Survey, Dynamic Analysis
W.N. Martin and J.K. Aggarwal
Computer Graphics and Image Processing, Vol.7 No.3, June 1978

MARTIN and AGGARWAL(1978)
Computer Analysis of Dynamic Scenes Containing Curvilinear Figures
W.N. Martin and J.K. Aggarwal
Pattern Recognition, Vol. 11, December 1978, pp. 169-178.

MARTIN and AGGARWAL(1983)
Volumetric Description of Objects from Multiple Views
W.N. Martin and J.K. Aggarwal
IEEE PAMI, Vol.PAMI-5 No.2, 1983, pp.150-158

MORAVEC(1977)
Towards Automatic Visual Obstacle Avoidance
H.P. Moravec
International Joint Conference on Artificial Intelligenec, 1977, p584.

MORAVEC(1979a)
Visual Mapping by a Robot Rover
H.P. Moravec
IJCAI, Tokyo, Japan, 1979, pp.598-600

MORAVEC(1979b)
Obstacle Avoidance and Navigation in the Real World by a Seeing Robot Rover
H.P. Moravec
Ph.D Dissertation, Stanford University, Stanford, Calif.

NAGEL(1981a)
Image Sequence Analysis: What can we learn from Applications?
H.-H. Nagel
Image Sequence Analysis, T.S. Huang edt., Springer-Verlag, Berlin/Heidelberg/Newyork, 1981, pp.19-228

NAGEL(1981b)
Representation of Moving Rigid Objects Based on Visual Observations
H.-H. Nagel
IEEE on Computers, Vol.C-14, August 1981, pp.29-39

NAGEL(1981c)
On the Derivation of 3D Rigid Point Configurations from Image Sequences
H.-H. Nagel
Pattern Recognition and Image Processing, August, 1981

NAGEL and NEUMANN(1981d)
On 3D Reconstruction from Two Perspective Views
H.-H. Nagel and B. Neumann
7th IJCAI August, 1981

NAGEL and ENKELMANN(1982)
Investigation of Second Order Grey Value Variations to Estimate Corner Point Displacements
H.-H. Nagel and W. Enkelmann
International Conference on Pattern Recognition, 1982, pp.768-773

NAGEL(1983a)
Displacement Vectors Derived from Second-Order Intensity Variations in Image Sequences
H.-H. Nagel
Computer Vision, Graphics, and Image Processing, Vol.21, 1983, pp.85-117

NAGEL(1983b)
Constraints for the Estimation of Displacement Vector Fields from Image Sequences
H.-H. Nagel
Proc. ICJAI-83, 1983, pp.945-951

NAGEL and ENKELMANN(1984)
Towards the Estimation of Displacement Vector Fields by 'Oriented Smoothness' Constraints
H.-H. Nagel and W. Enkelmann
International Conference on Pattern Recognition 7, Montreal Canada, 1984, pp.6-8

NAKAYAMA and LOOMIS(1974)
Optic Velocity Patterns, Velocity Sensitive Neurons, and Space Perception: a Hypothesis
K. Nakayma and J.M. Loomis
Perception Vol.3, 1974, pp.63-80

NETRAVALI and ROBBINS(1979)
Motion-Compensated Television Encoding: Part I
A.N. Netravali and J.P. Robbins
Bell System Tech. J. Vol.58, 1979, pp.631-670

NETRAVALI and ROBBINS(1980)
Motion-Compensated Coding: Some New Results
A.N. Netravali and J.P. Robbins
Bell System Tech. J. Vol.59, 1980, pp.1735-1745

PAQUIN and DUBIOS(1983)
A Spatio-Temporal Gradient Method for Estimating the Displacement Field in Time-Varying Imagery
R. Paquin and E. Dubios
Computer Vision, Graphics, and Image Processing, Vol.21, 1983, pp.205-221

POTTER(1975)
Velocity as a Cue to Segmentation
J.L. Potter
IEEE Trans. Systems, Man, and Cybernetics, Vol.5, May 1975, pp.390-394

PRAGER and ARBIB(1983)
Computing the Optic Flow: The Match Algorithm and Prediction
Pragger and Arbib
Computer Vision, Graphics, and Image Processing, Vol.24, 1983, pp.276-304

PRAZDNY(1980)
Egomotion and Relative Depth Map from Optic Flow

K. Prazdny
Biological Cybernetics, Vol.36, 1980, pp.87-102

PRAZDNY(1981)
Determining the Instantaneous Direction of Motion from Optic Flow Generated by Curvilinear Moving Observer
K. Prazdny
Computer Graphics and Image Processing, Vol.17, pp.238-248, 1981

RENADE and ROSENFELD(1980)
Point Pattern Matching by Relaxation
S. Renade and A. Rosenfeld
Pattern Recognition, Vol.12, 1980, pp.269-275

RIEGER and LAWTON(1983)
Determining the Instantaneous Axis of Translation from Optic Flow Generated by Arbitrary Sensor Motion
J.M. Rieger and D.T. Lawton
ACM, 1983

ROACH and AGGARWAL(1979)
Computer Tracking of Objects Moving in Space
J.W. Roach and J.K. Aggarwal
IEEE Trans. on PAMI, Vol.PAMI-1 No.2, April 1979

ROACH and AGGARWAL(1980)
Determining the Movement of Objects from a Sequence of Images
J.W. Roach and J.K. Aggarwal
IEEE Trans. on PAMI, Vol.PAMI-2 No.6, November 1980, pp.554-562

ROSENFELD and VANDERBURG(1977)
Coarse Fine Template Matching
A. Rosenfeld and G.J. Vanderburg
IEEE Trans. on Systems, Man, and Cybernetics, Vol.7 No.2, Feb 1977, pp.104-107

SCHUNK(1984)
The Motion Constraint Equation for Optic Flow
B.G. Schunk
International Conference on Pattern Recognition 7, Montreal Canada, 1984, pp.20-22

SHAH and JAIN(1984)
Detecting Time-Varying Corners
M.A. Shah and R. Jain
Computer Vision, Graphics, and Image Processing, Vol.28, 1984, pp.345-355

SHAPIRO(1975)
Transformations for the Computer Detection of Curves in Noisy Pictures
S.D. Shapiro
Computer Graphics and Image Processing, Vol 4 No 4, pp 328-338, Dec 1975

SKLANSKY(1978)
On the Hough Technique for Curve Detection
J. Sklansky
IEEE Transaction on Computer, Vol c-27, No 10, Oct 1978

SNYDER et al.(1980)
Image Modelling, the Continuity Assumption and Tracking
W.E. Snyder, S.A. Rajala, and G. Hirzinger
International Conference on Pattern Recognition, 1980, pp.1111-1114

STULLER and KRISHNAMURPHY(1983)
Kalman Filter Formulation of Low-Level Television Image Motion Estimation
J. Stuller and G. Krishnamurphy
Computer Vision, Graphics, and Image Processing, Vol.21, 1983, pp.169-204 aaa

THOMPSON(1980)
Combining Motion and Contrast for Segmentation
W.B. Thompson
IEEE Trans. on PAMI, Vol.PAMI-2 No.6, Nov. 1980, pp.543-549

THOMPSON and BARNARD(1984)
Low-Level Estimation and Interpretation of Visual Motion
W.B. Thompson and S.T. Barnard
IEEE Computer, Vol.14,No.8, August 1981, pp20-28

TRETIAK and PASTOR(1984)
Velocity Estimation from Image Sequence with Second Order Differential Operator
O. Tretiak and L. Pastor
International Conference on Pattern Recognition 7, Montreal Canada, 1984, pp.16-19

TSAI and HUANG(1981)
Estimating Three-Dimensional Motion Parameters of a Rigid Planar Patch I
R.Y. Tsai and T.S. Huang
IEEE Trans. on ASSP, Vol. ASSP-29, Dec. 1981, pp.1147-1152

TSAI et al.(1982)
Estimating Three-Dimensional Motion Parameters of a Rigid Planar Patch II
R.Y. Tsai, T.S. Huang, and W. Zhu
IEEE Trans. on ASSP, Vol.ASSP-30 No.4, August 1982, pp.525-534

TSAI and HUANG(1984)
Uniqueness and Estimation of Three-Dimensional Motion Parameters of Rigid Objects with Curved Surfaces
R.Y. Tsai and T.S. Huang
IEEE on PAMI, Vol.PAMI-6 No.1, January 1984, pp.13-27

TSAI(1983)
Multiframe Image Point Matching and Surface Reconstruction
IEEE on PAMI, Vol. PAMI-5 No.2, March 1983, pp.159-174

ULLMAN(1979)
The Interpretation of Visual Motion
S. Ullman
MIT Press, Cambridge, Mass., 1979

ULLMAN(1981)
Analysis of Visual Motion by Biological and Computer System
S. Ullman
Computer, Vol. 14 No. 8, August 1981, pp.57-69

ULSTAD(1973)
An Algorithm for Estimating Small Scale Difference between Two Digital Images
M.S. Ulstad
Pattern Recognition Vol.5, 1973, pp.323-333

VANDERBURG and ROSENFELD(1977)
Two Stage Template Matching
G.J. Vanderburg and A. Rosenfeld
IEEE Trans. Computers, Vol.C-26, April 1977, pp.384-393

WILLIAMS(1980)
Depth from Camera Motion in a Real World Scene
T.D. Williams
IEEE Trans. on PAMI, Vol.PAMI-2 No.6, November 1980, pp.511-516

WOHN et al.(1983)
Motion Estimation Based on Multiple Local Constraints and Nonlinear Smoothing
K. Wohn, L.S. Davis, and P. Thrift
Pattern Recognition, Vol.16 No.6, 1983, pp.563-70

YACHIDA(1983)
Determining Velocity Map by Spatio-Temporal Nwighborhoods from Image Sequence
M. Yachida
Computer Vision, Graphics, and Image Processing, Vol.21, 1983, pp.262-279

YALAMANCHILI et al.(1982)
Extraction of Moving Object Descriptions via Differencing
S. Yalamanchili, W.N. Martin, and J.K. Aggarwal
Computer Graphics and Image Processing, Vol.18, 1982, pp.188-201

YEN and HUANG(1983)
Determining 3-D Motion and Structure of a Rigid Body Using the Spherical Projection
B.L. Yen and T.S. Huang
Computer Vision, Graphics, and Image Processing, Vol.21, 1983, pp.21-32

The vita has been removed from the scanned document